Mémoire d'Habilitation à Diriger les Recherches

Faculté de Science d'Orsay - Université Paris-Sud

Specialité: Astroparticules

Dark Matter Indirect Detection

Marco Cirelli

IPhT, CNRS, URA 2306 & CEA/Saclay, F-91191 Gif-sur-Yvette, France

Octobre 2014

Contents

Foreword

My scientific career has developed so far at the borders between particle physics, cosmology and astrophysics, in what is commonly identified as the field of **astroparticle physics**.

The **'flow' of my research** can be generically captured by the following definitions: models with extra space dimensions for particle physics (2001) $\rightarrow$ models with neutrinos in extra-dimensions (2002) $\rightarrow$ sterile neutrinos and neutrino cosmology (2003-2006) $\rightarrow$ neutrinos produced from Dark Matter annihilations (2005) $\rightarrow$ constructions of Dark Matter (DM) models (2006-2008) $\rightarrow$ phenomenology of indirect detection of DM (2008-2014) $\rightarrow$ exploration of alternative models for DM production (2012) $\rightarrow$ phenomenology of DM direct detection and collider detection (2013-2014).

Hence, what is arguably the dominant core interest of my recent activity right now is the exploration of **DM Indirect Detection (ID) methods**. These consists in using cosmic rays (gamma rays, charged particles and neutrinos), produced by the annihilations or decays of DM particles in our galactic halo and beyond, in order to reveal the existence (and eventually study the properties) of the Dark Matter itself.

In this context, I have in particular put a special attention into the ID phenomenology of the DM models recently proposed in the wake of the excitement for 'anomalies' in the data, such as the PAMELA positron excess, the FERMI gamma-ray line, the GeV gamma-ray Galactic Center excess etc.

This *mémoire* is divided in two parts. In **Part A** I briefly present myself and my scientific activities up to now (october 2014). In **Part B** I present a selection of results in DM Indirect Detection. The logical structure of Part B, in turn, is twofold: 1) it presents the basic concepts and formulæ that are used in the field, in the form of a 'matter of fact', (hopefully) useful collection of tools; 2) it presents briefly the status of the searches and sketch the research directions that have stemmed from them.

Part A

Curriculum Vitæ and presentation of the scientific activities

Curriculum Vitæ - Marco CIRELLI

Date of Birth:	June 20th, 1975
Place of Birth:	Milano, Italy
Citizenship:	Italian (original) & French (pending)

Present position and address:

from 10.2007 **CNRS Researcher** (currently CR1) in Theoretical Physics at the Institut de Physique Théorique of **CEA-Saclay**

IPhT - CEA/Saclay, Orme de Merisiers, Bât. 774
F-91191, Gif-sur-Yvette Cedex, France
phone: +33 (0)1 69 08 81 14 – fax: +33 (0)1 69 08 81 20
www.marcocirelli.net – marco.cirelli@cea.fr

Education and Past Employment:

10.2009 – 09.2012 **CERN Fellow** at CERN Theory Division
on leave from CNRS

10.2006 – 09.2007 **Post-Doc**, Institut de Physique Théorique at **CEA-Saclay**, France
awarded INFN postdoc fellowship, *first place - 97.5/100*

09.2003 – 09.2006 **Post-Doc**, Physics Dept., **Yale University**, New Haven, CT, USA
Particle Theory group (Prof. Thomas Appelquist)

17.04.2004 **Ph.D. in Physics** from **Scuola Normale Superiore**:
70/70 magna cum laude
Thesis: “Sterile neutrinos in 4D and 5D in supernovæ and the cosmo”
Advisors: R. Barbieri (Scuola Normale Superiore, Pisa),
A. Romanino (Scuola Normale Superiore, Pisa and CERN)
Board of external referees: A.Yu. Smirnov (ICTP, Trieste) and
A. Dolgov (INFN, Ferrara).

06 – 07.2003 Short Term Visitor at CERN Theory Division, Geneva, Switzerland
supported by Scuola Normale studentship

2001 – 2003 Ph.D. Student at Scuola Normale Superiore, Pisa, Italy
Research Interest: High Energy Physics, Extra dimensions, Neutrino Physics
Key courses: Elementary Particle Theory (R. Barbieri) - Cosmology (A. Riotto) -
Critical Phenomena (S. Caracciolo) - Monopoles (V. Zakharov) -
Non Perturbative aspects in Quantum Field Theory (F. Strocchi) -
String Theory (M. Porrati) - High Energy Astrophysics (M. Vietri)

11.07.2000 **Laurea in Physics** from **Milano University**:
110/110 magna cum laude
Thesis: “Soft Gluon Resummation in Drell-Yan processes in QCD”
Advisors: G. Marchesini (now Milano-Bicocca University, Italy)
P. Nason (now INFN, Milano-Bicocca, Italy)

1994 – 1999 Undergraduate studies in Physics, Milano University
Exams average: *29.8/30*

Languages:

Italian (native), English, French.

Miscellaneous awards:

- Laureate of European Research Council (**ERC**) **Starting Grant** 2011
- “Nuclear Physics B Most Cited Article 2006-2010” Award, for paper [17] below
- Referee Award from Phys. Lett. B, November 2009

Professional Activities:

- Grants and Grant Administration:
  - ERC Starting Grant, project ‘*NewDark*’ ($\sim$ 1.5 M€ over 5 yr), 2012–2017
  - travel and collaboration grant funded by *PEPS CNRS* (5 K€/yr), 2010–2011 (main coordinator P. Serpico)
  - one postdoctoral recruitment funded by *Physique des 2 Infinis* Consortium (100 K€), 2008–2010, with IAP
  - ‘scientist in charge’ of the Saclay node of the European RTN Network *UniverseNet*, 2008-2011 (main coordinator S. Sarkar, Oxford)
- Advisor of PhD Students:
  - PhD of Marta Maria Perego (jointly with SPP CEA/Saclay), 2014-2017
  - PhD of Andrea Vittino (jointly with Torino University), 2012-2015
  - PhD of Gaëlle Giesen, 2012-2015
  - PhD of Paolo Panci (jointly with L’Aquila University), 2009-2011
- Supervision of other Students and Post-docs:
  - Internship of Jatan Buch, 2014
  - CERN summer student project of Caner Ünal, 2010
  - post-doctoral appointment of Fabio Iocco (with IAP), 2008-2009
  - ‘mentoring’ of Andrzej Hryczuk, within the *UniverseNet* network, from 2009
  - Master research stage of Carolin Bräuninger (Tübingen University), 2008–2009

- PhD research project of Yi-Zen Chu (Yale University), 2005–2006
- (member of PhD committee: Marco Farina at Scuola Normale Superiore Pisa, October 2013)
- (member of PhD committee: Daniel Albornoz-Vasquez at Annecy, September 2011)
- (member of PhD committee: Gilles Vertongen at ULB Bruxelles, September 2009)

▷ Conference Organization:

- Planck 2014 "From the Planck scale to the electroweak scale",
  Paris, May 2014 – organizer with K. Benakli, E. Dudas, S. Lavignac and H. Partouche
- PONT d'Avignon 2014 "Progress on Old and New Themes in cosmology",
  Avignon, April 2014 – organizer with C. Caprini, G. Servant and Ph. Brax
- ICTP Workshop on the Future of Dark Matter Astro-Particle Physics,
  Trieste, Oct 2013 – organizer with G. Zaharijas, P. Serpico et al.
- TeVPA 2013 "TeV Particle Astrophysics Conference",
  Irvine, California, August 2013 – member of the Scientific Organizing Committee
- TeVPA 2012 "TeV Particle Astrophysics Conference",
  Mumbai, India, December 2012 – member of the Scientific Organizing Committee
- DMUH11 "CERN TH-Institute: Dark Matter Undeground and in the Heavens",
  CERN, Geneva, July 2011 – main organizer
- PPC 2011 "Workshop on the Interconnections between Particle Physics & Cosmology",
  CERN, Geneva, June 2011 – member of the local organizing committee
- PONT d'Avignon 2011 "Progress on Old and New Themes in cosmology",
  Avignon, April 2011 – organizer with C. Caprini, G. Servant and Ph. Brax
- DMaa "Dark Matter All Around",
  Paris, December 2010 – member of the local organizing committee
- ICHEP 2010 "International Conference on High Energy Physics",
  Paris, July 2010 – member of scientific committee, of local committee, proceedings editor
- TeVPA 2010 "TeV Particle Astrophysics Conference",
  Paris, July 2010 – member of the local organizing committee
- TANGO in PARIS "Testing Astroparticle with the New GeV-TeV Observations: Positrons And electRons, Identifying the Sources",
  Paris, May 2009 – member of the local organizing committee
- PONT d'Avignon 2008 "Progress on Old and New Themes in cosmology",
  Avignon, April 2008 – organizer with G. Servant and Ph. Brax

▷ Conference Converships:

- IFT Madrid Workshop - "Physics Challenges in the face of LHC-13",
  Madrid, September 2014 – session organizer: "Dark Matter"
- APP 2014 "AstroParticle Physics 2014",
  Amsterdam, June 2014 – session co-organizer: "Indirect Dark Matter Searches"
- IFAE 2014 "Incontri di Fisica delle Alte Energie 2014",
  L'Aquila, Italy, April 2014 – session co-organizer: "Cosmic Frontier (DM, neutrinos, CRs)"

– WIN 2013 “XXIV Weak Interactions and Neutrino Workshop”,
  Natal, Brazil, September 2013 – session co-organizer: “Astroparticle Physics”
– ICATPP 2011 “Astroparticle, Particle, Space Physics & Detectors for Physics Appl.s”,
  Como, Oct 2011 – session co-org.: “Production of CR from Exotic Matter & Astro Sources”
– ECFA Study of “Physics and Detectors for a Linear Collider 2010”,
  Geneva, October 2010 – co-convener: “Connection to Cosmology”
– CRICATPP 2010 “CR Int. Conf. on Advanced Technology in Particle Physics”,
  Como, October 2010 – session co-organizer: “Production of CR from exotic matter”
– COSMO 2009,
  CERN, September 2009 – parallel session convener: “Dark Matter”
– ENTApP Dark Matter Visitor’s Program,
  DESY - 25-29 Feb 2008, Hamburg, Germany – convener

▷ Meeting Series Organization:
– yearly mini-workshops at IPhT on Dark Matter (*NewDark* project)
  from 2013 – local organization
– french GDR TeraScale
  from 2013 – Dark Matter coordinator with E. Moulin
– french GDR Neutrino
  from 2008 to 2013 – theory coordinator with S. Lavignac
– Rencontres IPhT/SPP, regular tri-annual meetings theorists ↔ experimentalists in particle physics and cosmology at Saclay
  2008–2009 – organizer with E. Mazzucato
– mini-workshops at IPhT on the Physics of ElectroWeak Symmetry Breaking and LHC
  2008–2009 – local organization

▷ Seminar Organization:
– AstroParticle and Phenomenology friday seminar series, CERN-TH, 2010
– Particle and Cosmology seminar series, IPhT CEA/Saclay, 2007–2009
– High Energy Theory seminar series, Yale University, 2004–2005

▷ Grant Reviewer:
– for the CONICYT, Chile, 2014
– for the ERC (European Research Council), 2009, 2014
– for the European Commission Research Executive Agency, 2014
– for the Italian Ministry of University & Research (FIRB and PRIN), Italy, 2013
– for the ANVUR (Research and University Evaluation National Agency), Italy, 2012
– for the Région Rhônes-Alpes, France, 2012
– for the Académie universitaire Louvain, Belgium, 2011
– for the NSERC (Natural Science and Engineering Research Council) of Canada, 2008

- Journal Referee (since 2004):
  - Nature, Physical Review Letters, Astrophysical Journal Letters, Nuclear Physics B, Physics Letters B, JHEP, JCAP, Physical Review D, Progress of Theoretical Physics, Advanced Space Research, MNRAS, European Journal of Physics C, International Journal of Modern Physics A, Frontiers, Advances in High Energy Physics

- Membership in research networks:
  - French *Groupement de Recherche* (GDR) TeraScale
    since 2013
  - *UniverseNet* European Research and Training Network (coordinator S. Sarkar)
    2008 – 2011
  - *UniLHC* European Research and Training Network (coordinator I. Antoniadis)
    2009 – 2013
  - *Phys@Col&Cos* Agence Nationale de la Recherche (ANR) grant (coordinators C. Savoy)
    2006 – 2008
  - *DarkPhys* ANR grant (coordinators G. Servant et P. Brax)
    2006 – 2008
  - French *Groupement de Recherche* (GDR) Neutrinos
    since 2006

- Memberships:
  - Société Française de Physique (2007-2014)
  - Associazione Alunni Scuola Normale Superiore

- Outreach:
  - CERN hang-out on Dark Matter (2013): collective online interview and discussion
    around 500 online participants and around 5000 offline viewers
  - general public seminars: CERN (several occasions, 2010 to 2012)
  - CERN official guide, including CMS and AD (since 2010)
  - Popular articles, communications and interviews: see on page 15

List of Publications

The list includes Conference Proceedings, only if published and containing original material.
Other non-published (refereed and non-refereed) works can be found on my personal webpage.

40. M. Cirelli, F. Sala, M. Taoso,
"Wino-like Minimal Dark Matter and future colliders",
arXiv:1407.7058 [hep-ph].

39. M. Cirelli, D. Gaggero, G. Giesen, M. Taoso, A. Urbano,
"Antiproton constraints on the GeV gamma-ray excess: a comprehensive analysis",
arXiv:1407.2173 [hep-ph].

38. M. Cirelli, N. Fornengo, M. Taoso, A. Vittino,
"Anti-helium from Dark Matter annihilations",
JHEP **1408** (2014) 009, arXiv:1401.4017 [hep-ph].

37. P. Baratella, M. Cirelli, A. Hektor, J. Pata, M. Piibeleht, A. Strumia,
"PPPC 4 DMν: A Poor Particle Physicist Cookbook for ν from DM annihil. in the Sun",
JCAP **1403** (2014) 053, arXiv:1312.6408 [hep-ph].

36. M. Cirelli, P. D. Serpico, G. Zaharijas,
"Bremsstrahlung gamma rays from light Dark Matter",
JCAP **1311** (2013) 035, arXiv:1307.7152 [astro-ph.HE].

35. E. Del Nobile, M. Cirelli, P. Panci,
"Tools for model-independent bounds in direct dark matter searches",
JCAP **1310** (2013) 019, arXiv:1307.5955 [hep-ph].

34. M. Cirelli, G. Giesen,
"Antiprotons from Dark Matter: Current constraints and future sensitivities",
JCAP **1304** (2013) 015, arXiv:1301.7079 [hep-ph].

33. G. Belanger, C. Boehm, M. Cirelli, J. Da Silva, A. Pukhov,
"PAMELA and FERMI-LAT limits on the neutralino-chargino mass degeneracy",
JCAP **1211** (2012) 028, arXiv:1208.5009 [hep-ph].

32. M. Cirelli, E. Moulin, P. Panci, P. D. Serpico, A. Viana,
"Gamma ray constraints on Decaying Dark Matter"
Phys. Rev. **D86** (2012) 083506, arXiv:1205.5283 [astro-ph.CO].

31. G. Brooijmans, B. Gripaios, F. Moortgat, Jose Santiago, P. Skands, C. Balazs *et al.*,
"Les Houches 2011: Physics at TeV Colliders New Physics Working Group Report",
Proceedings of Les Houches workshop 2011, arXiv:1203.1488 [hep-ph].

30. M. Cirelli,
"Indirect Searches for Dark Matter: a status review",
Proceedings of Lepton-Photon 2011, arXiv: 1202.1454 [hep-ph].

29. M. Cirelli, P. Panci, G. Servant, G. Zaharijas,
"Consequences of DM/antiDM Oscillations for Asymmetric WIMP Dark Matter",
JCAP **1203** (2012) 015, arXiv: 1110.3809 [hep-ph].

28. P. Ciafaloni, M. Cirelli, D. Comelli, A. De Simone, A. Riotto, A. Urbano,
"Initial State Radiation in Majorana Dark Matter Annihilations",
JCAP **1110** (2011) 034, arXiv:1107.4453 [hep-ph].

27. P. Ciafaloni, M. Cirelli, D. Comelli, A. De Simone, A. Riotto, A. Urbano,
"On the Importance of EW Corrections for Majorana Dark Matter Indirect Detection",
JCAP **1106** (2011) 018, arXiv:1104.2996 [hep-ph].

26. M. Cirelli, G. Corcella, A. Hektor, G. Hutsi, M. Kadastik, P. Panci, M. Raidal, F. Sala, A. Strumia,
"PPPC 4 DM ID: A Poor Particle Physicist Cookbook for Dark Matter Indirect Detection",
JCAP **1103** (2011) 051, arXiv:1012.4515 [hep-ph].

25. M. Cirelli, J. Cline,
"Can multistate DM annihilation explain the high-energy cosmic ray lepton anomalies?"
Phys. Rev. **D 82** (2010) 023503, arXiv:1005.1779 [hep-ph].

24. P. Brun, G. Bertone, M. Cirelli, E. Moulin, J.-F. Glicenstein, F. Iocco, L .Pieri
"The Cosmic Ray Lepton Puzzle"
Proceedings of the French Astronomy and Astrophyics Society, arXiv:1001.5408 [astro-ph.HE].

23. M. Cirelli, P. Panci, P. D. Serpico
"Diffuse gamma ray constraints on annihilating or decaying Dark Matter after Fermi"
Nucl. Phys. B **840** (2010) 284-303, arXiv:0912.0663 [astro-ph.CO].

22. M. Cirelli, F. Iocco, P. Panci
"Constraints on DM annihilations from reionization and heating of the intergalactic gas"
JCAP 10 (2009) 009, arXiv:0907.0719 [astro-ph.CO].

21. M. Cirelli, P. Panci
"Inverse Compton constraints on the Dark Matter e+e- excesses"
Nucl. Phys. B **821** (2009) 399-416, arXiv:0904.3830 [astro-ph.CO].

20. C. B. Braeuninger, M. Cirelli
"Anti-deuterons from heavy Dark Matter"
Phys. Lett. B **678** (2009) 20-31, arXiv:0904.1165 [hep-ph].

19. M. Cirelli, A. Strumia
"Minimal Dark Matter: Model and results"
New J. of Phys. 11 (2009) 105005 *(invited review)*, arXiv:0903.3381 [hep-ph].

18. G. Bertone, M. Cirelli, A. Strumia, M. Taoso
"Gamma-ray and radio tests of the e+e- excess from DM annihilations"
JCAP 03 (2009) 009, arXiv:0811.3744 [hep-ph].

17. M. Cirelli, M. Kadastik, M. Raidal, A. Strumia
“Model-independent implications of the $e^{\pm}, \bar{p}$ cosmic ray spectra on properties of DM”
Nucl. Phys. B **813** (2009) 1-21, arXiv:0809.2409 [hep-ph].

16. M. Cirelli, A. Strumia
“Minimal Dark Matter predictions and the PAMELA positron excess”
Proceedings of Physics, PoS(iDM2008)089, arXiv:0808.3867 [astro-ph].

15. M. Cirelli, R. Franceschini, A. Strumia
“Minimal Dark Matter predictions for galactic positrons, anti-protons, photons”
Nucl. Phys. B **800** (2008) 204-220, arXiv:0802.3378 [hep-ph].

14. M. Cirelli, A. Strumia, M. Tamburini
“Cosmology and Astrophysics of Minimal Dark Matter”
Nucl. Phys. B **787** (2007) 152-175, arXiv:0706.4071 [hep-ph].

13. M. Cirelli, Y.-Z. Chu
“Sterile neutrinos, lepton asymmetries, primordial light elements: how much of each?”
Phys. Rev. D **74** (2006) 085015, arXiv:astro-ph/0608206.

12. M. Cirelli, A. Strumia
“Cosmology of neutrinos and extra light particles after WMAP3”
JCAP 12 (2006) 013, arXiv:astro-ph/0607086.

11. M. Cirelli, N. Fornengo, A. Strumia
“Minimal Dark Matter”
Nucl. Phys B **753** (2006) 178, arXiv:hep-ph/0512090.

10. M. Cirelli, N. Fornengo, T. Montaruli, I. Sokalski, A. Strumia and F. Vissani
“Spectra of neutrinos from dark matter annihilations”
Nucl. Phys. B **727** (2005) 99, arXiv:hep-ph/0506298.

9. M. Cirelli, M.C. Gonzalez-Garcia, C. Peña-Garay
“Mass varying neutrinos in the Sun”
Nucl. Phys. B **719** (2005) 219, arXiv:hep-ph/0503028.

8. M. Cirelli,
“Sterile Neutrinos in Astrophysical and Cosmological Sauce”,
Proceedings of Pascos 2004 and of IFAE 2004, arXiv:astro-ph/0410122.

7. M. Cirelli, G. Marandella, A. Strumia. F. Vissani
“Probing Oscillations into Sterile Neutrinos with astrophysics, cosmology and experiments”
Nucl. Phys. B **708** (2005) 215-267, arXiv:hep-ph/0403158.

6. M. Cirelli
“Neutrinos in Extra Dimensions and Supernovae”
Proceedings of the 38th Rencontres de Moriond – Electroweak Interactions and unified theories, ed. J. Trân Thanh Vân, World Publishers, arXiv:hep-ph/0305141.

5. G. Cacciapaglia, M. Cirelli, A. Romanino
"Signatures of Supernova Neutrino Oscillations into Extra Dimensions"
Phys. Rev. D **68** (2003) 033013, arXiv:hep-ph/0302246.

4. G. Cacciapaglia, M. Cirelli, Y. Lin, A. Romanino
"Bulk neutrinos and core collapse supernovae"
Phys. Rev. D **67** (2003) 053001, arXiv:hep-ph/0209063.

3. M. Cirelli
"Muon g-2 in a model with one extra dimension"
Proceedings of the 37th Rencontres de Moriond EW, arXiv:hep-ph/0205140.

2. G. Cacciapaglia, M. Cirelli, G. Cristadoro
"Muon anomalous magnetic moment in a calculable model with one extra dimension"
Nucl. Phys. B **634** (2002) 230-246, arXiv:hep-ph/0111288.

1. G. Cacciapaglia, M. Cirelli, G. Cristadoro
"Gluon fusion production of the Higgs boson in a calculable model with one extra dimension"
Phys. Lett. B **531** (2002) 105-111, arXiv:hep-ph/0111287.

Popular Articles and other publications:

+ M. Cirelli,
"Dark matter candidates",
Newsletter of the Euclid Education & Public Outreach activity, 2014.

+ P. Brun, M. Cirelli,
"Shedding light on the dark sides of the Universe" (in french),
ScintillationS (CEA/IRFU magazine), June 2012.

+ M. Cirelli, C. Bonvin
"Theory of Dark Matter" (in french)
Clefs du CEA, October 2009

+ M. Cirelli, F. Zamponi
"On the academic recruitment system in Italy" (in italian and in english),
La Stampa (italian daily newspaper), October 2007

+ interviews with Nature (UK), Scientific American (USA), ScienceNews (USA), Cosmos Magazine (Australia), The Australian (Australia), The Times Online (UK), Mumbai News (India), EmmeCiQuadro and ilSussidiario.net (Italy), Physics Today (UK), Radio DeeJay (Italy), Science & Vie (France), CERN Bulletin (Switzerland), Physics World (UK), Science & Avenir (France)...

+ long interview with Hugo Ctiborsky, in the context of the "Scientific research: the Invisible" project, La Femis (french National High School of Image and Sound Professions)

Editor:

– ICHEP 2010 Proceedings, published by Proceedings of Science 2011, PoS ICHEP2010 (2010).

Conferences and Seminars

Main invited plenary talks at Conferences

- PANIC 2014 - Particles and Nuclei International Conference - 25-29 Aug 2014, Hamburg, Germany
- DISCRETE 2012 - Physics of Discrete Symmetries, 3-7 Dec 2012, Lisbon, Portugal
- Strong and Electroweak Matter (SEWM) 2012 - 9-13 Jul 2012, Swansea, UK
- Lepton-Photon 2011 - 22-27 Aug 2011, Mumbai, India
- NOW 2010 - 5-11 Sep 2010, Conca Specchiulla, Italy
- PASCOS 2009 - 6-10 Jul 2009, Hamburg, Germany
- Moriond EW 2009 - 7-13 Mar 2009, La Thuile, Italy
- NUFACT 06 - 24-30 Aug 2006, Irvine CA, Usa

Lectures

- *invited lectures* – “Dark Matter models and Indirect Detection”,
  Doctoral Program of ‘Suisse Romande’, 16h lectures, Nov-Dec 2013, Lausanne, Switzerland
- *invited lectures* – “Dark Matter ”,
  Sixth TRR33 Winter School, 4h lectures, 9-14 Dec 2012, Passo del Tonale, Italy
- *invited lectures* – “Dark Matter searches”,
  Retreat of the graduate school ‘Symmetry Breaking’, 22-24 Sep 2012, Mainz, Germany
- *invited lectures* – “Dark Matter”,
  ICTP Summer School on Cosmology 2012, 16-17 Jul 2012, Trieste, Italy
- *invited lectures* – “Introduction to the Dark Components of the Universe” and “Neutrinos as a dark component of the Universe”,
  ISAPP (International School on Astro-Particle Physics) - 8 -15 Jul 2011, Heidelberg, Germany
- *invited lecture* – “Dark Matter indirect detection”,
  UniverseNet School and Meeting - 12 -18 Sep 2010, Lecce, Italy
- *invited lectures* – “Hoping to indirectly detect Dark Matter with cosmic rays”,
  Carpathian Summer School of Physics 2010 - 20 Jun - 3 Jul 2010, Sinaia, Romania
- *invited lectures* – “Dark Matter”,
  UniverseNet School and Meeting - 28 Sep - 2 Oct 2009, Autonoma Barcelona, Spain
- *invited lectures* – “Dark Matter in cosmic rays”,
  Ecole de Physique des Astroparticules - 7-12 Sep 2009, OHP, Saint Michel l’Observatoire, France

- *invited lectures* – “Dark Matter”, Roma 2 Tor Vergata - 5-6 Feb 2009, Roma, Italy

Other conferences

- 4th Amsterdam-Paris-Stockholm meeting - 29 sep-1 oct 2014, Amsterdam, The Netherlands
- *invited talk* – 100esimo Congresso Società Italiana di Fisica - 22-26 Sep 2014, Pisa, Italy
- *convener* – IFT Madrid Workshop Physics Challenges of LHC-13, 15-26 Sep 2014, Madrid, Spain
- *invited talk* – Rencontres du Vietnam VHEPU 2014, 3-9 Aug 2014, Quy Nhon, Vietnam
- *invited talk* – ICHEP 2014 - 2-9 Jul 2014, Valencia, Spain
- *invited talk* – Higgs Symposium - 30 Jun - 4 Jul 2014, Edinburgh, Scotland
- Astroparticle Physics 2014 - 23-28 Jun 2014, Amsterdam, The Netherlands
- *invited talk* – SWAPS - Strategy Workshop on Astroparticle, 11-13 Jun 2014, Cartigny, Switzerland
- *invited talk* – APC-Perimeter-Solvay workshop, 10-13 Jun 2014, Paris, France
- *organizer* – Planck 2014 - 26-30 May 2014, Paris, France
- *invited talk* – Workshop on the future of AstroParticle Physics in space, 8-9 May 2014, Pisa, Italy
- *invited talk* – Ibericos Meeting, 28-30 Apr 2014, Aveiro, Portugal
- *organizer* – PONT d’Avignon 2014 - 14-18 Apr 2014, Palais des Papes, Avignon, France
- Rencontres de Physique des Particules, 20-22 Jan 2014, Strasbourg, France
- A passion for particles: A conference in honour of Riccardo Barbieri - 19-20 Dec 2013, Pisa, Italy
- 3rd Amsterdam-Paris-Stockholm meeting, 16-18 Dec 2013, Paris, France
- *organizer* – ICTP Workshop on the Future of DM Astro-Particle Physics, Oct 2013, Trieste, Italy
- *invited talk* – From Higgs to Dark Matter Symposium, 6 Dec 2013, Roma3, Roma, Italy
- *invited talk* – The Violent Universe, IoP Research Meeting, 31 Oct - 1 Nov 2013, London, UK
- *invited talk* – GDR TeraScale, 28-30 Oct 2013, Annecy, France
- *invited talk* – New Perspectives in DM Workshop, 22-25 Oct 2013, Lyon, France
- *convener* – WIN 2013, Weak Interactions & Neutrino Workshop, 16-21 Sep 2013, Natal, Brazil

- *invited talk* – Corfu Summer Institute 2013, 31 Aug-11 Sep 2013, Corfu, Greece
- *invited discussion* – Invisibles13 Workshop, 15-19 Jul 2013, Durham, UK
- Planck 2013 - 20-24 May 2013, Bonn, Germany
- *invited talk* – Portoroz 2013, 14-18 April 2013, Portoroz, Slovenia
- *invited talk* – Second Amsterdam-Paris-Stockholm meeting, 25-27 Mar 2013, Stockholm, Sweden
- *invited talk* – Neutrinos at the forefront of EP- and astro-physics, 22-24 Oct 2012, Lyon, France
- *invited talk* – 2nd KIAS Phenomenology Workshop, 10-14 Sep 2012, Seoul, South Korea
- *invited talk* – New Paths to Particle DM - 29-30 March 2012, Oxford, UK
- *invited talk* – Rencontres de Physique de la Vallee d'Aoste - 26 Feb - 3 Mar 2012, La Thuile, Italy
- *invited talk* – Bethe Program, Nov 2011, Bonn, Germany
- *invited talk* – IDEALS Workshop, 10-12 Nov 2011, SISSA Trieste, Italy
- *talk* – CERN-TH retreat - 2-4 Nov 2011, Les Houches, France
- *invited talk* – GGI Dark Workshop, 25-27 Oct 2011, Galileo Galilei Institute, Firenze, Italy
- *invited talk* – DESY 2011 - Desy Theory Workshop, 27-30 Sep 2011, DESY, Hamburg, Germany
- *invited talk* – LC11 Workshop, 12-16 Sep 2011, Trento, Italy
- *talk* – 15th Lomonosov Conf. on Elementary Particle Physics - 18-24 Aug 2011, Moskow, Russia
- *invited talk* – IDAPP 2days Meeting, 20-22 Jun 2011, Paris, France
- *organizer* – PONT d'Avignon 2011 - 18-22 Apr 2011, Palais des Papes, Avignon, France
- *invited talk* – Rencontres de Physique des Particules, 14 Jan 2011, Clermont-Ferrand, France
- *convener* – IWLC2010, Int. Workshop on Linear Colliders, 18-22 Oct 2010, Geneva, Switzerland
- *convener* – CRICATPP 2010, 7-8 Oct 2010, Como, Italy
- *talk* – COSMO 2010 - 27 Sep - 1 Oct 2010, Tokyo, Japan
- *invited talk* – IoA Conference Darkness Visible - 2-6 Aug 2010, I. of Astronomy, Cambridge, UK
- *organizer* – ICHEP 2010 - 21-28 Jul 2010, Palais des Congres, Paris, France

- *organizer* – TeVPA - 19-23 Jul 2010, Paris, France
- Planck 2010, From the Planck scale to the EW scale, 31 May - 4 Jun 2010, CERN, Switzerland
- *invited talk* – GGI DM conference - 17-21 May 2010, Galileo Galilei Institute, Firenze, Italy
- *invited talk* – Rencontres de Physique de la Vallee d'Aoste - 28 Feb - 6 Mar 2010, La Thuile, Italy
- KITP workshop Direct, Indirect & Collider Signals of DM - 7-18 Dec 2010, Santa Barbara, CA
- 13$^{\text{th}}$ JLAC Journée des Lacs Alpins de Cosmologie - 24 Nov 2010, Genève, Switzerland
- *invited talk* – Gamma ray diffuse emission mini-workshop - 18 Nov 2009, Zürich, Switzerland
- *talk* – CERN-TH retreat - 4-6 Nov 2010, Les Houches, France
- GDR Neutrino - 28-29 Oct 2009, Strasbourg, France
- *invited talk* – CCAPP Symposium - 12-14 Oct 2009, Columbus, OH
- *convener* – COSMO 2009 - 7-11 September 2009, CERN, Geneva, Switzerland
- *invited talk* – 12th Marcel Grossmann Meeting on GR - 12-18 Jul 2009, Unesco, Paris, France
- *invited talk* – Joint ICTP-INFN-SISSA conference on LHC - 29 Jun - 2 Jul 2009, Trieste, Italy
- *invited talk* – New Lights on Dark Matter - 11-13 Jun 2009, Perimeter Institute, Waterloo, Canada
- *invited talk* – Rencontre at the Colegio de España - 4-5 Jun 2009, Paris, France
- *invited talk* – TANGO workshop - 4-6 May 2009, IAP, Paris, France
- GDR Neutrino - 27-28 Apr 2009, LPNHE Jussieu, Paris, France
- *invited talk* – GDR TeraScale - 30 Mar - 1 Apr 2009, Grenoble, France
- *invited talk* – Rencontres Physique Particules - 23-25 Mar 2009, Ecole Polytechnique, France
- *invited review talk* – Dutch Astroparticle Meeting, 20 Mar 2009, Leiden, The Netherlands
- *invited talk* – Frontiers in Neutrino Physics - 16-18 Mar 2009, APC, Paris, France
- *invited talk* – Neutrino Telescopes Venice 2009 - 10-13 Mar 2009, Venice, Italy
- *invited talk* – IPhT Departmental Meeting - 15-17 Oct 2008, Batz-sur-Mer, France
- *invited talk* – UniverseNET school and meeting - 22-26 Sep 2008, Oxford, UK

- *talk* – NOW 2008, Neutrino Oscillation Workshop - 6-13 Sep 2008, Conca Specchiulla, Italy
- *talk* – iDM2008, Identification of Dark Matter - 18-22 Aug 2008, Stockholm, Sweden
- 12th Paris Cosmology Colloquium 2008 Ecole Chalonge - 17-19 Jul 2008, Paris, France
- PLANCK 2008, From the Planck scale to the EW scale - 19-23 May 2008, Barcelona, Spain
- *organizer* – PONT d'Avignon 2008 - 21-25 Apr 2008, Palais des Papes, Avignon, France
- GDR Neutrino - 10-11 Apr 2008, Saclay, France
- *convener* – ENTApP DM Visitor's Program DESY - 25-29 Feb 2008, Hamburg, Germany
- Dark Matter at Small Scales - 13-15 Feb 2008, APC, Paris, France
- *invited talk* – GDR SuSy - 12-14 Nov 2007, Bruxelles, Belgium
- *invited talk* – The Path to Neutrino Masses - 3-6 Sep 2007, Aarhus, Denmark
- *invited talk* – TeV Particle AstroPhysics - 27-31 Aug 2007, Venice, Italy
- *invited talk* – LHC-Cosmology Interplay CERN Theory Institute - 9-20 Jul 2007, CERN
- *invited talk* – GDR Neutrinos Plenary Meeting - 21-22 Jun 2007, APC, Paris, France
- *invited review talk* – Rencontre at the Colegio de España - 17-18 May 2007, Paris, France
- *invited talk* – GDR Neutrinos Plenary Meeting - 13-14 Mar 2007, LAPP, Annecy, France
- *invited short talk* – CERN Dark Matter Visitor Program - 5-9 Mar 2007, CERN
- *talk* – Rencontres de Physique de Particules 2007 - 28 Feb - 2 Mar 2007, Grenoble, France
- *invited talk* – Aspen Conference on Neutrinos Astrophysics - 28 Jan - 3 Feb 2007, Aspen
- Nobel Conference, Ecole d'Astrophysique D. Chalonge - 16 Dec 2006, Paris, France
- *talk* – ENTApP Annual Meeting (Theoretical Astroparticle) - 12-14 Dec 2006, Paris, France
- High Energy Physics in the LHC Era - 13-17 Nov 2006, LPNHE Jussieu, Paris, France
- Astroparticle Workshop - 23 Oct - 4 Nov 2006, Galileo Galilei Institute, Firenze, Italy
- *talk* – IFAE (Incontri sulla Fisica delle Alte Energie) - 19-21 April 2006, Pavia, Italy
- XI IFT-UAM/CSIC Christmas Workshop - 14 -16 Dec 2005, UAM, Madrid, Spain
- *talk* – QUEST Meeting 2005 - 12-13 Dec 2005, UAM, Madrid, Spain
- Tribute to John Bahcall - 29 Oct 2005, IAS, Princeton NJ
- *talk* – INFO 05, Implications of Neutrino Flavor Oscillations - 11-15 Jul 2005, Santa Fe NM
- Cosmic Connections – 17-23 Apr 2005, Quarrata, Italy

- COSMO 2004 - 17-21 Sep 2004, Toronto, Canada
- *talk* – PASCOS 2004 - 16-22 Aug 2004, Northeastern University, Boston MA, Usa
- IFAE (Incontri sulla Fisica delle Alte Energie) - 14-16 Apr 2004, Torino, Italy
- CAPP 2003, Cosmology And Particle Physics - 12-17 June 2003, CERN
- PLANCK 2003 – 26-31 May 2003, Madrid, Spain
- Pisa Week on Astro-Particle Physics and Cosmology: LSS and CMB, 5-9 May 2003
- *talk* – IFAE (Incontri sulla Fisica delle Alte Energie) - Lecce, Italy, 23-26 April 2003
- *talk* – Moriond 2003, EW Interactions & Unified Theories - 15-22 Mar 2003, Les Arcs, France
- PLANCK 2002 - Kazimierz, Poland, 25-29 May 2002
- *short talk* – Moriond 2002, EW Interactions & Unified Theories - 9-16 Mar 2002, France
- Corfu 2001, Summer Institute on Elementary Particles - 31 Aug-21 Sep 2001, Corfu, Greece
- PLANCK 2001 - 11-16 May 2001, La Londe les Maures, France
- IX National Seminar of Theoretical Physics - 4-15 Sep 2000, Parma, Italy

Invited Colloquia

- Laboratoire Francis Perrin, CNRS/CEA, France (December 2011)
- Dutch National Seminar, Amsterdam, The Netherlands (November 2011)
- CERN-TH Colloquium, CERN Theory Division (February 2011)
- 'Helmholtz Alliance' National German Seminar, Bonn, Th. Phys. Dep., Germany (January 2011)
- Heidelberg University Physics Department, Germany (May 2009)
- Federal University of Rio de Janeiro, Brazil (December 2008)
- IFT Saõ Paulo & University of Saõ Paulo, Brazil (November-December 2008)
- CERN-TH Colloquium, CERN Theory Division (October 2008)

Invited Seminars and other short term visits

- Gran Sasso Science Institute, L'Aquila, Italy (Mar 2014)
- IAP Paris, France (Feb 2014)
- TOTEM seminar, CERN, Geneva, Switzerland (Oct 2013)
- Aachen Doctoral School, Aachen, Germany (Oct 2013)

- Geneva University Physics Dept, Geneva, Switzerland (Oct 2013)
- DAMPT, Cambridge, UK (Apr 2013)
- Roma3 Physics Dept, Roma, Italy (Apr 2013)
- LPTHE/ENS Joint Seminar, Paris, France (Mar 2013)
- LPT Paris XI Orsay, France (Feb 2013)
- Scuola Normale Superiore, Pisa, Italy (Jan 2013)
- Padova Physics Department (Nov 2012)
- King's College London, UK (Nov 2012)
- ATLAS Astroparticle Forum, CERN, Switzerland (Nov 2012)
- Freiburg Physics Department, Germany (Jun 2012)
- CERN Collider Cross Talk, CERN, Switzerland (May 2012)
- Basel Physics Department, Switzerland (May 2012)
- SISSA, Trieste, Italy (Nov 2011)
- Niels Bohr Institute, Copenhagen, Denmark (Oct 2011)
- LNGS Gran Sasso, Italy (Mar 2011)
- SHEP Southampton, UK (Nov 2010)
- CP^3-Origins Center, Odense, Southern Denmark (Nov 2010)
- RWTH Aachen, Germany (May 2010)
- Université de Genève, Switzerland (Mar 2010)
- LPSC Grenoble, France (Dec 2009)
- LPNHE Jussieu, Paris, France (Nov 2009)
- IFT Granada, Spain (Nov 2009)
- Milano-Bicocca University, Italy (Oct 2009)
- ITP Warsaw, Poland (Oct 2009)
- IPHC Strasbourg, France (Sep 2009)
- LAPP, Annecy, France (Jun 2009)
- Imperial College, London, UK (May 2009)
- AstroParticle Theory group, Bielefeld, Germany (May 2009)

- ETH Zürich, Switzerland (April 2009)
- Max Planck Institute Heidelberg, Germany (January 2009)
- APC, Paris, France (December 2008)
- Autonoma University Barcelona, Spain (December 2008)
- LPT Paris XI Orsay, France (November 2008)
- Colloquium IPhT, Saclay, France (March 2008)
- CPT, Ecole Polytechnique, Palaiseau, France (March 2008)
- LPT, Paris XI Orsay, France (February 2008)
- LUTH, Observatoire de Paris, Meudon, France (November 2007)
- ULB Brussels, Belgium (October 2007)
- CPT Marseille, France (May 2007)
- IPN Lyon, France (April 2007)
- University of Wisconsin-Madison WI, Usa (February 2007)
- Fermilab, Batavia IL, Usa (February 2007)
- SPhT CEA/Saclay, France (April 2006)
- University of Washington, Seattle WA, Usa (February 2006)
- Harvard University, Cambridge MA, Usa (February 2006)
- New York University, New York NY, Usa (February 2006)
- EPFL, Lausanne, Switzerland (January 2006)
- Torino University, Italy (January 2006)
- ICTP, Trieste, Italy (January 2006)
- SPhT CEA/Saclay, France (December 2005)
- Institute for Advanced Study, Princeton NJ (October 2005)
- Zürich University, Switzerland (June 2005)
- Brookhaven National Lab, Upton NY (April 2005)
- SUNY Stony Brook NY, Usa (April 2005)
- UC Riverside CA, Usa (April 2005)
- UC Los Angeles CA (April 2005)

- UC Berkeley CA (April 2005)
- Harvard University, Cambridge MA, Usa (March 2005)
- Los Alamos National Lab, NM, Usa (March 2005)
- Cornell University, Ithaca NY, Usa (April 2004)
- Milano-Bicocca University, Italy (2003, 2004, 2006)
- Department of Physics at Pisa University (2002-2003)

Part B

Results in Dark Matter Indirect Detection

Chapter 1

Introduction to Dark Matter and Indirect Detection

The existence of Dark Matter is firmly established by observations from galactic to cosmological scales. However these observations only probe the gravitational coupling of Dark Matter, namely its total mass and (somewhat) its spatial distribution. To really understand *what* Dark Matter is we need to observe its other possible interactions with ordinary matter.

Three are the **main avenues of investigation** that are pursued:

- Direct Detection, which aims at detecting the recoil event produced by a passing DM particle hitting one of the nucleus of a super-shielded and closely monitored underground detector, made of ultrapure semiconductors, noble gasses, pristine crystals etc.

- Indirect Detection, discussed in detail in all the rest of this work, which aims at detecting in cosmic rays the signature of DM annihilations or decays.

- accelerator searches, which aim at producing DM particles in a controlled environment (at this time essentially the *pp* collisions at the Large Hadron Collider at CERN, but also possibly in e^+e^- colliders and in beam dump experiments) and then detecting their presence via missing energy or other signatures.

In each of these directions very many experimental efforts are deployed. Fig. 1.1 reports a good fraction of them and shows that they are distributed over many continents and different environments. In addition, most if not all of the experiments are run by international collaborations comprising tens to thousands of scientists from many institutions. It is truly a global effort of the scientific community. Hence, it is important and timely that the theoretical community supports this effort by providing, on one side, plausible predictions of the expected candidates and, on the other side, precision tools that allow to compute the expected signals in the different search channels. This also with the need in mind of comprehensive tools that allow cross-correlating the results obtained in such different channels. Concretely, what is needed is a unified framework that allows to convert a signal detected, say, in cosmic antiprotons into an expected signature in high energy neutrinos from the Galactic Center, or (if possible) into rate of events in a noble gas detector. While this remains an unreached goal for the time being (except for specific frameworks), steps have been taken along this way and in particular within the Indirect Detection approach. Some of these steps will be illustrated in the rest of this thesis.

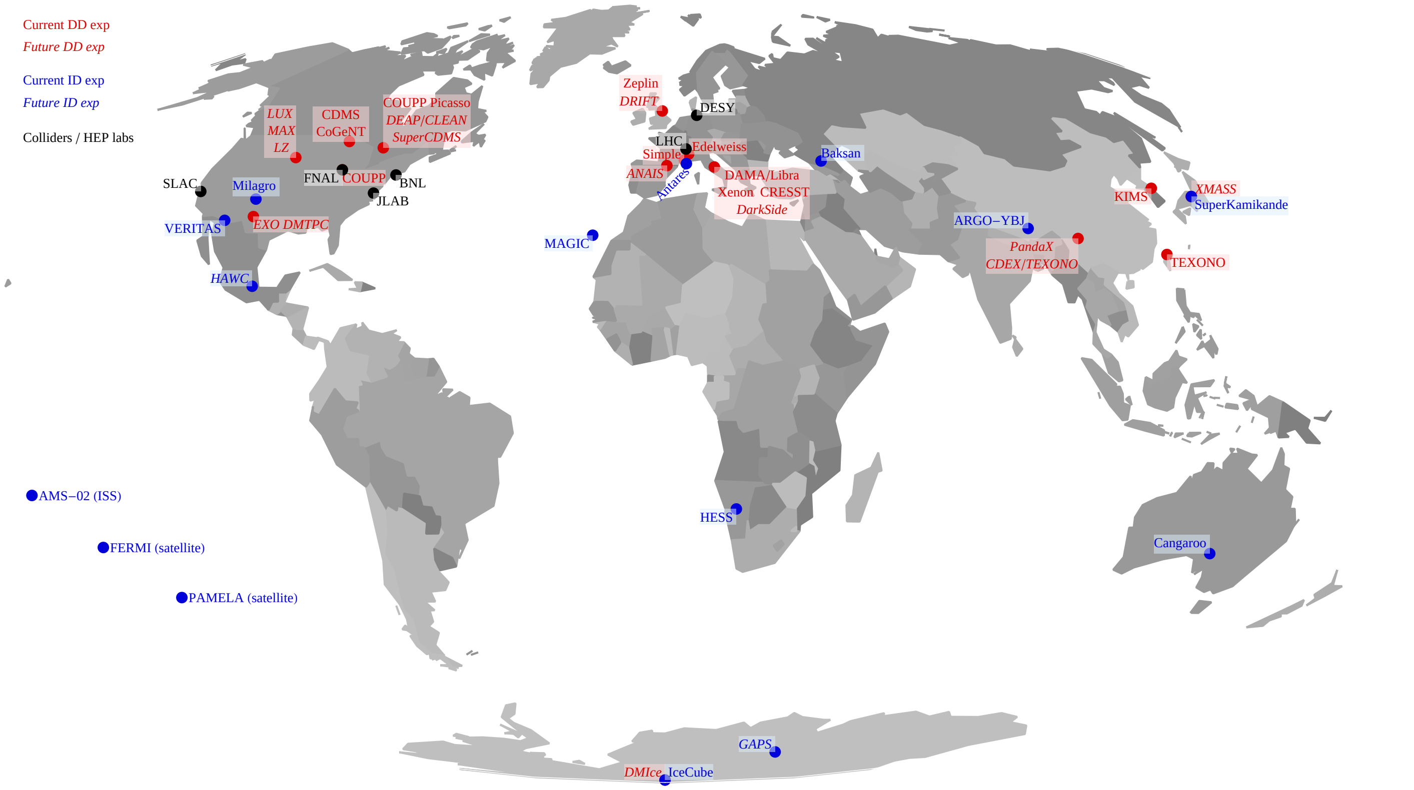

Figure 1.1: *Lots of experiments all around the planet and outside of it.*

Indirect detection of Dark Matter is the core subject of this dissertation. It consists in searching for the following signal: Dark Matter particles annihilate in pairs (or Dark Matter particles decay) giving rise to Standard Model particles, that can be detected by looking, in cosmic rays collected on Earth, for an excess with respect to the presumed astrophysical contribution. Promising sources are generically the regions where DM is expected to be densest, such as the center of our Galaxy, the inner halo of our Galaxy, nearby galaxies dominated by Dark Matter, the center of the Sun, the center of the Earth... However, some of these regions are also the most complicated from the point of view of the underlying astrophysics (notably: the Galactic Center) and so the best detection opportunities might come from selecting targets which are not necessarily the richest in DM but for which the signal over background ratio is most favorable. This also depends on which species of cosmic ray one is looking for. In general terms, the SM particles that we hope to detect are photons, neutrinos, positrons, electrons, antiprotons, antideuterium and maybe even more exotic antinuclei such as antihelium. Each one of them has advantages or disadvantages:

- *High-energy photons (γ-rays).* They freely propagate, in the galactic environment, such that the information lies in both the energy and angular spectrum (in the extragalactic/cosmological environment, however, absorption can occur, but its practical impact is limited). However DM is electrically neutral, so that photons can be produced only via some subdominant mechanism (e.g. loops involving charged particles) or as secondary radiation: the spectrum is expected to be suppressed and highly model dependent.

- *Low-energy photons (X-rays, radio waves).* In the case of heavy ($\sim$ GeV-TeV) DM, low energy photons are typically produced as secondary radiation (synchrotron, Inverse Compton or bremsstrahlung) by the electrons and positrons originating from DM. They do therefore constitute a signal ascribable to DM, but they are 'doubly indirect' and very dependent on the environment (magnetic field, ambient light distribution, gas density...). On the other hand, X-rays and other low energy radiation can also arise directly from the decay of light ($\sim$KeV or MeV) DM particles, e.g. in models featuring sterile neutrinos.

- *Positrons.* Positrons diffuse in the galactic magnetic fields losing energy via synchrotron emission, Coulomb scattering, ionization, bremsstrahlung and Inverse Compton (IC) processes. The DM contribution is dominated by the nearby regions of the galaxy, and the information lies in the energy spectrum. However, below a few GeV, this spectrum is distorted by solar activity.

- *Electrons.* Similar to positrons, with the disadvantage of a higher astrophysical background and the advantage that it is easier to measure at high energy the electron + positron flux rather than the positron flux alone.

- *Antiprotons.* They diffuse in the galactic magnetic fields with negligible energy losses, up to some scatterings on matter in the galactic plane. Therefore even far-away regions of the Galaxy can contribute to the flux collected on Earth and, as a consequence, its normalization has significant astrophysical uncertainties. The information lies in the energy spectrum which, again, is distorted by solar activity below a few GeV.

- *Antideuterons and antihelium.* Nuclei of antideuterium can be synthetized via the coalescence of an anti-proton and an anti-neutron produced in the DM annihilation (or decay) process. The expected yield is very small. On the other hand, the astrophysical background is also expected to be small and, notably, it is expected to peak in a range of energies different from the one of the DM signal, thanks to the peculiar kinematics of the production mechanisms. The propagation in the galactic environment is analogous to the antiproton case. Heavier antinuclei, such as antihelium, can be produced in a completely analogous way, with the important penalty of a much suppressed flux, due to the need of coalescing more antinucleons.

- *Neutrinos.* TeV-scale neutrinos propagate freely in the Galaxy and can also propagate through the dense matter of the Sun and the Earth. The low interaction cross sections make more difficult to detect neutrinos than, e.g., gamma rays. Furthermore, they are measured indirectly via the detection of charged particles (e.g. up-going muons) produced by a neutrino interaction in the rock or water surrounding a neutrino telescope and therefore their energy can be reconstructed only partially. On the other hand, the interaction cross section increases with energy, thus partly compensating the decrease in flux for large DM masses. Possible sources are the same already discussed for photons, plus the center of the Sun and (less promising) of the Earth.

The rest of this Part is dedicated to discussing in detail these different messengers. First, however, in Chapter 2, we will review the basic knowledge on how Dark Matter is presumed to be distributed in the Galaxy. Then, in Chapter 3, we discuss the production of each messenger from DM and their energy spectrum. In Chapter 4 we describe the propagation of each messenger and therefore the observable fluxes at Earth. In Chapter 5 we finally present the status of the DM Indirect searches, with particular attention to the recent anomalies in charged cosmic rays and gamma rays.

Chapter 2

Dark Matter distribution

In this Chapter we briefly remind the current state of the art concerning the presumed distribution of Dark Matter density and velocity in the Galaxy.

Tentative determinations of the DM density profile $\rho(r)$ proceed in two steps:

1. Guesses of the functional form of the spherical $\rho(r)$ in terms of a minimal number of free parameters, as discussed in section 2.1.

2. Determination of the free parameters in terms of safe observations of DM in our Galaxy, or in other galaxies, as discussed in section 2.1.1.

The DM velocity distribution is inferred by simple arguments and then checked against numerical simulations, as discussed in section 2.2. The velocity in the galactic rest frame has then to be converted into the solar rest frame (e.g. for computation concerning the scatterings of DM particles on the nuclei of the Sun, relevant for DM capture and production of high energy neutrino fluxes) or the Earth rest frame (relevant for Direct Detection). These aspects are discussed in sections 2.2.1 and 2.2.2.

2.1 DM density distribution

For the galactic distribution $\rho(r)$ we list the functional forms considered more plausible:

$$\begin{aligned}
\text{NFW}: \quad \rho_{\rm NFW}(r) &= \rho_s \frac{r_s}{r}\left(1+\frac{r}{r_s}\right)^{-2} \\
\text{Einasto}: \quad \rho_{\rm Ein}(r) &= \rho_s \exp\left\{-\frac{2}{\alpha}\left[\left(\frac{r}{r_s}\right)^{\alpha}-1\right]\right\} \\
\text{Isothermal}: \quad \rho_{\rm Iso}(r) &= \frac{\rho_s}{1+(r/r_s)^2} \\
\text{Burkert}: \quad \rho_{\rm Bur}(r) &= \frac{\rho_s}{(1+r/r_s)(1+(r/r_s)^2)} \\
\text{Moore}: \quad \rho_{\rm Moo}(r) &= \rho_s \left(\frac{r_s}{r}\right)^{1.16}\left(1+\frac{r}{r_s}\right)^{-1.84}
\end{aligned} \tag{2.1}$$

All profiles assume spherical symmetry and r is the coordinate centered in the Galactic Center; r_s, ρ_s and α are free parameters. These functions are motivated by the following considerations.

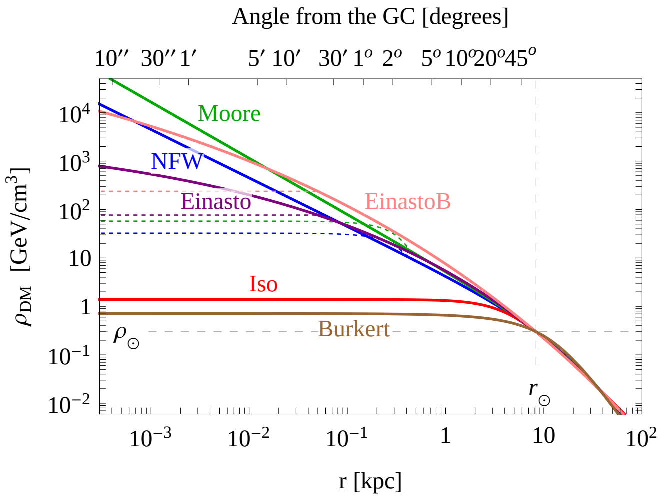

DM halo	α	r_s [kpc]	ρ_s [GeV/cm^3]
NFW	–	24.42	0.184
Einasto	0.17	28.44	0.033
EinastoB	0.11	35.24	0.021
Isothermal	–	4.38	1.387
Burkert	–	12.67	0.712
Moore	–	30.28	0.105

Figure 2.1: ***DM profiles*** *and the corresponding parameters to be plugged in the functional forms of eq. (2.1). The dashed lines represent the smoothed functions adopted for some of the computations in Sec.* **??**. *Notice that we here provide 2 (3) decimal significant digits for the value of r_s (ρ_s): this precision is sufficient for most computations, but more would be needed for specific cases, such as to precisely reproduce the J factors (discussed in Sec.*??*) for small angular regions around the Galactic Center.*

- The Navarro, Frenk and White (**NFW**) [10] profile (peaked as r^{-1} at the Galactic Center (GC)) is a traditional benchmark choice motivated by N-body simulations.

- The **Einasto** [11, 12] profile (not converging to a power law at the GC and somewhat more chubby than NFW at kpc scales) is emerging as a better fit to more recent numerical simulations; the shape parameter α varies from simulation to simulation, but 0.17 seem to emerge as a central, fiducial value, adopted here.

- Numerical DM simulations that try to include the effects of the existence of baryons have consistently found modified profiles that are steeper in the center with respect to the DM-only simulations [13]. Most recently, [14] has found such a trend re-simulating the haloes of [11, 12]: steeper Einasto profiles (smaller α) are obtained when baryons are added. To account for this possibility we include a modified Einasto profile (denoted as EinastoB, EiB in short in the following) with an α parameter of 0.11.

- Cored profiles, such as the truncated **Isothermal** profile [15, 16] or the **Burkert** profile [17], might be instead more motivated by the observations of galactic rotation curves, but seem to run into conflict with the results of numerical simulations.

- On the other hand, profiles steeper that NFW had been previously found by **Moore** and collaborators [18]. Such profiles, despite being less plausible, are often considered because imply larger DM indirect signals from the center of the Galaxy.

In some of the considered profiles $\rho(r)$ diverges as $r \to 0$, but in all profiles $r^2\rho(r) \to 0$ such that the central region of the Galaxy contains a small amount of DM.

Authors	Date	Ref.	$\rho_\odot$ [GeV/cm^3]	Notes
Turner	1986	[21, 22]	0.28	'uncertainty of about a factor of 2'
Flores	1988	[23]	$0.3 \to 0.43$	
Kuijken & Gilmore	1991	[24]	0.42 ($\pm$20%)	
Widrow et al.	2008	[25]	0.304 ± 0.053	
Catena & Ullio	2009	[26]	0.385 ± 0.027	Einasto
			0.389 ± 0.025	NFW
Weber & de Boer	2009	[27]	$0.2 \to 0.4$	
Salucci et al.	2010	[28]	$0.43 \pm 0.11 \pm 0.10$	
McMillan	2011	[29]	0.40 ± 0.04	
Garbari et al.	2011	[30]	$0.11^{+0.34}_{-0.27}$	isothermal stellar tracers
			$1.25^{+0.30}_{-0.34}$	non-isothermal stellar tracers
Iocco et al.	2011	[31]	$0.2 \to 0.56$	
Bovy & Tremaine	2012	[32]	0.3 ± 0.1	
Zhang et al.	2012	[33]	0.28 ± 0.08	
Piffl et al.	2014	[34]	0.59 ($\pm$15%)	

Table 2.1: ***DM density at the location of the Sun*** *as determined by historical and recent studies. Note that the position of the Sun may not be exactly the same for all the authors, that key assumptions might differ and that relative renormalizations might be necessary.*

2.1.1 Determination of the Milky Way parameters

Next, one has to determine the parameters r_s (typical scale radius) and ρ_s (typical scale density) that enter in the tentative DM distributions $\rho(r)$. This can be done in different ways, e.g. extracting their values from numerical simulations of Milky Way-like halos, or determining them in some way from observations of similar outer galaxies. We choose to fix them by imposing that the resulting profiles satisfy the following 'safe' findings of astrophysical observations of the Milky Way:

A) The density of Dark Matter at the location of the Sun is

$$\rho_\odot = \rho(r_\odot) = 0.3\,\mathrm{GeV/cm^3}. \tag{2.2}$$

This is the canonical value routinely adopted in the literature, with a typical associated error bar of ± 0.1 GeV/cm^3 and a possible spread up to $0.2 \to 0.8$ GeV/cm^3 (sometimes referred to as 'a factor of 2'). Recent computations (performed especially from 2008 to 2012) found higher or lower central values and smaller or larger associated error, still subjects to intense debate (see e.g. [19] for a recent discussion on the systematic uncertainties).[1] Table 2.1 lists some of the results; for a dedicated and more thorough discussion see however [35]. Data from the upcoming Gaia mission [36] should allow a precision determination of $\rho_\odot$, although determining how precise this precision will be seems difficult.

B) The total Dark Matter mass contained in 60 kpc (i.e. a bit larger than the distance to the Large Magellanic Cloud, 50 kpc) is $M_{60} \equiv 4.7 \times 10^{11} M_\odot$. This number is based on the recent kinematical surveys of stars in SDSS [37]. We adopt the upper edge of their 95%

[1] It made the news in 2012 the claim of [20] which found $\rho_\odot = 0.000 \pm 0.004$ GeV/cm^3, later ascribed to poor modelling.

C.L. interval to conservatively take into account that previous studies had found somewhat larger values (see e.g. [38, 39]).

Notice that the distance of the Sun from the Galactic Center is itself somehow uncertain: we assume $r_\odot = 8.33$ kpc (see [40, 41, 42]), with an uncertainty of about ± 0.2 kpc.

The parameters that we adopt are given in fig. 2.1, where we also plot the resulting profiles. The values of the parameters that we adopt do not differ much (at most 20%) from the parameter often conventionally adopted in the rest of the literature.

While the various density profiles give similar results above a few kiloparsecs, and in particular around the location of the Earth. they differ considerably — by orders of magnitudes — at smaller distances where there are no data and the results is uniquely determined by the assumed asymptotic functional form as $r \to 0$. As a consequence, indirect DM signals from the inner Galaxy (e.g. gamma ray fluxes from regions a few degrees around the GC) will be highly sensitive to the choice of profile, unlike DM signals that depend on the DM density around the Earth or in the local environment (e.g. the fluxes of high energy positrons, produced at most a few kpc away from the Earth) or that probe regions distant from the GC (e.g. gamma rays from high latitudes).

2.2 Dark Matter velocity distribution

The energy E of a DM particle changes with time because DM partices collectively are forming a dynamical gravitational bound system, where the gravitational potential φ is changing with time, such that $dE/dt = \partial\varphi/\partial t$. This effectively amounts to tell that DM particles undergo many gravitational scatterings. As a consequence their final velocities are given by a sum of many random contributions. The Central Limit Theorem then says that their distribution is approximatively Gaussian.

However, DM particles that happen to acquire a velocity larger than the escape velocity $v_{\rm esc}$ from the Galaxy tend to evaporate away. Consequently, the DM velocity distribution in the galactic rest frame is often assumed to be a Maxwell-Boltzmann (MB) sharply cut off by a finite escape velocity,

$$f(v) = N \times e^{-v^2/v_0^2}\ \Theta(v_{\rm esc} - v)\,, \tag{2.3}$$

where the normalisation constant N is fixed such that $\int d^3v\ f(v) = 1$. It is explicitly given as $N = 1/(\sqrt{\pi} v_0)^3$ in the limit $v_{\rm esc} \to \infty$. Here v_0 is the root mean square velocity which presumably lies in the range,

$$220\,\mathrm{km/s} < v_0 < 270\,\mathrm{km/s} \tag{2.4}$$

and $v_{\rm esc}$ is the escape velocity from the Milky Way, with presumably lies in the range [43].

$$450\,\mathrm{km/s} < v_{\rm esc} < 650\,\mathrm{km/s}. \tag{2.5}$$

N-body simulations [44, 45, 46, 47] suggest a smoother cut-off at $v < v_{\rm esc}$, which can be parameterized as

$$f(v) = N\left[\exp\left(\frac{v_{\rm esc}^2 - v^2}{k v_0^2}\right) - 1\right]^k \Theta(v_{\rm esc} - v) \tag{2.6}$$

with $1.5 < k < 3.5$ [48]. The MB distribution is reobtained in the limit $k \to 0$. These velocity distributions are plotted in fig. 2.2a.

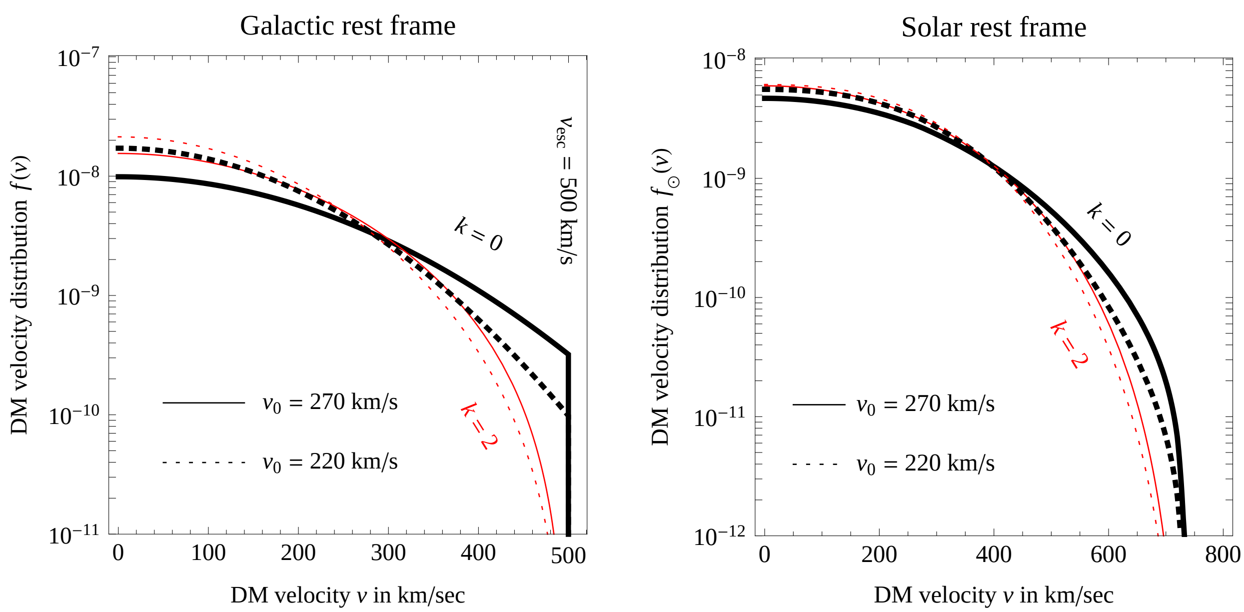

Figure 2.2: ***DM velocity distributions**: the Maxwell-Boltzmann with sharp cutoff at* $v = v_{esc} = 500\,\mathrm{km/s}$ *(thick black curve), the distribution, eq.* (2.6)*, with a smooth cutoff computed for* $k = 2$ *(red). Two different values of* v_0 *are shown:* 220 km/s *(dotted) and* 270 km/s *(solid). The DM velocity distribution is plotted with respect to the galactic rest frame in the left picture and with respect to the solar rest frame in the right picture.*

2.2.1 DM velocity with respect to the Sun

The DM velocity distribution with respect to the solar local frame, $f_\odot(\vec{v})$, is obtained in terms of the velocity distribution in the galactic frame, $f(v)$, through $f_\odot(\vec{v}) = f(|\vec{v} + \vec{v}_\odot|)$ where

$$\vec{v}_\odot = (0, 220, 0)\frac{\mathrm{km}}{\mathrm{sec}} + (10, 13, 7)\frac{\mathrm{km}}{\mathrm{sec}} \tag{2.7}$$

is the velocity of the Sun, here written as the sum of the local Galactic rotation velocity plus the Sun peculiar velocity. We here used Galactic coordinates, where $\hat{x}$ is the direction to the Galactic center, $\hat{y}$ is the direction of disk rotation and $\hat{z}$ the north galactic pole. The modulus of $\vec{v}_\odot$ is $v_\odot \approx 233$ km/ sec.

When computing DM capture by the Sun, we will later need the angular average of $f_\odot$, given by

$$f_\odot(v) = \frac{1}{2}\int_{-1}^{+1} d\cos\theta\; f(\sqrt{v^2 + v_\odot^2 + 2vv_\odot\cos\theta}) \tag{2.8}$$

The numerical result is plotted in fig. 2.2b.

2.2.2 DM velocity with respect to the Earth

The DM velocity distribution with respect to the Earth local frame, $f_\oplus(v, t)$, is obtained in terms of the velocity distribution in the galactic frame, $f(v)$, through

$$f_\oplus(\vec{v}, t) = f(|\vec{v} + \vec{v}_\oplus(t)|)\,. \tag{2.9}$$

Here $\vec{v}_\oplus(t)$ is the relative motion of the Earth with respect to the galactic frame. It is given by

$$\vec{v}_\oplus(t) = \vec{v}_\odot + V_\oplus \left[\hat{\varepsilon}_1 \cos\omega(t - t_1) + \hat{\varepsilon}_2 \sin\omega(t - t_1) \right] \tag{2.10}$$

where $\vec{v}_\odot$ is the velocity of the Sun, $V_\oplus = 29.8\,\mathrm{km/\,sec}$ is the Earth orbital speed, $\omega = 2\pi/\,\mathrm{yr}$, $t_1 = 0.218\,\mathrm{yr}$ = March 21 is the time of the spring equinox, $\hat{\varepsilon}_1$ and $\hat{\varepsilon}_2$ are the orthogonal direction versors of the Earth at spring equinox and summer solstice (at $t_1 +\, \mathrm{yr}/4$). In Galactic coordinates (defined in section 2.2.1) one has

$$\begin{aligned}
\hat{\varepsilon}_1 &= (0.9931, 0.1170, -0.0103) && (2.11)\\
\hat{\varepsilon}_2 &= (-0.0670, 0.4927, -0.8676). && (2.12)
\end{aligned}$$

Consequently the modulus of the Earth velocity is

$$v_\oplus(t) = \sqrt{v_\odot^2 + V_\oplus^2 + 2bv_\odot V_\oplus \cos[\omega(t - t_c)]} \simeq v_\odot + \frac{V_\oplus^2}{2v_\odot} + bV_\oplus \cos[\omega(t - t_c)] \tag{2.13}$$

where

$$b = \frac{\sqrt{(\hat{\varepsilon}_1 \cdot \vec{v}_\odot)^2 + (\hat{\varepsilon}_2 \cdot \vec{v}_\odot)^2}}{v_\odot} \approx 0.490 \tag{2.14}$$

is the sine of the angle between $\vec{v}_\odot$ and the normal to the orbital plane of the Earth, and

$$t_c = t_1 + \frac{1}{\omega} \arctan \frac{\hat{\varepsilon}_2 \cdot \vec{v}_\odot}{\hat{\varepsilon}_1 \cdot \vec{v}_\odot} \approx 0.415\,\mathrm{yr} = \text{June 2} \tag{2.15}$$

is the time at which $v_\oplus(t)$ is maximal, $v_\oplus(t_1) \approx 249\,\mathrm{km/\,sec}$. The minimal Earth velocity is $v_\oplus(t_1 +\, \mathrm{yr}/2) \approx 220\,\mathrm{km/\,sec}$.

Chapter 3

Energy spectra of cosmic rays from DM, at production

In this chapter we discuss the production of the spectra of cosmic rays from DM annihilations and decays in the Galaxy. A special section (sec. 3.3) is dedicated to neutrino fluxes from the center of the Sun, as they have a completely different production history.

3.1 Introduction and method

We consider (see [1]) DM annihilations (parameterized by the DM DM cross section σv) and decays (described by the DM decay rate $\Gamma = 1/\tau$) into the following primary channels:

$$
\begin{aligned}
&e^+_L e^-_L,\ e^+_R e^-_R,\ \mu^+_L \mu^-_L,\ \mu^+_R \mu^-_R,\ \tau^+_L \tau^-_L,\ \tau^+_R \tau^-_R,\\
&q\bar{q},\ c\bar{c},\ b\bar{b},\ t\bar{t},\ \gamma\gamma,\ gg,\\
&W^+_L W^-_L,\ W^+_T W^-_T,\ Z_L Z_L,\ Z_T Z_T,\\
&hh,\\
&\nu_e\bar{\nu}_e,\ \nu_\mu\bar{\nu}_\mu,\ \nu_\tau\bar{\nu}_\tau,\\
&VV \to 4e,\ VV \to 4\mu,\ VV \to 4\tau,
\end{aligned}
\tag{3.1}
$$

where $q = u, d, s$ denotes a light quark and h is the Standard Model Higgs boson, with a mass fixed at 125 GeV. The last three channels denote models in which the annihilation or decay first happens into some new (light) boson V which then decays into a pair of leptons, along the lines of the models inspired by the charged cosmic ray excesses in Pamela, Fermi, Hess, Ams-02 etc (see chapter 5). The subscripts L and R on the leptonic channels refer to their left and right polarization, while the L and T on the vector boson ones refer to their longitudinal and transverse polarizations. It is important to distinguish such polarizations for the purposes of electroweak radiation, which we will discuss shortly below. Of course, the corresponding unpolarized channels can be recovered by means of the following averages:

$$
e^+e^- = \frac{e^+_L e^-_L + e^+_R e^-_R}{2}, \qquad W^+W^- = \frac{2\,W^+_T W^-_T + W^+_L W^-_L}{3}.
$$

Our approach here is to consider all the channels in eq. (3.1) on equal footing, in a manner which is completely independent of the DM model. In any given model, annihilation or decay branching ratios into the specific channels will instead be dictated by the underlying theory. Some channels (such as $\gamma\gamma$, $\nu\bar{\nu}$, gg) are 'unusual' as they are often suppressed in many models, but from a model-independent point of view they are as viable as any other, so that we shall include them and discuss them further below. Operationally, as discussed e.g. in [2], s-wave non-relativistic DM DM annihilation can be seen as equivalent to the decay of a $\mathscr{D}$ resonance with mass $M_{\mathscr{D}} = 2M_{\rm DM}$, where $M_{\rm DM}$ is the DM particle mass. Decays of $\mathscr{D}$ into any pair of Standard Model (SM) particles can therefore be computed and implemented in Monte Carlo generators.

These primary particles undergo parton showers and hadronization, in such a way to produce fluxes of $e^\pm, \bar{p}, \bar{d}, \gamma, \overset{(-)}{\nu}_{e,\mu,\tau}$. This process is followed in most DM studies with the use of Monte Carlo simulation programs. Pythia (version 8.135), is the one on which we base the results presented here (with the exception of neutrinos from the center of the Sun, see section 3.3). Other MonteCarlo codes can be used to perform the computation of the spectra at production. In particular [1] has investigated the differences using Herwig (version 6.510). In fact, the algorithms implemented in Herwig and Pythia are quite different, in both parton showers and hadronization. A detailed comparison for the different channels and spectra is beyond my current scope. Overall, the uncertainty connected with the numerical tools can be estimated to be of the order of 20%, although larger discrepancies can appear in some specific cases.

However, in its current version, Pythia's parton showering algorithms include gluon and photon radiation, but not the emissions of W's and Z's, which is called collectively ElectroWeak bremsstrahlung.

3.1.1 Inclusion of ElectroWeak radiation

Electroweak radiation effects have been recognized as relevant for the purposes of DM indirect detection only relatively recently [49]. At large DM masses, such bremsstrahlung corrections are enhanced by one or more powers of $\ln(M_{\rm DM}/M_W)$ logarithms, which become large for $M_{\rm DM} \gg M_W$, compensating the suppression due to the additional weak coupling.

Phenomenologically, electroweak radiation effects can be particularly relevant for the leptonic and $\gamma\gamma$ channels. In fact, the emission of W's and Z's yields to further hadrons in the final state, and therefore it significantly modifies the flux of γ's and $e^\pm$ at energies $E \ll M$, M being the DM mass. Moreover, W/Z radiation leads to a $\bar{p}$ contribution, which is instead absent if weak corrections are neglected; this is also true for the the neutrino channels, that thereby also give $e^\pm$'s, γ's and $\bar{p}$'s.

We therefore include electroweak bremsstrahlung (at leading order in the electroweak couplings) by 'post-processing' the output of the MonteCarlo. We refer to [50] for a dedicated discussion and a detailed presentation of the computational techniques. The enhanced terms are model-independent: in the numerical results presented here they have been turned on abruptly when $M_{\rm DM} \gtrsim M_W$. In a full DM model, these effects would actually appear in a smooth model-dependent way when increasing the DM mass.The finite non-logarithmic terms, that cannot be computed in a model-independent way, have instead been neglected.

3.1.2 Comments on some specific channels

The annihilation into SM Higgs, tau, photon and gluon pairs deserves a few comments.

hh. A particle very consistent with the SM Higgs boson has been discovered recently (see [51] in case you have been on Mars lately) and we include the corresponding channel in the list of possible annihilations. On the other hand, the detailed properties of such a particle are obviously still under very active investigation, so that we have to make some guesses/assumptions. For its mass, we assume $m_h = 125$ GeV. For its branching ratios, we take those predicted by the Standard Model and embedded in the MonteCarlo codes. The values in Herwig and Pythia can differ by up to 25% for a light higgs: Herwig has a slightly smaller BR into WW and ZZ with respect to Pythia, while it has has a slightly larger BR into $b\bar{b}$. Such discrepancies are due to the different accuracy which is used to compute the partial widths (see, e.g., [52]). For example, in the decays into WW/ZZ Pythia allows both vector bosons to be off-shell, whereas in Herwig at least one is forced to be on-shell. In the rate of $h \to b\bar{b}$ processes, Herwig includes also the resummation of mass logarithms $\sim \alpha_S^n(m_h^2)\ln^n(m_h/m_b)$, which are not resummed in Pythia. Hereafter, we shall stick to the default branching fractions for the two codes. We stress that the mentioned branching ratios are obtained for the Standard Model Higgs boson and that, Beyond the Standard Model, the Higgs decay fractions will clearly be different. Should the investigations at the LHC highlight a non-SM behavior of the h particle, these assumptions will clearly have to be revised.
$\boldsymbol{\tau^+\tau^-}$**.** As for τ leptons, Herwig and Pythia treat them as unpolarized and implement the Standard Model three-body decay matrix elements. Alternatively, the two Monte Carlo codes could be interfaced with the Tauola package [55], which fully includes polarization effects and implements several lepton and hadron decay modes, by means of hadronic matrix elements. In the following, we shall nonetheless use the standard routines even for the purpose of τ decays and subsequent showers and hadronization. In fact, this is a reasonable approximation for the observables which we shall investigate, namely the hadron/lepton/photon energy fraction in the Dark Matter rest frame and averaged over many, many events. A remarkable impact of the inclusion of the τ polarization should instead be expected if one looked at other quantities, such as angular correlations between the τ decay products from the same event.
$\boldsymbol{\gamma\gamma}$**.** We include $\gamma\gamma$ as a primary channel: Dark Matter, being dark, has no tree-level coupling to photons, but $\gamma\gamma$ production can occur at one loop. This is not to be confused with photons emitted by charged particles or produced in three-body annihilations or radiative hadron decays, such as $\pi^0 \to \gamma\gamma$. Photons in final-state showers or hadron decays are of course included in the fluxes yielded by Herwig and Pythia. Including instead DM annihilation into three-body final states would require a specific model of Dark Matter (see e.g. [56, 57]), whereas in this work we shall stick to model-independent results.
gg. Neglecting the case of colored Dark Matter, the DM DM $\to gg$ mode can also take place only at one loop. In the Monte Carlo codes which will be employed later on, we shall implement the $\mathscr{D} \to gg$ decay in the same fashion as $h \to gg$, i.e. with an effective $\mathscr{D}gg$ vertex, assuming that DM is color neutral.

3.2 Results

In fig. 3.1 we present some examples of the spectra produced by the annihilation of two DM particles with mass $M_{\rm DM}$ (normalized per annihilation), for four values of $M_{\rm DM}$. They correspond to the fluxes from the decay of a DM particle with mass $2M_{\rm DM}$.

Some specifications on these fluxes are in order.
About γ ray fluxes: We specify that of course the fluxes here include only the prompt emission and

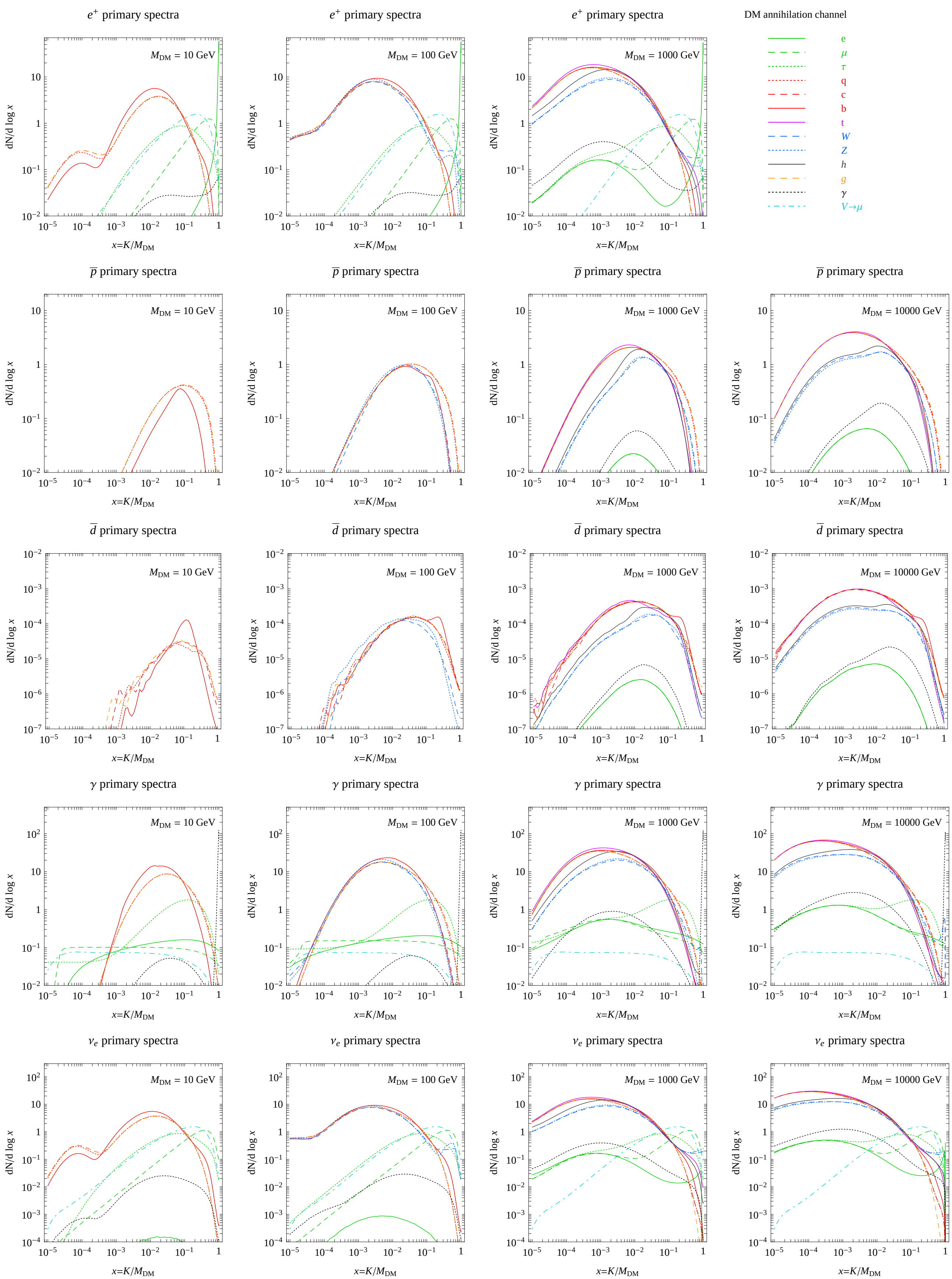

Figure 3.1: ***Primary fluxes*** *of* $e^{\pm}$, $\bar{p}$, $\bar{d}$, γ *and* ν_e.

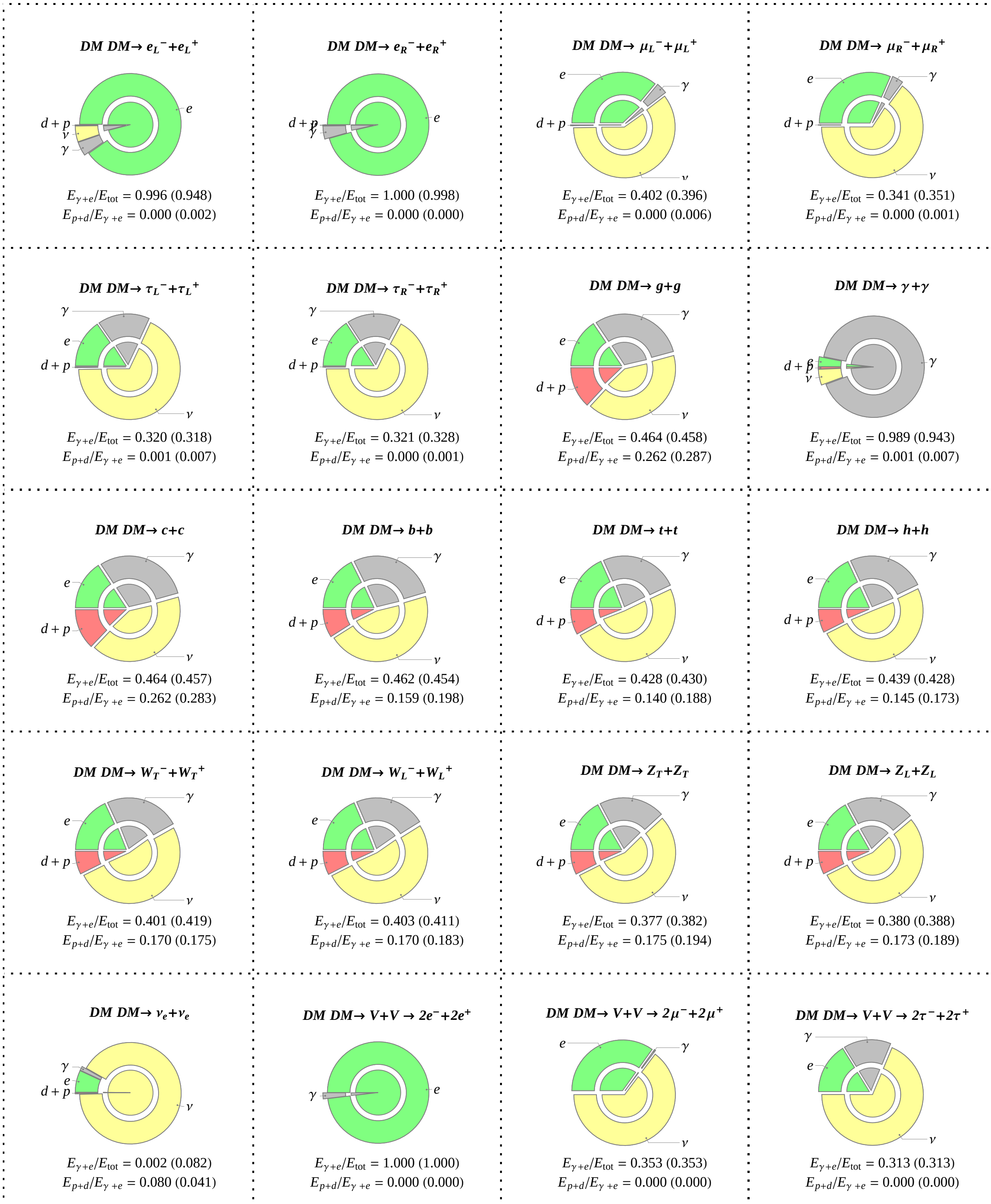

Figure 3.2: ***Energy distribution between the final states particles***: *$e^\pm$, hadrons $(p+d)$, γ and ν, for a set of characteristic annihilation channels. The inner (outer) pie refers to a DM mass of 200 GeV (5 TeV). For each pie chart, the first caption gives the energy fraction going into γ and $e^\pm$ $(E_{\gamma+e})$ with respect to the total. The second caption gives the energy fraction into hadronic final states (E_{p+d}) with respect to γ and $e^\pm$.*

not the secondary radiation (e.g. due to Inverse Compton processes) that we discuss in Sec. 4.5.1. Furthermore, we recall that by 'prompt emission' we here mean all photons in final-state showers or hadron decays as given by PYTHIA, including those from (IR-enhanced model-independent) QED and EW bremsstrahlung as discussed above and in [50]. But further contributions to prompt emission can come from other three-body final states such as *internal* bremsstrahlung [56, 57]: these can only be computed in the framework of a precise DM model because one needs to know the higher order QED annihilation/decay diagram. These are not included.
About fluxes of anti-deuterons: They are computed taking into account the jet structure of the annihilation products. The yield scales with the cube of the uncertain coalescence parameter, here fixed to $p_0 = 160\,\mathrm{MeV}$; for details on the computation we refer the reader to [58].
About fluxes of neutrinos and anti-neutrinos: Those that we provide here are of course the neutrino spectra at production; the corresponding fluxes at detection are affected by oscillations (if travelling in vacuum, such as for neutrinos from DM annihilations/decays at the Galactic Center) and/or by interactions with matter (if e.g. from DM annihilations/decays in the center of the Sun). The fluxes at detection of neutrinos having traveled in vacuum from a distant astrophysical source can be obtained taking into account average oscillations with the formula

$$P(\nu_\ell \to \nu_{\ell'}) = P(\bar\nu_\ell \to \bar\nu_{\ell'}) = \sum_{i=1}^{3} |V_{\ell i} V_{\ell' i}|^2 \approx \begin{pmatrix} 0.6 & 0.2 & 0.2 \\ 0.2 & 0.4 & 0.4 \\ 0.2 & 0.4 & 0.4 \end{pmatrix} \tag{3.2}$$

where i runs over neutrino mass eigenstates, and the elements $|V_{\ell i}|$ of the neutrino mixing matrix can depend on its unknown CP-violating phases. The case of neutrinos from the center of the Sun is more complicated and is discussed separately in sec. 3.3.

To conclude this quantitative presentation of the DM fluxes, in fig. 3.2 we show some characteristic energy distributions between the final-states particles: $e^\pm$, hadrons $(p+d)$, γ and ν. The inner pie refers to a DM mass of 200 GeV (a typical SuSy WIMP value) while the outer pie to 5 TeV (taken as a typical multi-TeV case). One can see that the portion of energy which goes into gamma rays and $e^\pm$ is often the most important one and always dominates over the energy fraction of the hadronic final states for all the channels. This is especially relevant in the context of extragalactic gamma rays signatures, where the energy fraction in $e^\pm$ is quickly converted to gamma rays due to Inverse Compton radiation. For the channels involving $\mu^+\mu^-$ and $\tau^+\tau^-$ and of course for the $\nu\bar\nu$ channels, the portion of energy carried away by neutrinos becomes the dominant one. The fractions are rather independent of the mass of the DM particle, with some exceptions. For example, in the $\nu\nu$ channels, primary neutrinos start to radiate gamma rays and charged leptons due to radiative weak corrections when $M_{\rm DM}$ is above the electroweak scale (i.e. for the outer pie in the figure) and this increases the energy fraction of γ and $e^\pm$.

3.3 Neutrinos from the center of the Sun

The Dark Matter (DM) particles that constitute the halo of the Milky Way have a small but finite probability of scattering with a nucleus of a massive celestial body like the Sun if their orbit passes through it. If their velocity after the scattering is smaller than the escape velocity from that body, they become gravitationally bound and start orbiting around the body. Upon additional scatterings, they eventually sink into the center of the body and accumulate, building up a local DM overdensity concentrated in a relatively small volume. There they annihilate into Standard

Model particles, giving origin to fluxes of energetic neutrinos [59]. These neutrinos are the only species that can emerge, after experiencing oscillations and interactions in the dense matter of the astrophysical body. The detection of high-energy neutrinos from the center of the Sun, on top of the much lower energy neutrino flux due to nuclear fusion or radioactive processes, would arguably constitute one of the best proverbial smoking guns for DM, as there are no known astrophysical processes able to mimic it (except possibly for the flux of neutrinos produced in the atmosphere of the Sun, which however are expected to have a different spectral shape [60]). It is therefore worthwhile to compute the expected yield and the expected spectra of such neutrino fluxes, in terms of the usual primary DM properties such as the mass and the annihilation channel. With respect to those presented in the previous section, however, the computation here is made more complex by the fact that the annihilations occur in a very dense medium, that affects significantly the hadronization and showering process. Also, the produced neutrinos are subject to oscillations (in matter and in vacuum) and interactions with matter along their journey to the Earth. In this section we will address the computation of the fluxes at production while in sec. 4.6 we will discuss their propagation.

GEANT4 is a toolkit for the simulation of the passage of particles through matter [61], a very suitable tool for modeling cascades in the environment of the solar core. Following the approach of [62, 63], we couple it to PYTHIA in the following sense. Hadronization of the quarks and gluons produced by DM annihilations is performed by PYTHIA; the stable and metastable hadronization products (e, $\nu_{e,\mu,\tau}$, μ, K_{L0}, π, K, n, p, $N_{\rm D,He}$) are injected into GEANT4 which adds the effect of particle/matter interactions. We model the matter around the solar core following the Solar Standard Model, but with a simplified chemical composition (we just include 74.7 % by mass of H and 25.3 % of He). In our GEANT4 code, we consider a sphere with radius of 1 km, that is big enough for our purposes: we verified that only neutrinos from the cascades can reach its surface, while secondary products are contained.

Fig. 3.3 presents, for reference, an example of our final results for the neutrino spectra at production [3]. We plot the spectra of ν (first column) and $\bar{\nu}$ (second column) for all the channels that we consider for a sample DM mass of 1 TeV. The spectra are normalized per one annihilation of two DM particles. The considered range of $x = E/M_{\rm DM}$ covers from 10^{-8} to 1. In the third column we zoom on the high energy part, relevant for neutrino detectors such as ICECUBE.

In very general terms, moving from low to high $x = E/M_{\rm DM}$, the obtained spectra are characterized by some very pronounced low energy humps or spikes, an intermediate energy smooth shoulder and, for some channels, a high energy peak. These features are easily understood.

- The high energy peak occurs when DM annihilate into particles that directly decay into neutrinos. This is visible in the W^+W^-or ZZ channel. For large DM masses, i.e. for large boosts of the primary W and Z, this feature smears into a smooth spectrum.

- The smooth component of the spectrum arises from the neutrinos produced in the cascading event by primary and secondary particles (hadrons and leptons), that lose energy and rapidly decay.

- The low energy humps and spikes essentially arise from relatively long-lived particles that have been stopped in solar matter and then decay, essentially at rest. More precisely, recalling that n, π^-, μ^- and K^- are mostly absorbed or captured by matter, the low energy neutrino peaks arise from the following processes:

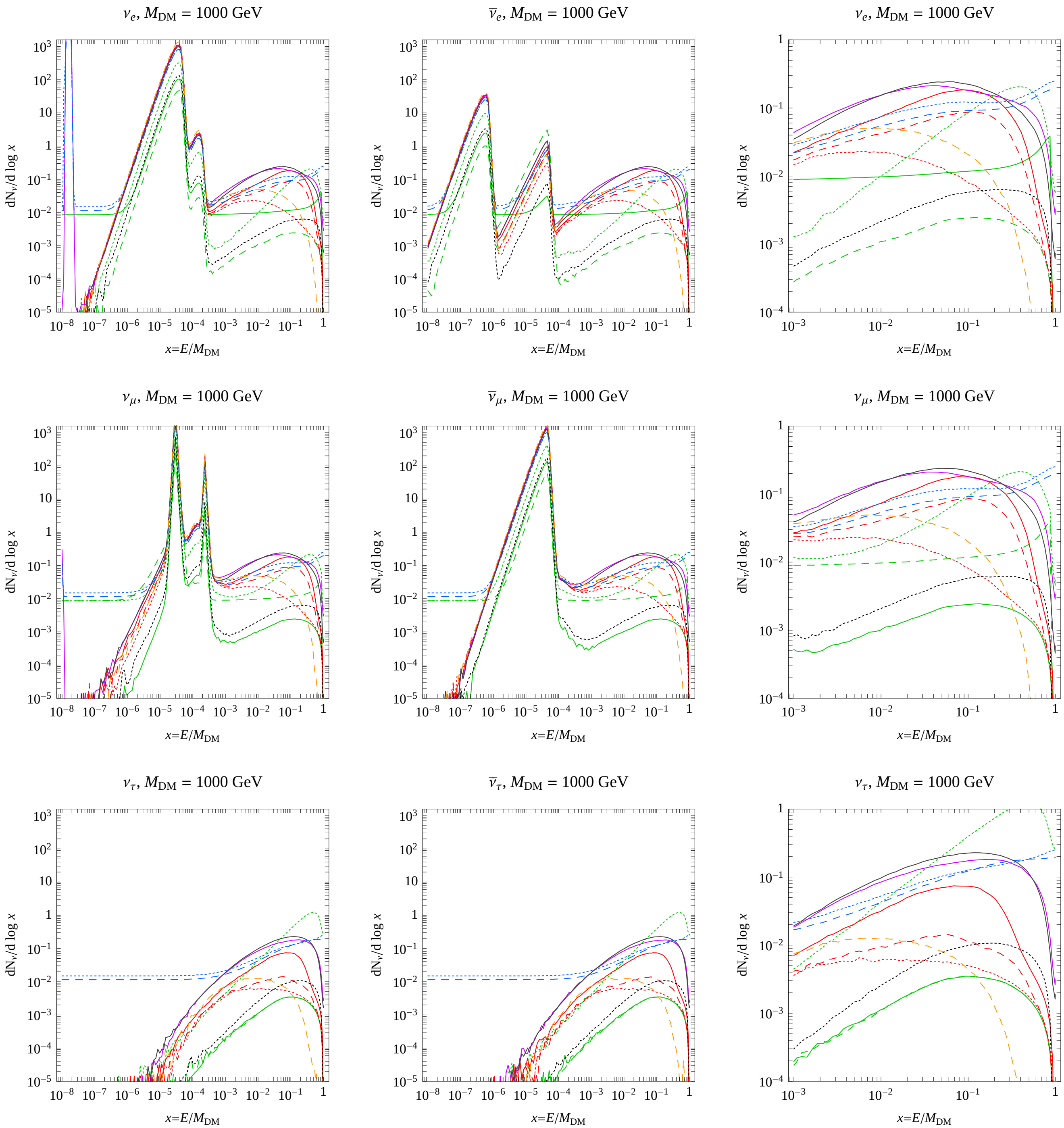

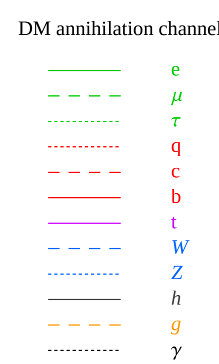

Figure 3.3: *Final results for the* ***neutrino spectra at production****, including all effects (in particular ElectroWeak corrections). Left column: neutrino spectra. Central column: antineutrino spectra. Right column: zoom on the high energy portion of the neutrino spectra. Upper row: e flavor; middle row: μ flavor; bottom row: τ flavor.*

- $\pi^+ \to \mu^+\nu_\mu$ decays, which produce a monochromatic line in the ν_μ spectra, at $E_\nu = 29.8\,\text{MeV}$. For numerical reasons we artificially broaden it.
- $\mu^+ \to \bar{\nu}_\mu\nu_e e^+$ decays, which contribute to the $\nu_e, \bar{\nu}_\mu$ energy spectra producing the typical three body decay bump with an end-point at $m_\mu/2 \approx 53\,\text{MeV}$ and peaked at $E \approx m_\mu/3 \approx 35\,\text{MeV}$.
- $\mu^- \to \nu_\mu\bar{\nu}_e e^-$ decays, which similarly contribute to the $\bar{\nu}_e, \nu_\mu$ energy spectra, although the resulting bump is about two orders of magnitude less intense than the bump in $\nu_e, \bar{\nu}_\mu$. Indeed π^- are absorbed by matter before decaying into μ^-.
- K^+ decays with 63% branching fraction into a monochromatic ν_μ at $E_\nu = 240\,\text{MeV}$. Three body decays have smaller branching ratios (5.1% BR into $\pi^0\ e^+\ \nu_e$ and 3.4% BR into $\pi^0\ \mu^+\ \nu_\mu$) producing bumps below about $m_K/2 \approx 250\,\text{MeV}$.
- K^- get absorbed, synthesised by nuclei into a Λ which decays into nucleons and pions. Their rare free decays negligibly affect the neutrino spectra.
- Decays of K_L^0 into neutrinos are blocked by matter effects that break the quantum coherence between K_S^0 and K_L^0, such that K_S^0 are continuously regenerated and quickly decay hadronically.

These spectra also include the effect of ElectroWeak radiations, added on top of the GEANT computation as discussed in the analogous case of sec. 3.1.1. In fig. 3.3 this is visible in the low energy plateaux and in the fact that, for instance, the spectrum for the e channel extends to $x = 1$ (in absence of EW radiation, the process DM DM $\to e^+e^-$ would not produce any neutrino except the low energy ones from the stopping of light leptons and hadrons in the matter cascade).

These spectra will then have to be propagated through the matter of the Sun, the vacuum and the matter of the Earth as we will discuss in sec. 4.6.

Chapter 4

Computation of the propagation and thus the observable CR fluxes at Earth

Having at disposal the energy spectra of charged particles, gamma rays and neutrinos per annihilation at production, as generated by MonteCarlos and as discussed in the previous chapter, we next need to consider where these fluxes of particles are produced (essentially everywhere in the galactic halo for what concerns charged species, but also in specific sources such as the Galactic Center or the center of the Sun for gamma rays or neutrinos) and how they propagate to the Earth.

For simplicity, we start by presenting separately the propagation formalism for electrons or positrons, for antiprotons, for antideuterons and antihelium nuclei. In these latter two cases, only a few trivial changes have to be implemented with respect to antiprotons, as we discuss below. We then move to discuss gamma rays and neutrinos.

4.1 Propagation of electrons and positrons

The differential $e^{\pm}$ flux [1] per unit of energy from DM annihilations or decays in any point in space $\vec{x}$ and time t is given by $d\Phi_{e^{\pm}}/dE\,(t,\vec{x},E) = v_{e^{\pm}} f/4\pi$ (units $1/\,\mathrm{GeV}\cdot\mathrm{cm}^2\cdot\mathrm{s}\cdot\mathrm{sr}$) where $v_{e^{\pm}}$ is the velocity (essentially equal to c in the regimes of our interest). The $e^{\pm}$ number density per unit energy, $f(t,\vec{x},E) = dN_{e^{\pm}}/dE$, obeys the diffusion-loss equation [64]:

$$\frac{\partial f}{\partial t} - \nabla\left(\mathcal{K}(E,\vec{x})\nabla f\right) - \frac{\partial}{\partial E}\left(b(E,\vec{x}) f\right) = Q(E,\vec{x}) \tag{4.1}$$

with diffusion coefficient function $\mathcal{K}(E,\vec{x})$ and energy loss coefficient function $b(E,\vec{x})$. They respectively describe transport through the turbulent magnetic fields and energy loss due to several processes, such as synchrotron radiation and Inverse Compton scattering (ICS) on CMB photons and on infrared or optical galactic starlight, as we discuss in more detail below. Notice that other terms would be present in a fully general diffusion-loss equation for Cosmic Rays, such as diffusive re-acceleration terms (describing the diffusion of CR particles in momentum space, due to their interactions on scattering centers that move in the Galaxy with an (Alfvén) velocity V_a) and convective terms. These are however negligible for $e^{\pm}$, see e.g. [64, 65].

[1] Notice that with the notation $e^{\pm}$ we always refer to the independent fluxes of electrons e^- or positrons e^+, which share the same formalism, and not to their sum (for which we use the notation $e^+ + e^-$ when needed) which of course differs by a trivial factor 2.

	Electrons or positrons		Antiprotons (and antideuterons)			
Model	δ	$\mathcal{K}_0$ [kpc^2/Myr]	δ	$\mathcal{K}_0$ [kpc^2/Myr]	$V_{\rm conv}$ [km/s]	L [kpc]
MIN	0.55	0.00595	0.85	0.0016	13.5	1
MED	0.70	0.0112	0.70	0.0112	12	4
MAX	0.46	0.0765	0.46	0.0765	5	15

Table 4.1: ***Propagation parameters*** *for charged particles in the Galaxy (from [74, 75]).*

Eq. (4.1) is solved in a diffusive region with the shape of a solid flat cylinder that sandwiches the galactic plane, with height $2L$ in the z direction and radius $R = 20\,\text{kpc}$ in the r direction [66]. The location of the solar system corresponds to $\vec{x} = (r_\odot, z_\odot) = (8.33\,\text{kpc}, 0)$. Boundary conditions are imposed such that the $e^\pm$ density f vanishes on the surface of the cylinder, outside of which electrons and positrons freely propagate and escape.[2] Assuming that steady state conditions hold (as it is if one assumes that the typical time scales of the DM galactic collapse and of the variation of propagation conditions are much longer than the time scale of propagation itself, of the order of 1 Myr at 100 GeV energies [68]), the first term of eq. (4.1) vanishes and the dependence on time disappears.[3]

Before illustrating the solution method, we briefly comment on the different pieces of the equation. We dedicate a special attention to the energy loss function and the processes it encodes.

First we briefly discuss the *diffusion coefficient* function $\mathcal{K}$. This is in principle dependent on the position, since the distribution of the diffusive inhomogeneities of the magnetic field changes throughout the galactic halo. However, a detailed mapping of such variations is prohibitive: e.g. they would have different features inside/outside the galactic arms as well as inside/outside the galactic disk, so that they would depend very much on poorly known local galactic geography. Moreover, including a spatial dependence in $\mathcal{K}$ would make the semi-analytic method described below much more difficult to implement numerically. We therefore leave these possible refinements aside [4] and, as customary, we adopt the parameterization $\mathcal{K}(E, \vec{x}) = \mathcal{K}_0 (E/\,\text{GeV})^\delta = \mathcal{K}_0\, \epsilon^\delta$. The values of the propagation parameters δ, K_0 and L (the height of the diffusion cylinder defined above) are deduced from a variety of cosmic ray data and modelizations. It is customary to adopt the sets presented in Table 4.1, which are found to minimize or maximize the final fluxes. [5]

Next, we discuss DM DM annihilations or DM decays in each point of the halo with DM density $\rho(\vec{x})$, which provide the *source term* Q of eq. (4.1). It reads

$$Q = \frac{1}{2}\left(\frac{\rho}{M_{\rm DM}}\right)^2 f_{\rm inj}^{\rm ann}, \qquad f_{\rm inj}^{\rm ann} = \sum_f \langle\sigma v\rangle_f \frac{dN^f_{e^\pm}}{dE} \qquad \text{(annihilation)}, \tag{4.2}$$

[2] See [67] for the impact of not neglecting the propagation outside the cylinder.

[3] A caveat on this point is that the time-independence of the diffusion process might not be justified in extreme environments such as the galactic central regions, where the propagation conditions may possibly change on a short enough time scale that they make this assumption invalid. E.g. recently the Fermi satellite has pointed out the existence of large gamma-ray structures (dubbed 'Fermi bubbles') above and below the Galactic Center [69]. A detailed modeling of the impact of these possible features on CR propagation is, for the moment, well beyond the scope of our analysis and probably of most DM related ones.

[4] See [70] for a recent analysis for antiprotons.

[5] We stress, however, that the determination of these parameters is a whole evolving research area, which will certainly update these values in the future as more refined modelizations and further CR data become available. See e.g. [71, 72, 73] for recent references. The choices presented in Table 4.1 should be seen as the current bracketing of sensible possibilities.

$$Q = \left(\frac{\rho}{M_{\rm DM}}\right) f_{\rm inj}^{\rm dec}, \qquad f_{\rm inj}^{\rm dec} = \sum_f \Gamma_f \frac{dN^f_{e^\pm}}{dE} \qquad \text{(decay)}, \tag{4.3}$$

where f runs over all the channels with $e^\pm$ in the final state, with the respective thermal averaged cross sections σv or decay rate Γ.

We now discuss in some detail the energy loss coefficient function $b(E, \vec{x})$ and its ingredients.

4.1.1 An improved energy loss function for $e^\pm$ in the Galaxy

We want here to present the computation of a 'state-of-the-art' function describing the energy losses of electrons and positrons during their propagation in the Galaxy. It includes energy losses by Coulomb interactions with the interstellar gas, by ionization of the same gas, by bremsstrahlung on the same gas, by ICS (using an updated InterStellar Radiation Field (ISRF) presented below) and by synchrotron emission, with the choice of the three magnetic field models discussed below. Schematically:

$$b_{\rm tot}(E_{e^\pm}, r, z) \equiv -\frac{{\rm d}E_{e^\pm}}{{\rm d}t} = b_{\rm Coul+ioniz} + b_{\rm brem} + b_{\rm ICS} + b_{\rm syn} \tag{4.4}$$

where $E_{e^\pm}$ is the energy of the electron or positron and r and z are cylindrical galactic coordinates. Details can be found in standard references such as [76, 77] as well as in [1, 4].

- **Energy losses by Coulomb interaction and ionization** on neutral matter are described by

$$b^{\rm neut}_{\rm Coul+ioniz}(E_{e^\pm}, r, z) = \frac{9}{4}\, c\, \sigma_{\rm T}\, m_e \sum_i n_i Z_i \left(\log\frac{E_{e^\pm}}{m_e} + \frac{2}{3}\log\frac{m_e}{\Delta E_i}\right) \tag{4.5}$$

  where c is the speed of light, $\sigma_T = 8\pi r_e^2/3$, with $r_e = \alpha_{\rm em}/m_e$, is the Thompson cross section, n_i is the number density of gas species i with atomic number Z_i and ΔE_i is its average excitation energy (it equals 15 eV for hydrogen and 41.5 eV for helium).

  On ionized matter, one has

$$b^{\rm ion}_{\rm Coul+ioniz}(E_{e^\pm}, r, z) = \frac{3}{4}\, c\, \sigma_{\rm T}\, m_e\, n_e \left(\log\frac{E_{e^\pm}}{m_e} + 2\log\frac{m_e}{E_{\rm pla}}\right) \tag{4.6}$$

  where n_e is the electron density and $E_{\rm pla} = \sqrt{4\pi\, n_e\, r_e^3}\, m_e/\alpha$ corresponds to the characteristic energy of the plasma.

  The total energy losses for Coulomb interactions and ionization processes will therefore be given by the sum of eq. (4.5) and eq. (4.6) with, respectively, the densities of ionized and neutral gas species. In both cases, energy losses are *essentially independent* on $E_{e^\pm}$, since the constant terms in the brackets are numerically dominant. The input gas maps are discussed below.

- **Energy losses by bremsstrahlung** are described by

$$b_{\rm brem}(E_{e^\pm}, r, z) = c \sum_i n_i(r, z) \int_0^{E_{e^\pm}} {\rm d}E_\gamma\, E_\gamma \frac{{\rm d}\sigma_i}{{\rm d}E_\gamma}, \tag{4.7}$$

Magnetic field configurations

Model	ref.	B_0 [μG]	R_D [kpc]	z_D [kpc]
MF1	[85]	4.78	10	2
MF2	[82, 86]	5.1	8.5	1
MF3	[89]	9.5	30	4

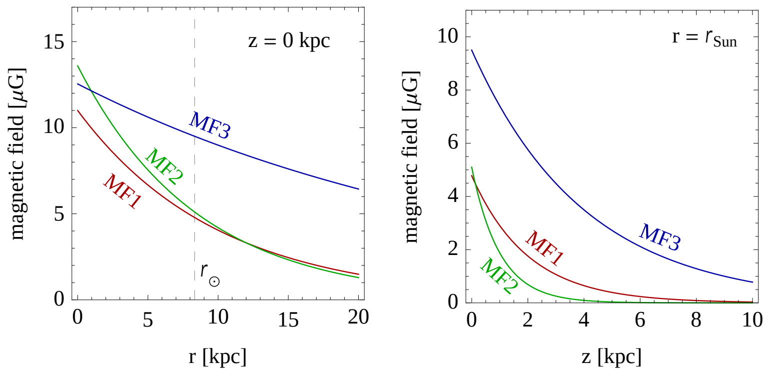

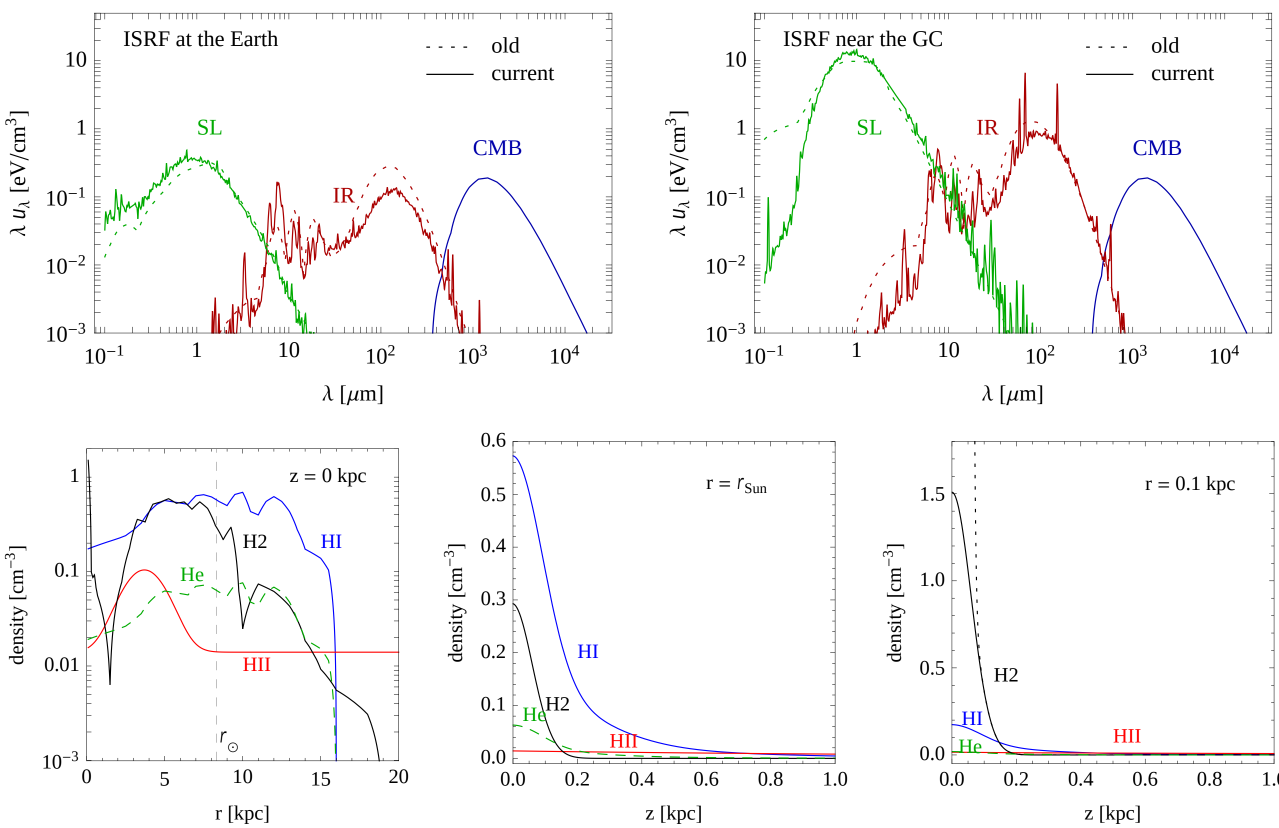

Figure 4.1: *Collection of the* ***astrophysical ingredients*** *we use. Top row: parameters of the magnetic field configurations. Middle row: illustration of the ISRF in two sample locations. Bottom row: illustration of the galactic gas densities (figure from [5]).*

where E_γ corresponds to the energy of the gamma ray emitted in each bremsstrahlung process. The differential cross-section reads

$$\frac{\mathrm{d}\sigma_i(E_{e^\pm}, E_\gamma)}{\mathrm{d}E_\gamma} = \frac{3\,\alpha_{\rm em}\sigma_T}{8\pi\,E_\gamma}\left\{\left[1+\left(1-\frac{E_\gamma}{E_{e^\pm}}\right)^2\right]\phi_1^i - \frac{2}{3}\left(1-\frac{E_\gamma}{E_{e^\pm}}\right)\phi_2^i\right\}\,, \tag{4.8}$$

where $\phi^i_{1,2}$ are scattering functions depending on the properties of the scattering system.

For a completely ionized gas plasma with charge Z one has

$$\phi_1^{\rm ion}(E_{e^\pm}, E_\gamma) = \phi_2^{\rm ion}(E_{e^\pm}, E_\gamma) = 4(Z^2+Z)\left\{\log\left[\frac{2E_{e^\pm}}{m_e\,c^2}\left(\frac{E_{e^\pm}-E_\gamma}{E_\gamma}\right)\right] - \frac{1}{2}\right\}\,, \tag{4.9}$$

and thus the energy losses in this regime ('weak shielding') read

$$b^{\rm ion}_{\rm brem} = \alpha_{\rm em}\frac{3\,\sigma_{\rm T}}{2\pi}n_i\;Z(Z+1)\left(\log\left(2\,\frac{E_{e^\pm}}{m_e}\right) - \frac{1}{3}\right)E_{e^\pm}\,. \tag{4.10}$$

On the other hand, for atomic neutral matter the scattering functions have a more complicated dependence, which is usually parameterized in terms of the quantity $\Delta = \frac{E_\gamma m_e}{4\alpha_{\rm em}E_{e^\pm}(E_{e^\pm}-E_\gamma)}$. For the relativistic regime we are interested in, since $E_{e^\pm} \gtrsim 1$ MeV always, one basically cares for the limit $\Delta \to 0$ for which these functions are constant and take the following numerical values:

$$\begin{aligned}
\phi_1^{\rm H}(\Delta=0) &\equiv \phi^{\rm H}_{1,\rm ss} = 45.79,\\
\phi_2^{\rm H}(\Delta=0) &\equiv \phi^{\rm H}_{2,\rm ss} = 44.46,\\
\phi_1^{\rm He}(\Delta=0) &\equiv \phi^{\rm He}_{1,\rm ss} = 134.60,\\
\phi_2^{\rm He}(\Delta=0) &\equiv \phi^{\rm He}_{2,\rm ss} = 131.40,\\
\phi^{\rm H_2}_{(1,2)}(\Delta=0) &\simeq 2\,\phi^{\rm H}_{(1,2),\rm ss}.
\end{aligned} \tag{4.11}$$

The subscript $_{\rm ss}$ in this notation refers to the fact that this regime is usually called 'strong-shielding' because the atomic nucleus is screened by the bound electrons and the impinging $e^\pm$ have to force the shield. In this limit the energy losses read

$$b^{\rm neut}_{\rm brem} = \alpha_{\rm em}\frac{3\,\sigma_{\rm T}}{8\pi}n_i\left(\frac{4}{3}\phi^i_{1,\rm ss} - \frac{1}{3}\phi^i_{2,\rm ss}\right)E_{e^\pm}\,. \tag{4.12}$$

The total energy losses for bremsstrahlung will therefore be given by the sum of eq. (4.10) and eq. (4.12) with, respectively, the densities of ionized and neutral gas species. In both cases, at leading order, energy losses are *linearly dependent* from $E_{e^\pm}$. A further logarithmic dependence arises for scattering in ionized medium, while a small additional energy dependence is also found in neutral medium if one accounts for the effect of finite Δ.

The input gas maps are as follows.

- **Gas maps**. We use the gas maps described in [78] and already used in [5]. They are illustrated in fig. 4.1. The relevant species are atomic (HI) and molecular (H_2) neutral hydrogen, ionized hydrogen (HII), neutral atomic helium (He) and ionized helium (which is however irrelevant for all practical purposes). These maps represent a reliable description of the coarse grained distribution of gas in the Galaxy, but miss important features at small scales. In particular, they do not take into account the regions characterized by a much higher gas density (up to 2 or 3 orders of magnitude with respect to the coarse grained maps) which are known to exist close to the galactic center (typically at $\mathbf{r} \lesssim 200$ pc scales).

- **Energy losses by Inverse Compton Scattering** are described, in their exact form, by

$$b_{\rm ICS} = 3\sigma_{\rm T} \int_0^\infty d\epsilon\, \epsilon \int_{1/4\gamma^2}^1 dq\; n(\epsilon) \frac{(4\gamma^2 - \Gamma_\epsilon)q - 1}{(1+\Gamma_\epsilon q)^3} \left[2q \ln q + q + 1 - 2q^2 + \frac{1}{2}\frac{(\Gamma_\epsilon q)^2}{1+\Gamma_\epsilon q}(1-q) \right], \tag{4.13}$$

where $n(\epsilon, r, z)$ is the number density (per unit volume and unit energy) of photons of the ISRF, with energy ϵ, $\gamma = E_{e^\pm}/m_e$ is the relativistic factor of the electrons and positrons and $\Gamma_\epsilon = 4\epsilon\gamma/m_e$.

In the Thomson limit (valid for low electron energies), it reduces to the particularly compact expression

$$b_{\rm ICS} = \frac{4\,\sigma_{\rm T}}{3\,m_e^2}\, E_{e^\pm}^2 \int_0^\infty d\epsilon\; \epsilon\; n(\epsilon, r, z) \qquad \text{[Thomson limit]}, \tag{4.14}$$

which makes the energy density in the photon bath $u_{\rm ISRF} = \int d\epsilon\, \epsilon\, n(\epsilon, r, z)$ apparent.

The ICS energy losses are *proportional to* $E_{e^\pm}^2$ (as evident in the Thomson expression, but also in eq. (4.13) noting that $4\gamma^2 q$ is the dominant piece at the numerator) for small $E_{e^\pm}$. For large $E_{e^\pm}$, the dependence softens.

- ○ **InterStellar Radiation Field** (ISRF). A detailed description of the radiation field against which electrons and positrons scatter in the ICS process is important in order to reliably compute the energy losses. We adopt the latest radiation maps extracted from Galprop. These replace the ones formerly used in the literature, and in particular in [1]. In fig. 4.1 we draw the two maps in two sample locations (at the Earth and near the galactic center) and compare them. One clearly sees the 3 different components (StarLight SL, InfraRed IR and the CMB blackbody spectrum). The current map is much more detailed and normalization differences of the order of a factor 2 are visible, but the overall behavior is confirmed. We will see that these small differences have a (equally small) impact on the observables entering $e^\pm$ propagation.

- **Energy losses by synchrotron emission** are described by

$$b_{\rm syn} = \frac{4\,\sigma_{\rm T}}{3\,m_e}\, E_{e^\pm}^2\, \frac{B^2}{8\pi} \tag{4.15}$$

where B is the strength of the magnetic field, discussed below. This formula is in close analogy to the one for ICS losses: the integral term in (4.14) and the B^2 term in (4.15) correspond to the energy density in the photon bath and in the magnetic field respectively. In particular, synchrotron energy losses are also *proportional to* $E_{e^\pm}^2$.

- ○ **Galactic magnetic field** Our Galaxy has a complicated magnetic field structure, and dedicated efforts by several groups have been performed in order to map it: for some recent overviews and sets of references see for instance [79, 80, 81]. We here recall the salient features of the inferred magnetic field and then define the simplified functional form that we will adopt.

The total galactic magnetic field $\vec{B}_{\rm tot}$ is the sum of a regular $\vec{B}_{\rm reg}$ and a turbulent $\vec{B}_{\rm turb}$ component. The regular field, in turn, can be decomposed in a disk $\vec{B}^{\rm disk}_{\rm reg}$ and a halo $\vec{B}^{\rm halo}_{\rm reg}$ contribution. Several observational techniques are employed to map the different components. The regular magnetic field is caused by dynamo effects in the galaxy and their direction can be determined by Faraday rotation measurements of the signals from nearby pulsar and high latitude radio sources, or by measurements of the polarized synchrotron intensity. On the other hand, the turbulent (random) magnetic fields are tangled by turbulent gas flows and can be traced looking for their unpolarized synchrotron emission. In addition, the distribution of cosmic-ray electrons and their induced γ-rays are other tools that allow to test the modeling of magnetic field. For instance, a complete model has been recently proposed in [82].

Rather than the detailed magnetic field geography, the overall intensity is more important for the purposes of DM indirect detection. In general terms, in spiral galaxies, like ours, the strength of the total magnetic field is expected to be of the order of 10 μG $-$ 1 mG and to follow the spiral pattern [83]. Radio-faint galaxies, like our neighbor Andromeda (M31) have instead weaker fields $\sim 5\mu G$. In the Milky Way, measurements point to a value around 6 μG at the position of the Sun and an increase to $20-40$ μG close to the Galactic Center [84]. In addition, despite the spiral pattern, a magnetic field reversal is present at the Sun's radius.

While we keep in mind that the complicated cartography sketched above can have an impact on the determination of the synchrotron emission from DM, we choose to model the disk field strength by a double exponential in z and in r, as proposed e.g. by [85] and [86] for the radial part, neglecting the halo component.

$$B_{\rm tot} = B_0 \exp\left(-\frac{R-R_\odot}{R_D} - \frac{|z|}{z_D}\right) \tag{4.16}$$

We then adopt several configurations for the values for the parameters B_0, R_D and z_D, as shown in the table in fig. 4.1:

- Model 1 (MF1 for "Magnetic Field 1" hereafter) is the configuration used in [1] and very similar to the one used in the original GALPROP code (it differs by the normalization factor B_0, which has changed a few times in the GALPROP literature [85, 87, 88]).
- Model 2 ("MF2") is loosely based of the findings of [82] (and previous [86]). Following one of the models in [82] we take a value of 2.1 μG for the intensity of the disk regular field at solar location (we report it to our value for $R_\odot$); we then add an intensity of 3 μG to account for the random component. The resulting field is steeper in r and in z than MF1 and reaches slightly higher values at the GC.
- Model 3 ("MF3") is modeled following [89]. It is substantially higher at the location of the Earth and has larger scale heights both in r and in z, i.e. it extends much farther out in both directions.

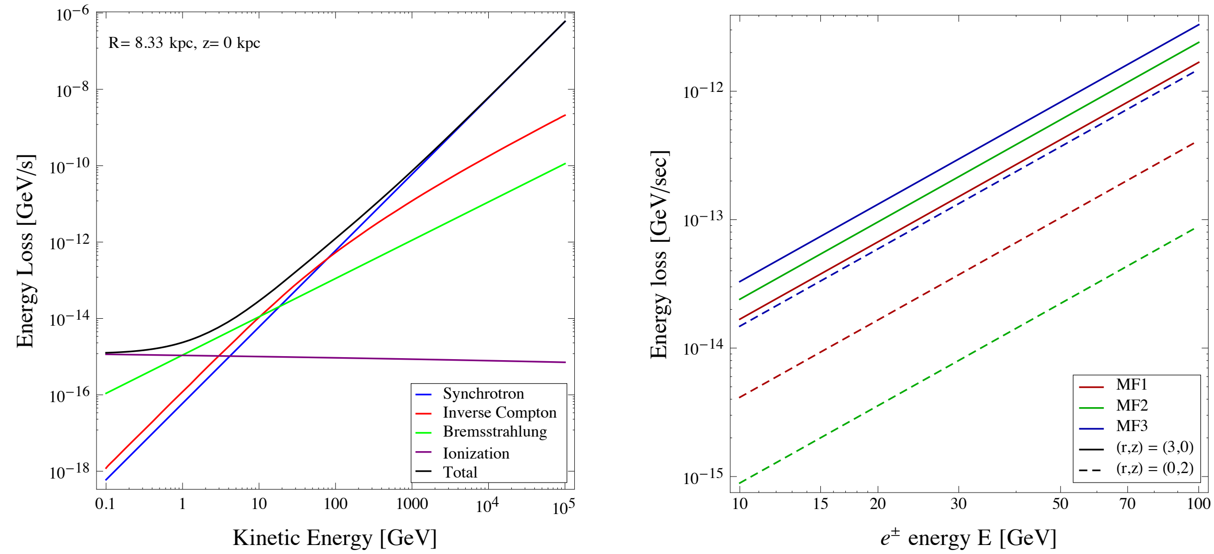

Figure 4.2: *Left panel: the* ***different processes*** *contributing to the energy loss coefficient function, at the location of the Earth. Right panel: the dependence of the energy loss coefficient function (synchrotron only) on the* ***choice of magnetic field model****, in two locations.*

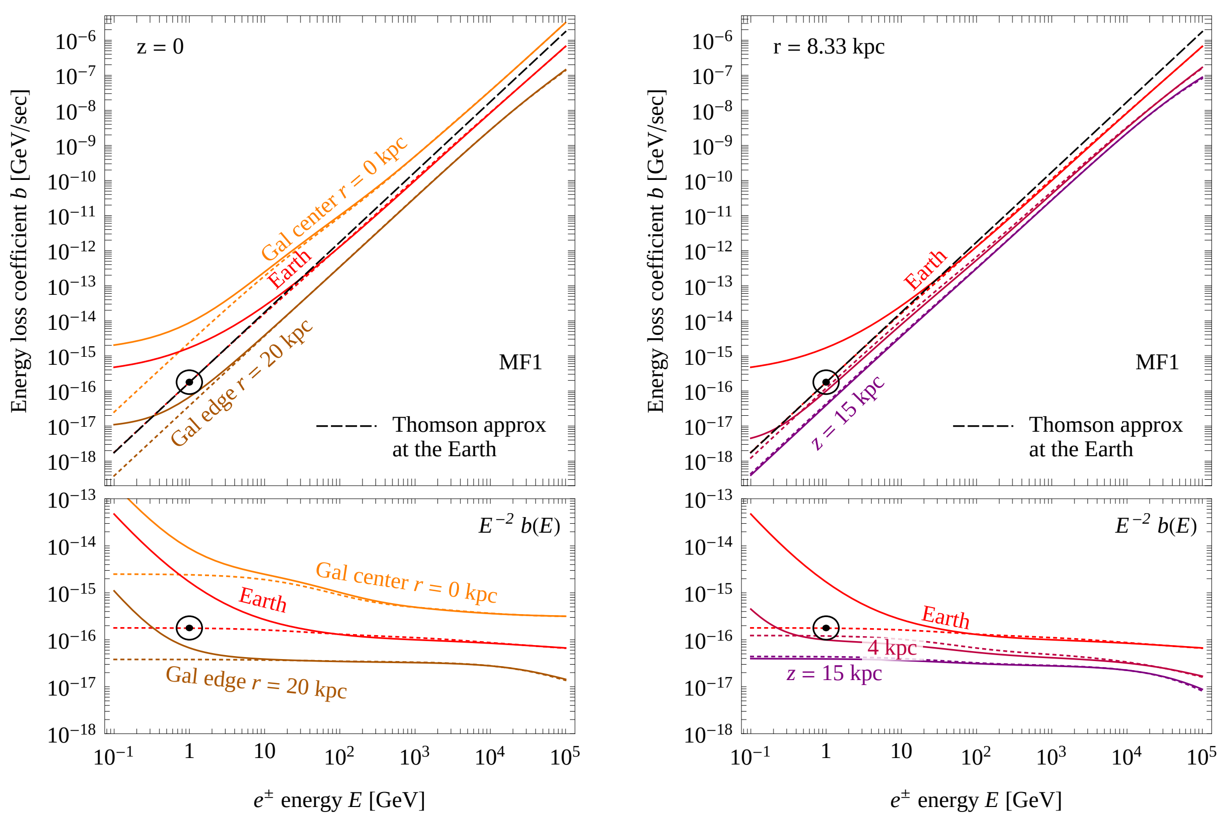

Figure 4.3: ***Energy loss coefficient function*** *for electrons and positrons in the Milky Way. Left panel: in the galactic disk ($z = 0$), at several locations along the radial coordinate r. Right panel: above (or below) the location of the Earth along the coordinate z. Here the magnetic field model MF1 has been fixed for definiteness. The circled dot identifies the constant value sometimes adopted. The dotted colored lines are the same function before the improvements listed in Sec. 4.1.1. This figure replaces the analogous one (fig. 5) of [1].*

In fig. 4.2, left panel, we plot the different energy losses discussed above, at the location of the Earth. The different dependences on the $e^{\pm}$ energy are clearly shown. Hence, the dominant process in the different energy ranges are, in order, ionization (including Coulomb), bremsstrahlung, ICS and synchrotron.

In fig. 4.3 we plot the total energy loss function in several locations in the galactic plane (left panel) and at several galactic altitudes at the location of the Earth (right panel). We compare it with the previous version of the same function not including the improvements that we are now implementing (dashed colored lines). The main modification is apparent at low energies and it is due to the inclusion of bremsstrahlung, ionization and Coulomb losses. Being related to the presence of gas, it disappears at the locations outside of the galactic disk.

The modifications due to the use of the new ISRF is minimal and mostly concentrated at low energy, so it is hidden by the dominant bremsstrahlung, ionization and Coulomb losses in most cases except well outside of the plane where the absence of gas makes it indeed visible (see the slight difference between the solid and dashed purple lines corresponding to $z = 15$ kpc in the right panel).

While in fig. 4.2 left and in fig. 4.3 we have chosen the MF1 for definiteness, in fig. 4.2 right we explore the impact of changing the magnetic field model. Not surprisingly, in the $(r, z) = (3, 0)$ kpc the synchrotron energy losses are larger than in the $(r, z) = (0, 2)$ kpc one, and the ordering reflects the intensity of the magnetic field in the corresponding model (see fig. 4.1).

4.1.2 Electrons or positrons: result

Armed with the energy loss function described in detail in the previous subsection, as well as with the other ingredients, we can write down the solution of the diffusion-loss equation (4.1) as follows. The *differential flux of* $e^{\pm}$ $d\Phi_{e^{\pm}}/dE = v_{e^{\pm}} f/4\pi$ in each given point of our Galaxy for any injection spectrum can be written as

$$\frac{d\Phi_{e^{\pm}}}{dE}(E,\vec{x}) = \frac{v_{e^{\pm}}}{4\pi\, b(E,\vec{x})} \begin{cases} \displaystyle \frac{1}{2}\left(\frac{\rho(\vec{x})}{M_{\rm DM}}\right)^2 \sum_f \langle\sigma v\rangle_f \int_E^{M_{\rm DM}} dE_{\rm s}\, \frac{dN^f_{e^{\pm}}}{dE}(E_{\rm s})\, I(E,E_{\rm s},\vec{x}) & \text{(annihilation)} \\ \displaystyle \left(\frac{\rho(\vec{x})}{M_{\rm DM}}\right) \sum_f \Gamma_f \int_E^{M_{\rm DM}/2} dE_{\rm s}\, \frac{dN^f_{e^{\pm}}}{dE}(E_{\rm s})\, I(E,E_{\rm s},\vec{x}) & \text{(decay)} \end{cases} \tag{4.17}$$

where $E_{\rm s}$ is the $e^{\pm}$ energy at production ('s' stands for 'source') and the *generalized halo functions* $I(E, E_{\rm s}, \vec{x})$ are essentially the Green functions from a source with fixed energy $E_{\rm s}$ to any energy E. In other words, the halo functions I encapsulate all the astrophysics (there is a halo function I for each choice of DM distribution profile and choice of $e^{\pm}$ propagation parameters) and are independent of the particle physics model: convoluted with the injection spectra $dN^f_{e^{\pm}}/dE$ (discussed in detail in Sec. 3), they give the final spectrum searched for. They obey $I(E, E, \vec{x}) = 1$ and $I(E, E_{\rm s}, \vec{x}) = 0$ on the boundary of the diffusion cylinder. Neglecting diffusion (i.e. setting $\mathcal{K} = 0$) one would have $I(E, E_{\rm s}, \vec{x}) = 1$. Plugged in eq. (4.17), they allow to compute the $e^{\pm}$ flux everywhere in the Galaxy.

Some examples of the functions particularized to the location of the Earth, that is: $I(E, E_{\rm s}, \vec{r}_{\odot})$, are plotted in fig. 4.4. Plugged in eq. (4.17), these allow to compute the $e^{\pm}$ flux at the location of the Earth, $\Phi(\epsilon, r_{\odot}, z_{\odot})$.

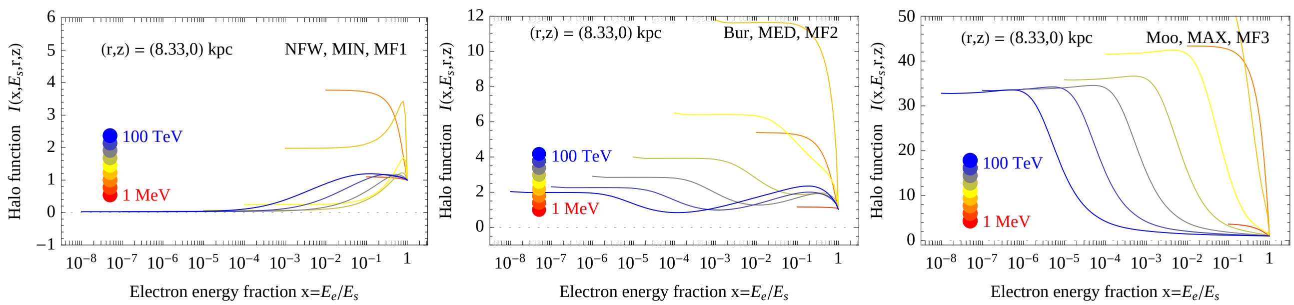

Figure 4.4: ***Generalized halo functions for electrons or positrons***, *at the location of the Earth, for several different values of the injection energy ϵ_S (color coded) and for some illustrative choices of the profile, propagation and magnetic field parameters.*

The generalized halo functions I are computed as follows. Due to numerical issues it is convenient to search for the solution of eq. (4.1) using an ansatz similar to eq. (4.17) but somewhat different:

$$f(\epsilon,\vec{x}) = \frac{1}{b_{\rm T}(\epsilon)} \begin{cases} \frac{1}{2}\left(\frac{\rho_\odot}{M_{\rm DM}}\right)^2 \int_\epsilon^{M_{\rm DM}} d\epsilon_{\rm s}\, f_{\rm inj}^{\rm ann}(\epsilon_{\rm s})\, \tilde{I}(\epsilon,\epsilon_{\rm s},\vec{x}) & \text{(annihilation)} \\ \left(\frac{\rho_\odot}{M_{\rm DM}}\right) \int_\epsilon^{M_{\rm DM}/2} d\epsilon_{\rm s}\, f_{\rm inj}^{\rm dec}(\epsilon_{\rm s})\, \tilde{I}(\epsilon,\epsilon_{\rm s},\vec{x}) & \text{(decay)} \end{cases} \tag{4.18}$$

where $\epsilon = E/\mathrm{GeV}$. Here we adopted the (arbitrary but convenient) normalizing factor $b_{\rm T}(\epsilon) = \epsilon^2\,\mathrm{GeV}/\tau_\odot$, with $\tau_\odot = \mathrm{GeV}/b(1\,\mathrm{GeV},\vec{x}_\odot) = 5.7\times 10^{15}$ sec, which is the energy loss coefficient at Earth in the Thomson limit regime. Plugging now the ansatz (4.18) in the differential equation (4.1) one can recast (4.1) into a partial differential equation for $\tilde{I}(\epsilon,\epsilon_{\rm s},\vec{x})$ (this extends the solution method first discussed (to our knowledge) in [90]). Indeed, (4.1) becomes

$$\begin{aligned} &- \quad \mathcal{K}_0\tau_\odot\epsilon^{\delta-2}\int_\epsilon^{M_{\rm DM}(M_{\rm DM}/2)} d\epsilon_{\rm s}\, f_{\rm inj}(\epsilon_{\rm s})\,\nabla^2\tilde{I}(\epsilon,\epsilon_{\rm s},\vec{x}) + \left.\frac{b(\epsilon,\vec{x})\, f_{\rm inj}(\epsilon)\tilde{I}(\epsilon,\epsilon_{\rm s},\vec{x})}{b_{\rm T}(\epsilon)}\right|_{\epsilon=\epsilon_{\rm s}} + \\ &- \quad \int_\epsilon^{M_{\rm DM}(M_{\rm DM}/2)} d\epsilon_{\rm s}\, f(\epsilon_{\rm s})\frac{\partial}{\partial\epsilon}\left(\frac{b(\epsilon,\vec{x})}{b_{\rm T}(\epsilon)}\tilde{I}(\epsilon,\epsilon_{\rm s},\vec{x})\right) = f_{\rm inj}(\epsilon)\left(\frac{\rho(\vec{x})}{\rho_\odot}\right)^\eta, \end{aligned} \tag{4.19}$$

where $\eta = 1, 2$ for decay or annihilation scenarios respectively and the upper integration limit changes accordingly. One then extracts the partial differential equation for $\tilde{I}$:

$$\nabla^2\tilde{I}(\epsilon,\epsilon_{\rm s},\vec{x}) + \frac{1}{\mathcal{K}_0\tau_\odot\epsilon^{\delta-2}}\frac{\partial}{\partial\epsilon}\left(\frac{b(\epsilon,\vec{x})}{b_{\rm T}(\epsilon)}\tilde{I}(\epsilon,\epsilon_{\rm s},\vec{x})\right) = 0, \tag{4.20}$$

with boundary conditions

$$\begin{cases} \tilde{I}(\epsilon_{\rm s},\epsilon_{\rm s},\vec{x}) = \frac{b_{\rm T}(\epsilon_{\rm s})}{b(\epsilon_{\rm s},\vec{x})}\left(\frac{\rho(\vec{x})}{\rho_\odot}\right)^\eta, \\ \tilde{I}(\epsilon,\epsilon_{\rm s},\vec{x}_{\rm max}) = 0, \quad \text{with } \vec{x}_{\rm max} \equiv (R, L). \end{cases} \tag{4.21}$$

Finally the halo functions with the normalization conventions of eq. (4.17) are obtained as

$$I(E,E_{\rm s},\vec{x}) = \tilde{I}(\epsilon,\epsilon_{\rm s},\vec{x})\left[\frac{b_{\rm T}(\epsilon)}{b(\epsilon,\vec{x})}\left(\frac{\rho(\vec{x})}{\rho_\odot}\right)^\eta\right]^{-1}, \tag{4.22}$$

Solving numerically eq. (4.20) with (4.21) allows to compute the $\tilde{I}(\epsilon, \epsilon_{\rm s}, \vec{x})$ and in turn the $I(\epsilon, \epsilon_{\rm s}, \vec{x})$.

4.2 Propagation of antiprotons

The propagation of antiprotons through the galaxy is described by a diffusion equation analogous to the one for positrons and electrons. Again, the number density of antiprotons per unit energy $f(t, \vec{x}, K) = dN_{\bar{p}}/dK$ vanishes on the surface of the cylinder at $z = \pm L$ and $r = R$. $K = E - m_p$ is the $\bar{p}$ kinetic energy, conveniently used instead of the total energy E (a distinction which is of course not particularly relevant when one looks at fluxes originating from TeV-scale DM, i.e. at energies much larger than the proton mass m_p, but important for the low energy tails and in the case of small DM masses). Since $m_p \gg m_e$ one can neglect the energy loss term that was instead important for electrons/positrons. But new terms appear in the diffusion equation for f, which reads

$$\frac{\partial f}{\partial t} - \mathcal{K}(K) \cdot \nabla^2 f + \frac{\partial}{\partial z} \left(\mathrm{sign}(z)\, f\, V_{\rm conv}\right) = Q - 2h\, \delta(z)\, (\Gamma_{\rm ann} + \Gamma_{\rm non-ann}) f, \tag{4.23}$$

where:

- The pure *diffusion term* can again be written as $\mathcal{K}(K) = \mathcal{K}_0 \beta\, (p/\,\mathrm{GeV})^\delta$, where $p = (K^2 + 2m_p K)^{1/2}$ and $\beta = v_{\bar{p}}/c = \left(1 - m_p^2/(K + m_p)^2\right)^{1/2}$ are the antiproton momentum and velocity. δ and $\mathcal{K}_0$ are given in Table 4.1.

- The $V_{\rm conv}$ term corresponds to a *convective wind*, assumed to be constant and directed outward from the galactic plane, that tends to push away $\bar{p}$ with energy $T \lesssim 10\, m_p$. Its value is given in Table 4.1.

- The *source term* Q due to DM DM annihilations or DM decay has a form fully analogous to eq. (4.2) or (4.3), with E now formally replaced by K.

- The first part of the last term in eq. (4.23) describes the annihilations of $\bar{p}$ on interstellar protons in the galactic plane (with a thickness of $h = 0.1\,\mathrm{kpc} \ll L$) with rate $\Gamma_{\rm ann} = (n_{\rm H} + 4^{2/3} n_{\rm He}) \sigma^{\rm ann}_{p\bar{p}} v_{\bar{p}}$, where $n_{\rm H} \approx 1/\mathrm{cm}^3$ is the hydrogen density, $n_{\rm He} \approx 0.07\, n_{\rm H}$ is the Helium density (the factor $4^{2/3}$ accounting for the different geometrical cross section in an effective way) and $\sigma^{\rm ann}_{p\bar{p}}$ is given by [91, 92]

$$\sigma^{\rm ann}_{p\bar{p}} = \begin{cases} 661\, (1 + 0.0115\, K^{-0.774} - 0.984\, K^{0.0151})\ \mathrm{mbarn}, & \text{for } K < 15.5\,\mathrm{GeV} \\ 36\, K^{-0.5}\ \mathrm{mbarn}, & \text{for } K \geq 15.5\,\mathrm{GeV} \end{cases} . \tag{4.24}$$

The second part, similarly, describes the interactions on interstellar protons in the galactic plane in which the $\bar{p}$'s do not annihilate but lose a significant fraction of their energy. Technically, one should keep them in the flux, with a degraded energy: they are referred to as "tertiary antiprotons". We here adopt instead the simplifying approximation of treating them as if they were removed from the flux. The cross section that we need for the whole last term of eq. (4.23) is then the sum of $\sigma^{\rm ann}_{p\bar{p}} + \sigma^{\rm non-ann}_{p\bar{p}} = \sigma^{\rm inel}_{p\bar{p}}$. It is given in [91] as

$$\sigma^{\rm inel}_{p\bar{p}}(K) = 24.7\, (1 + 0.584\, K^{-0.115} + 0.856\, K^{-0.566})\ \mathrm{mbarn} \tag{4.25}$$

(at large energies this expression has to be replaced by a better approximation [93]). We find, anyway, that the precise expressions adopted for these cross sections do not significantly impact the final results.

- We neglect, as just said, the effect of "tertiary antiprotons". It can be re-included in terms of an absorption term proportional to a different $\sigma^{\rm non-ann}$, and of a re-injection term $Q^{\rm tert}$ proportional to the integrated cross section over $f(K)$. The full solution of the resulting integro-differential equation can be found in [93]. The effect of tertiaries is mainly relevant at low energies $K \lesssim$ few GeV.

Assuming steady state conditions the first term in the diffusion equation vanishes, and the equation can be solved analytically [94, 95, 96]. In the "no-tertiaries" approximation that we adopt, the solution for the antiproton differential flux at the position of the Earth $d\Phi_{\bar p}/dK\,(K,\vec r_\odot) = v_{\bar p}/(4\pi) f$ acquires a simple factorized form (see e.g. [75])

$$\frac{d\Phi_{\bar p}}{dK}(K,\vec r_\odot) = \frac{v_{\bar p}}{4\pi}\left\{\begin{array}{ll} \left(\dfrac{\rho_\odot}{M_{\rm DM}}\right)^2 R(K)\displaystyle\sum_f \frac{1}{2}\langle\sigma v\rangle_f \frac{dN^f_{\bar p}}{dK} & \text{(annihilation)} \\ \left(\dfrac{\rho_\odot}{M_{\rm DM}}\right) R(K)\displaystyle\sum_f \Gamma_f \frac{dN^f_{\bar p}}{dK} & \text{(decay)} \end{array}\right. . \tag{4.26}$$

The f index runs over all the annihilation channels with antiprotons in the final state, with the respective cross sections or decay rates; this part contains the particle physics input. The function $R(K)$ encodes all the astrophysics of production and propagation. [6] There is such a 'propagation function' for annihilations and for decays for any choice of DM galactic profile and for any choice of set of propagation parameters among those in Table 4.1.

4.2.1 Solar modulation in a force field approximation

In the final portion of their journey, antiprotons penetrate into the sphere of influence of the Sun and are subject to the phenomenon of solar modulation. In general terms, the solar CR wind and the solar magnetic field have the effect of decreasing the kinetic energy and momentum of the particles, especially low energy ($\lesssim 10$ GeV) ones. This can be effectively described in the so-called 'force field approximation': the energy spectra in the local interstellar environment $d\Phi_{\rm LIS}/dK$ (i.e. at the end of the galactic propagation but before entering into the solar sphere, which corresponds to the $d\Phi_{\bar p}/dK$ of eq. (4.26)) are modulated to obtain the flux at Earth $d\Phi_\oplus/dK$ in the following

[6] Formally, it is given by

$$R(K) = \sum_{n=1}^{\infty} J_0\left(\zeta_n \frac{r_\odot}{R}\right) \exp\left[-\frac{V_{\rm conv} L}{2\mathcal{K}(K)}\right] \frac{y_n(L)}{A_n \sinh(S_n L/2)} \tag{4.27}$$

with

$$y_n(Z) = \frac{4}{J_1^2(\zeta_n) R^2} \int_0^R dr\, r\, J_0(\zeta_n r/R) \int_0^Z dz \exp\left[\frac{V_{\rm conv}(Z-z)}{2\mathcal{K}(K)}\right] \sinh\left(S_n(Z-z)/2\right) \left(\frac{\rho(r,z)}{\rho_\odot}\right)^2 \tag{4.28}$$

The coefficients $A_n = 2h\Gamma_{\rm ann} + V_{\rm conv} + \mathcal{K}(K)\, S_n \coth(S_n L/2)$ with $S_n = \left(V^2_{\rm conv}/\mathcal{K}(K)^2 + 4\zeta_n^2/R^2\right)^{1/2}$ encode the effects of diffusion.

way

$$\frac{d\Phi_\oplus}{dK}(K) = \frac{d\Phi_{\rm LIS}}{dK}(K + \phi_F Z/A) \cdot \frac{K(K+2m)}{(K+m+\phi_F Z/A)^2 - m^2}. \tag{4.29}$$

Here Z, A and m are the atomic number, the mass number and the mass of the CR species. In our case, $Z = A = 1$ for protons and antiprotons. The force-field or Fisk potential ϕ_F parametrizes the effect of the solar modulation on CRs and will take a value which depends on several complex parameters of the solar activity and therefore ultimately on the epoch of observation [7]. For the analysis of the PAMELA data, for instance, one can choose a conservative interval 0.1 GV $< \phi_F <$ 1.1 GV. This is based on the fact that, using more refined tools such as `HelioProp` [97] to model the propagation in the heliosphere, ref. [6] has concluded that for the PAMELA data taking period the solar modulation conditions correspond to such a range. For the AMS-02 data, projections suggest an even more conservative interval of $0 < \phi_F < 2$ GV.

4.3 Propagation of antideuterium (and heavier antinuclei)

The propagation of antideuterons and heavier antinuclei (we will consider anti-^{3}He only) through the Galaxy follows closely that of antiprotons discussed above, with a few trivial changes. The diffusion equation is still the one in eq. (4.23). In it:

- Diffusion, being governed by the electromagnetic properties of the particles, is the same for antinuclei as for antiprotons, but of course the deuteron mass m_d or nucleus mass $m_{\bar{A}}$ should replace the proton mass in the expression for the kinetic energy and the momentum.

- It is actually customary for low Z nuclei to use as a variable $K_{d,\bar{A}}/n$: the kinetic energy per nucleon ($n = 2$ or $n = 3$ for the cases of antideuteron and anti-^{3}He). We will present all results as functions of this quantity.

- The treatment of spallations of $\bar{d}$ or $\bar{A}$ on the interstellar gas ('annihilating' and 'non-annihilating' reactions) is less straightforward than for $\bar{p}$, essentially for the scarcity of experimental nuclear data on $\bar{d}$ and even more on $\bar{A}$. We have therefore to adapt from existing data. For antideuterons, we still write $\Gamma_{\rm (non-)ann} = (n_{\rm H} + 4^{2/3} n_{\rm He})\sigma_{p\bar{d}}^{\rm (non-)ann} v_{\bar{d}}$ and so we now need $\sigma_{p\bar{d}}^{\rm inel}$. This can be obtained from related experimental measurements with the charge conjugated reaction $\bar{p}d$ or with the reaction $p\bar{p}$: we refer for more details to [98, 7] and references therein. All in all, we find that a good approximation is to effectively adopt $\sigma_{p\bar{d}}^{\rm inel} \simeq 2\,\sigma_{p\bar{p}}^{\rm inel}$. For antihelium, the same equation holds and for the nuclear cross sections we use the parametrizations in Table 4.5 of [99].

With the ingredients above one can compute, exactly as for antiprotons, an antideuteron/antinucleus propagation function $R_{d,A}(K_{d,A}/n)$ for annihilations and for decays for any choice of DM galactic profile and for any choice of set of propagation parameters among those in Table 4.1. Not suprisingly, since the changes are so minimal with respect to antiprotons and affecting subdominant processes only, the propagation functions resemble those for antiprotons closely.

[7] Note that, with the notation ϕ_F, we will always refer to the Fisk potential *for antiprotons*. The corresponding quantity for protons, ϕ_F^p can in principle be different (in which case one has 'charge dependent' solar modulation). Ref. [6], based on the same `HelioProp` runs mentioned below, finds that the two quantities typically do not differ by more than 50%. Moreover, dedicated runs find that the value for antiprotons tends to be larger than the one for protons, at least for the conditions of solar activity which are appropriate during the data taking period of PAMELA.

With these ingredients, it is straightforward to compute the antideuteron or antihelium differential flux at the position of the Earth as

$$\frac{d\Phi_{\bar{d},\overline{\rm He}}}{dE}(K,\vec{r}_\odot) = \frac{v_{\bar{d},\overline{\rm He}}}{4\pi} \begin{cases} \left(\dfrac{\rho_\odot}{M_{\rm DM}}\right)^2 R_{d,{\rm He}}(K_{d,{\rm He}}/n) \displaystyle\sum_f \frac{1}{2}\langle\sigma v\rangle_f \frac{dN^f_{\bar{d},\overline{\rm He}}}{dK_{d,\overline{\rm He}}} & \text{(annihilation)} \\ \left(\dfrac{\rho_\odot}{M_{\rm DM}}\right) R_{d,{\rm He}}(K_{d,{\rm He}}/n) \displaystyle\sum_f \Gamma_f \frac{dN^f_{\bar{d},\overline{\rm He}}}{dK_{d,\overline{\rm He}}} & \text{(decay)} \end{cases} . \tag{4.30}$$

Solar modulation can be applied as discussed for antiprotons, with the due changes.

4.4 Prompt gamma rays

The *differential flux of photons* from a given angular direction $d\Omega$ produced by the annihilation of self-conjugated DM particles (e.g. Majorana fermions) is

$$\frac{d\Phi_\gamma}{d\Omega\, dE} = \frac{1}{2}\frac{r_\odot}{4\pi}\left(\frac{\rho_\odot}{M_{\rm DM}}\right)^2 J \sum_f \langle\sigma v\rangle_f \frac{dN^f_\gamma}{dE}, \qquad J = \int_{\rm l.o.s.} \frac{ds}{r_\odot}\left(\frac{\rho(r(s,\theta))}{\rho_\odot}\right)^2 \qquad \text{(annihilation)} \tag{4.31}$$

where dN^f_γ/dE is the energy spectrum of photons produced per one annihilation [8] in the channel with final state f. If DM is not constituted by self-conjugated particles (e.g. in the case of Dirac fermions), then σv must be averaged over DM particles and antiparticles: in practice, the equation above has to be divided by an additional factor of 2 if only particle-antiparticle annihilations are present.

In the case of DM decay, an analogous equation holds

$$\frac{d\Phi_\gamma}{d\Omega\, dE} = \frac{r_\odot}{4\pi}\frac{\rho_\odot}{M_{\rm DM}} J \sum_f \Gamma_f \frac{dN^f_\gamma}{dE}, \qquad J = \int_{\rm l.o.s.} \frac{ds}{r_\odot}\left(\frac{\rho(r(s,\theta))}{\rho_\odot}\right) \qquad \text{(decay)} \tag{4.32}$$

Here the coordinate r, centered on the Galactic Center, reads $r(s,\theta) = (r_\odot^2 + s^2 - 2\, r_\odot\, s\cos\theta)^{1/2}$, and θ is the aperture angle between the direction of the line of sight and the axis connecting the Earth to the Galactic Center.

The J *factor* in eq. (4.31) and eq. (4.32) integrates the intervening matter along the line of sight (along which the variable s runs) individuated by the angular direction, and it is conventionally weighted by $r_\odot$ (here assumed to be 8.33 kpc) and the appropriate power of $\rho_\odot$ (here assumed to be 0.3 GeV/cm^3) so to be adimensional.[9] $J(\theta)$ is of course invariant under rotations around the axis which connects the Earth to the GC, due to the assumed spherical symmetry of the DM distribution $\rho(r)$.

The J factors are plotted in fig. 4.5 as a function of θ.

The recipes (4.31) and (4.32) are ready for consumption if one needs the flux of gamma rays from a given direction. More often, of course, one needs the *integrated flux* over a region $\Delta\Omega$, corresponding e.g. to the window of observation or the resolution of the telescope. The J factor is

[8] Not per initial state particle; not per final state primary particle.

[9] Alternatively, sometimes an analogous factor is defined as $\mathcal{J} = \int_{\rm l.o.s.} \rho^2(r) = r_\odot \rho_\odot^2\, J$ in units of GeV^2/cm^5 (annihilation) or $\mathcal{J} = \int_{\rm l.o.s.} \rho(r) = r_\odot \rho_\odot\, J$ in units of GeV/cm^2 (decay).

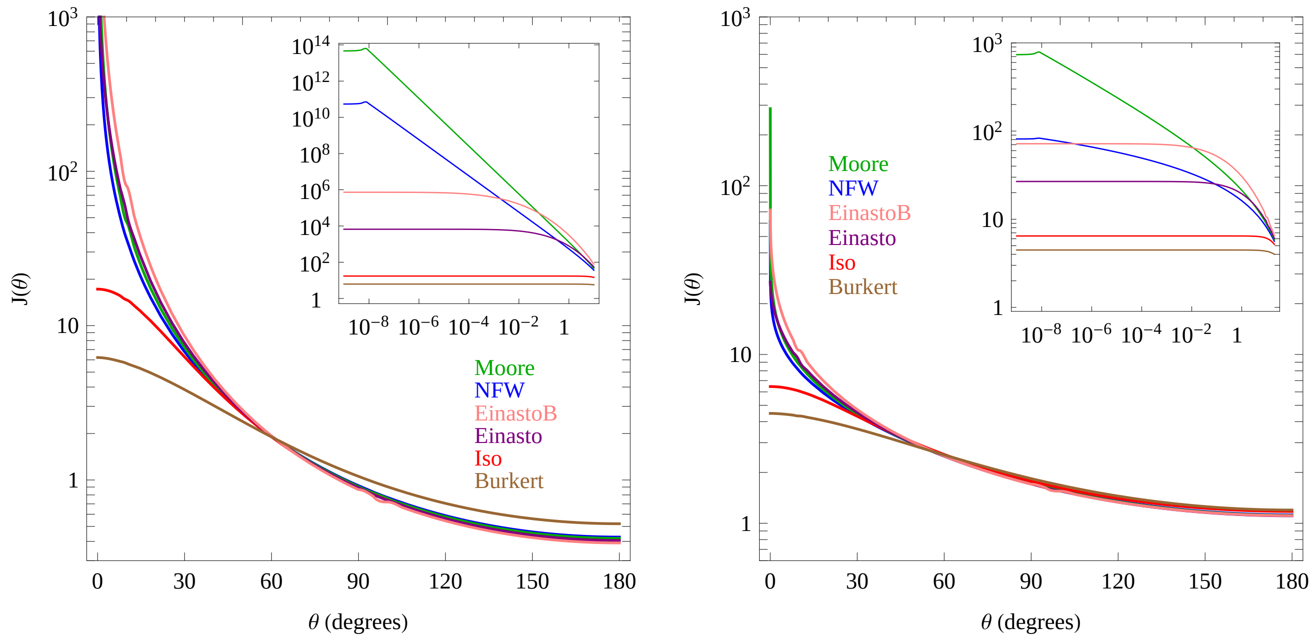

Figure 4.5: ***J(θ)* for annihilating** *(left)* **and decaying** *(right)* **Dark Matter***, for the different DM profiles. The color code individuates the profiles (Burkert, Isothermal, Einasto, EinastoB, NFW, Moore from bottom to top in the inset).*

then replaced by the *average J factor* for such region, simply defined as $\bar{J}(\Delta\Omega) = \left(\int_{\Delta\Omega} J\, d\Omega\right)/\Delta\Omega$. The following simple formulæ hold for regions that are disks of aperture $\theta_{\rm max}$ centered around the GC, annuli $\theta_{\rm min} < \theta < \theta_{\rm max}$ centered around the GC or generic regions defined in terms of galactic latitude b and longitude ℓ[10] (provided they are symmetric around the GC):

$$
\begin{aligned}
&\Delta\Omega = 2\pi \int_0^{\theta_{\rm max}} d\theta\, \sin\theta, && \bar{J} = \frac{2\pi}{\Delta\Omega}\int d\theta\, \sin\theta\, J(\theta), && \text{(disk)}\\
&\Delta\Omega = 2\pi \int_{\theta_{\rm min}}^{\theta_{\rm max}} d\theta\, \sin\theta, && \bar{J} = \frac{2\pi}{\Delta\Omega}\int d\theta\, \sin\theta\, J(\theta), && \text{(annulus)}\\
&\Delta\Omega = 4 \int_{b_{\rm min}}^{b_{\rm max}} \int_{\ell_{\rm min}}^{\ell_{\rm max}} db\, d\ell\, \cos b, && \bar{J} = \frac{4}{\Delta\Omega}\iint db\, d\ell\, \cos b\, J(\theta(b,\ell)), && (b\times\ell\ \text{region})
\end{aligned}
\tag{4.33}
$$

where the integration limits in the formulæ for $\bar{J}$ are left implicit for simplicity but obviously correspond to those in $\Delta\Omega$. For the '$b\times\ell$ region' the limits of the integration region are intended to be in one quadrant (e.g. the $b > 0°$, $0 < \ell < 90°$ one for definiteness), hence the factor of 4 to report it to the four quadrants.

The values of the $\bar{J}$ factors and $\Delta\Omega$ for some popular observational regions are reported in table 4.2, for the cases of annihilating and decaying DM and for the different halo profiles. Any

[10]Galactic polar coordinates (d, ℓ, b) are defined as

$$x = d\cos\ell\cos b, \qquad y = d\sin\ell\cos b, \qquad z = d\sin b$$

where the Earth is located at $\vec{x} = 0$ (such that d is the distance from us); the Galactic Center at $x = r_\odot$, $y = z = 0$; and the Galactic plane corresponds to $z \approx 0$. Consequently $\cos\theta = x/d = \cos b\cdot\cos\ell$.

Region	latitude b or aperture θ	longitude l	$\Delta\Omega$ [steradians]	$\bar{J}_{\rm ann}$ NFW	Ein	EinB	Iso	Bur	Moore	$\bar{J}_{\rm dec}$ NFW	Ein	EinB	Iso	Bur	Moore
'GC 0.1°'	$\theta < 0.1°$	–	$0.96\ 10^{-5}$	11579	3579	55665	17.2	6.21	81751	26.3	25.4	55.3	6.45	4.47	44.9
'GC 0.14°'	$\theta < 0.14°$	–	$0.19\ 10^{-4}$	8255	3206	43306	17.2	6.21	52395	25.1	25.0	52.9	6.45	4.47	41.5
'GC 1°'	$\theta < 1°$	–	$0.96\ 10^{-3}$	1118	1196	6945	17.2	6.21	3855	18.0	21.0	35.5	6.45	4.47	24.9
'GC 2°'	$\theta < 2°$	–	0.004	542	711	3103	17.2	6.19	1521	15.5	18.6	28.7	6.45	4.47	20.2
'Gal Ridge'	$0° < \|b\| < 0.3°$	$0° < \|\ell\| < 0.8°$	$0.29\ 10^{-3}$	1904	1605	11828	17.2	6.21	7927	19.6	22.2	39.9	6.45	4.47	28.4
'3 × 3'	$0° < \|b\| < 3°$	$0° < \|\ell\| < 3°$	0.011	306	443	1577	17.1	6.16	741	13.6	16.4	23.6	6.43	4.46	16.9
'5 × 5'	$0° < \|b\| < 5°$	$0° < \|\ell\| < 5°$	0.030	174	264	783	16.8	6.10	367	11.8	14.1	19.0	6.39	4.44	14.0
'5 × 30'	$0° < \|b\| < 5°$	$0° < \|\ell\| < 30°$	0.183	47.7	70.5	170	12.1	5.16	84.8	7.27	8.24	9.74	5.55	4.12	7.99
'10 × 10'	$0° < \|b\| < 10°$	$0° < \|\ell\| < 10°$	0.121	77.7	118	280	15.5	5.85	138	9.30	10.9	13.4	6.19	4.37	10.5
'10 × 30'	$0° < \|b\| < 10°$	$0° < \|\ell\| < 30°$	0.364	35.5	51.8	109	11.7	5.09	57.2	6.86	7.71	8.89	5.48	4.10	7.44
'10 × 60'	$0° < \|b\| < 10°$	$0° < \|\ell\| < 60°$	0.727	19.5	27.8	56.7	7.59	3.91	30.4	5.06	5.51	6.13	4.39	3.57	5.36
'GP w/o GC'	$0° < \|b\| < 5°$	$30° < \|\ell\| < 180°$	0.913	1.32	1.35	1.38	1.28	1.24	1.33	1.85	1.85	1.86	1.90	1.88	1.85
'sides of GC'	$0° < \|b\| < 10°$	$10° < \|\ell\| < 30°$	0.242	14.4	18.5	24.0	9.79	4.70	16.7	5.64	6.12	6.62	5.12	3.96	5.90
'outer Galaxy'	$0° < \|b\| < 10°$	$90° < \|\ell\| < 180°$	1.091	0.560	0.535	0.518	0.535	0.671	0.551	1.30	1.29	1.29	1.35	1.39	1.30
'10–20'	$10° < \|b\| < 20°$	$0° < \|\ell\| < 180°$	2.116	3.23	3.85	4.62	2.57	1.77	3.58	2.43	2.50	2.58	2.40	2.21	2.47
'20–60'	$20° < \|b\| < 60°$	$0° < \|\ell\| < 180°$	6.585	1.64	1.71	1.78	1.57	1.44	1.67	2.05	2.06	2.08	2.10	2.05	2.06
'Gal Poles'	$60° < \|b\| < 90°$	$0° < \|\ell\| < 180°$	1.684	0.992	0.965	0.947	0.964	1.11	0.982	1.77	1.75	1.75	1.82	1.88	1.77

Table 4.2: *Some popular observational regions, their angular area and the corresponding values of the* ***average $\bar{J}$ factor*** *for different DM halo profiles, in the case of annihilation and decay. 'GP' stands for Galactic Plane and 'GC' for Galactic Center. With a slight abuse of notation we indicate the absolute value of the longitude $|\ell|$ to signify that the considered regions are always symmetrical with respect to the $\ell = 0$ axis (for instance $0° < \ell < 3°$ actually means $\ell > 357°$, $\ell < 3°$).*

other region can be computed by using the formulæ in eq. (4.33) and the $J(\theta)$ functions provided above.

With these ingredients, one explicitly has for the differential γ ray flux from a region $\Delta\Omega$

$$\frac{d\Phi_\gamma}{dE}(E_\gamma) = \frac{r_\odot}{4\pi} \begin{cases} \frac{1}{2}\left(\frac{\rho_\odot}{M_{\rm DM}}\right)^2 \bar{J}\,\Delta\Omega \sum_f \langle\sigma v\rangle_f \frac{dN^f_\gamma}{dE_\gamma} & \text{(annihilation)} \\ \frac{\rho_\odot}{M_{\rm DM}} \bar{J}\,\Delta\Omega \sum_f \Gamma_f \frac{dN^f_\gamma}{dE_\gamma} & \text{(decay)} \end{cases} \tag{4.34}$$

4.5 Secondary photons

Galactic $e^\pm$ generated by DM in the diffusion volume lose essentially all their energy into photons by means of two processes: Inverse Compton and synchrotron radiation. In regions close to the galactic disk (where gas is abundant) and for low energy electrons, bremsstrahlung radiation is also important.

The resulting fluxes of ICS (and bremsstrahlung) γ rays and of microwave synchrotron radiation are thus possible signatures of DM. The ICS flux is particularly promising. One of its best features is that it originates from 'everywhere' in the diffusion volume of the galactic halo, including regions where the astrophysical background is reduced (e.g. at high latitudes). Moreover, essentially everywhere synchrotron energy losses are sub-dominant with respect to Inverse Compton energy losses (as discussed in Sec. 4.1.1), so that, thanks to energy conservation, the resulting ICS γ flux suffers only moderate astrophysical uncertainties.

The microwave synchrotron emission is generated in significant amount from the region close to the Galactic Center (where the intensity of the magnetic field and the density of Dark Matter is highest) and therefore is plagued by more uncertainty and more background. However it can also come from large latitudes, as recently appreciated [100, 101, 102, 103, 104, 105, 106, 107, 108].

Finally, the bremsstrahlung emission can be a relevant signature for DM in the conditions mentioned above (large gas density and $\lesssim$10 GeV $e^\pm$ energy) [5]. In any case, it has to be taken into account if one wants to consistently model the other emissions with which it competes [5].

In this section we describe in some detail the computation of ICS emission (sec. 4.5.1, based on [1] but upgraded with the results of sec. 4.1), of bremsstrahlung emission (sec. 4.5.2, based on [8]) and synchrotron radiation (sec. 4.5.3, based on [8]). The methods that we describe builds on standard EM formalism but they introduce new tools in the form of *generalized halo functions* (for ICS, bremsstrahlung and synchrotron). These functions, analogous to the halo functions for $e^\pm$ propagation, are computed once and for all and then allow to compute the emission by a simple convolution with the injection electron spectrum, making the phenomenology much faster to analyze for any DM model.

4.5.1 Inverse Compton gamma rays

The differential flux of ICS photons within an angular region $\Delta\Omega$ can be written in terms of the emissivity $j(E_\gamma, r)$ of a cell located at a distance $r \equiv |\vec{x}|$ from the Galactic Center as

$$\frac{d\Phi_{\rm IC\gamma}}{dE_\gamma\, d\Omega} = \frac{1}{E_\gamma} \int_{\rm l.o.s.} ds\, \frac{j(E_\gamma, r(s,\theta))}{4\pi} \tag{4.35}$$

In general, for any radiative process, the emissivity is obtained as a convolution of the spatial density of the emitting medium with the power that it radiates (see e.g. [109]). In this case therefore

$$j(E_\gamma, r) = 2\int_{m_e}^{M_{\rm DM}(/2)} dE_e\ \mathcal{P}_{\rm IC}(E_\gamma, E_e, r)\ \frac{dn_{e^\pm}}{dE_e}(r, E_e), \tag{4.36}$$

where $\mathcal{P} = \sum_i \mathcal{P}^i_{\rm IC}$ is the differential power emitted into photons due to ICS radiative processes (the sum runs over the different components of the photon bath: CMB, dust-rescattered light and starlight) and $dn_{e^\pm}/dE_e$ is the electron (or positron) number density after diffusion and energy losses, as computed in subsection 4.1.2 (notice that there it was denoted as f for simplicity, see page 46; $dn_{e^\pm}/dE_e$ just corresponds to eq. (4.17) removing the $v_{e^\pm}/4\pi$ factor). The minimal and maximal energies of the electrons are determined by the electron mass m_e and the mass of the DM particle $M_{\rm DM}$. The '/2' notation applies to the decay case. The overall factor of 2 takes into account the fact that, beside the electrons, an equal population of positrons is produced by DM annihilations/decays and radiates.[11]

The radiated power $\mathcal{P}_{\rm IC}$, in the full Klein-Kishina case, is given by (we refer the reader to [4, 110] and references therein for more details on the derivation)

$$\begin{aligned}&\mathcal{P}^i_{\rm IC}(E_\gamma, E_e, \vec{x}) = \\ &\frac{3\sigma_{\rm T}}{4\gamma^2}\int_{1/4\gamma^2}^{1} dq \left(E_\gamma - \frac{E_\gamma}{4q\gamma^2(1-\epsilon)}\right)\frac{n_i\big(E^0_\gamma(q), \vec{x}\big)}{q}\left[2q\ln q + q + 1 - 2q^2 + \frac{1}{2}\frac{\epsilon^2}{1-\epsilon}(1-q)\right].\end{aligned} \tag{4.37}$$

where $\gamma = E_e/m_e$ is the Lorentz factor of the scattering electron and the integrand is expressed in terms of

$$q = \frac{\epsilon}{\Gamma_E(1-\epsilon)}, \qquad \text{with } \Gamma_E = \frac{4E^0_\gamma E_e}{m_e^2}, \quad \epsilon = \frac{E_\gamma}{E_e}, \quad \text{in } \frac{1}{4\gamma^2} \simeq 0 \leq q \leq 1. \tag{4.38}$$

Here E^0_γ is the initial energy of the photon in the background bath. Correspondingly, E_γ lies in the range $E^0_\gamma/E_e \leq E_\gamma \leq E_e\,\Gamma_E/(1+\Gamma_E)$. The non-relativistic (Thompson) limit corresponds to $\Gamma_E \ll 1$, so that $\epsilon \ll 1$, the last term in the integrand of $\mathcal{P}$ is negligible, and $q \to y = E_\gamma/(4\gamma^2 E^0_\gamma)$ with $0 \leq y \leq 1$. Thus in the Thomson limit

$$\mathcal{P}^i_{\rm IC}(E_\gamma, E_e, \vec{x}) = \frac{3\sigma_{\rm T}}{4\gamma^2}E_\gamma\int_0^1 dy \frac{n_i\big(E^0_\gamma(y), \vec{x}\big)}{y}\left[2y\ln y + y + 1 - 2y^2\right] \qquad [\text{Thomson limit}]. \tag{4.39}$$

Plugging now $\mathcal{P}_{\rm IC}$ and $n_{e^\pm}$ in eq. (4.36), we can write the IC differential flux in the following convenient form:

$$\frac{d\Phi_{{\rm IC}\gamma}}{dE_\gamma\, d\Omega} = \frac{1}{E^2_\gamma}\frac{r_\odot}{4\pi}\begin{cases}\dfrac{1}{2}\left(\dfrac{\rho_\odot}{M_{\rm DM}}\right)^2\displaystyle\int_{m_e}^{M_{\rm DM}} dE_{\rm s}\sum_f \langle\sigma v\rangle_f \frac{dN^f_{e^\pm}}{dE}(E_{\rm s})\, I_{\rm IC}(E_\gamma, E_{\rm s}, b, \ell) & \text{(annihilation)}\\ \dfrac{\rho_\odot}{M_{\rm DM}}\displaystyle\int_{m_e}^{M_{\rm DM}/2} dE_{\rm s}\sum_f \Gamma_f \frac{dN^f_{e^\pm}}{dE}(E_{\rm s})\, I_{\rm IC}(E_\gamma, E_{\rm s}, b, \ell) & \text{(decay)}\end{cases} \tag{4.40}$$

[11] Recall from footnote 1 that with the notation $e^\pm$ we always refer to the independent fluxes of electrons e^- *or* positrons e^+ and not to the sum.

where $E_{\rm s}$ is the $e^\pm$ injection energy and $I_{\rm IC}(E_\gamma, E_{\rm s}, b, \ell)$ (with the dimension of an energy) is a halo function for the IC radiative process. This formalism allows therefore to express the flux of ICS γ as the convolution of the electron injection spectrum $dN_{e^\pm}/dE$ and this new kind of halo functions, in close analogy with the formalism for charged particles. Indeed, we can explicitly express $I_{\rm IC}$ in terms of the ICS ingredients discussed above and the generalized halo functions for $e^\pm$ that we introduced in Sec. 4.1.2. We get

$$I_{\rm IC}(E_\gamma, E_{\rm s}, b, \ell) = 2\, E_\gamma \int_{\rm l.o.s.} \frac{ds}{r_\odot} \left(\frac{\rho(r(s,\theta))}{\rho_\odot}\right)^\eta \int_{m_e}^{E_{\rm s}} dE\, \frac{\sum_i \mathcal{P}^i_{\rm IC}(E_\gamma, E, r(s,\theta))}{b(E, r(s,\theta))}\, I(E, E_{\rm s}, r(s,\theta)), \tag{4.41}$$

where again $\eta = 1, 2$ for the decay or annihilation scenarios respectively. The intensity of the interstellar radiation $\sum_i n_i$ cancels out in the ratio $\sum \mathcal{P}_i/b$, up to the sub-leading synchrotron contribution and provided that we are not interested in the contributions from the individual light baths.

The final step to obtain the differential ICS γ flux $d\Phi_{{\rm IC}\gamma}/dE_\gamma d\Omega$ consists in performing the convolution integral over $E_{\rm s}$ with any desired prompt $e^\pm$ energy spectrum from DM.

Finally one can compute the differential flux from a region $\Delta\Omega$ by integrating over b and ℓ as discussed in Sec. 4.4

$$\frac{d\Phi_{{\rm IC}\gamma}}{dE_\gamma} = \iint db\, d\ell\, \cos b\, \frac{d\Phi_{{\rm IC}\gamma}}{d\Omega\, dE_\gamma}. \tag{4.42}$$

Due to the intertwined dependence on b and ℓ and on E_γ and E_s of the halo functions, here the geometrical integral cannot be pulled out as for prompt γ rays, so a $\bar{J}$ factor cannot be defined in a simple way.

4.5.2 Bremsstrahlung gamma rays

The computation of the bremsstrahlung emission and its generalized halo functions follows quite closely the one for ICS in the previous subsection, using also the formalism for bremsstrahlung spelled out in sec. 4.1.1. We summarize here the main ingredients for completeness.

In exact analogy with eq. (4.40), the bremsstrahlung differential flux reads:

$$\frac{d\Phi_{{\rm brem}\gamma}}{dE_\gamma\, d\Omega} = \frac{1}{E_\gamma^2}\frac{r_\odot}{4\pi} \begin{cases} \dfrac{1}{2}\left(\dfrac{\rho_\odot}{M_{\rm DM}}\right)^2 \displaystyle\int_{m_e}^{M_{\rm DM}} dE_{\rm s} \sum_f \langle\sigma v\rangle_f \frac{dN^f_{e^\pm}}{dE}(E_{\rm s})\, I_{\rm brem}(E_\gamma, E_{\rm s}, b, \ell) & \text{(annihilation)} \\ \dfrac{\rho_\odot}{M_{\rm DM}} \displaystyle\int_{m_e}^{M_{\rm DM}/2} dE_{\rm s} \sum_f \Gamma_f \frac{dN^f_{e^\pm}}{dE}(E_{\rm s})\, I_{\rm brem}(E_\gamma, E_{\rm s}, b, \ell) & \text{(decay)} \end{cases} \tag{4.43}$$

where now (in analogy with eq. (4.41)) the generalized halo function for bremsstrahlung is

$$I_{\rm brem}(E_\gamma, E_{\rm s}, b, \ell) = 2\, E_\gamma \int_{\rm l.o.s.} \frac{ds}{r_\odot} \left(\frac{\rho(r(s,\theta))}{\rho_\odot}\right)^\eta \int_{m_e}^{E_{\rm s}} dE\, \frac{\mathcal{P}_{\rm brem}(E_\gamma, E, r(s,\theta))}{b(E, r(s,\theta))}\, I(E, E_{\rm s}, r(s,\theta)), \tag{4.44}$$

where as before $\eta = 1, 2$ for the decay or annihilation scenarios respectively and I is the $e^\pm$ generalized halo function. The bremsstrahlung power consists in

$$\mathcal{P}_{\rm brem}(E_\gamma, E, \vec{x}) = c\, E_\gamma \sum_i n_i(\vec{x}) \frac{d\sigma_i(E_\gamma, E)}{dE_\gamma} \tag{4.45}$$

where n_i are the number densities of the gas species and the bremsstrahlung cross section was given in eq. (4.46):

$$\frac{\mathrm{d}\sigma_i(E_{e^\pm}, E_\gamma)}{\mathrm{d}E_\gamma} = \frac{3\,\alpha_{\rm em}\sigma_T}{8\pi\,E_\gamma}\left\{\left[1+\left(1-\frac{E_\gamma}{E_{e^\pm}}\right)^2\right]\phi_1^i - \frac{2}{3}\left(1-\frac{E_\gamma}{E_{e^\pm}}\right)\phi_2^i\right\}. \tag{4.46}$$

4.5.3 Synchrotron radiation

The synchrotron power (in erg s^{-1} Hz^{-1}) of an isotropic distribution of relativistic electrons with energy E in a uniform magnetic field is

$$\mathcal{P}_{\rm syn}(\nu, E, \alpha) = \sqrt{3}\,\frac{e^3\,B\sin\alpha}{m_e\,c^2}F(x) \tag{4.47}$$

with

$$x = \nu/\nu_c', \qquad \nu_c' = \frac{1}{2}\nu_c\sin\alpha, \qquad \nu_c = \frac{3}{2\pi}\frac{e}{m_e c}B\gamma^2.$$

Here B is the strength of the magnetic field, α the angle between the line of sight and the magnetic field direction and $\gamma = E/m_e$ the Lorentz factor of the electron or positron. The synchrotron kernel $F(x)$ is

$$F(x) = x\int_x^\infty K_{5/3}(x')dx'$$

where K_n is the modified Bessel function of the second kind of order n.

In presence of a randomly oriented magnetic field, which is the case of our interest, the synchrotron power has to be averaged over the pitch angle α:

$$\mathcal{P}_{\rm syn}(\nu, E) = \frac{1}{2}\int_0^\pi d\alpha\,\sin(\alpha)\,\mathcal{P}_{\rm syn}(\nu, E, \alpha) \tag{4.48}$$

For relativistic electrons ($\gamma \geq 2$) this corresponds to [111]:

$$\mathcal{P}_{\rm syn}(\nu, E) = 2\sqrt{3}\,\frac{e^3\,B}{m_e c^2}y^2\left[K_{4/3}(y)K_{1/3}(y) - \frac{3}{5}y\Big(K_{4/3}(y)^2 - K_{1/3}(y)^2\Big)\right] \tag{4.49}$$

with $y = \nu/\nu_c$. Integrating this quantity over ν yields the total power emitted by an electron of energy E in all frequencies, i.e. eq. (4.15).

Next, the synchrotron emissivity has to be computed convolving the synchrotron power in eq. (4.49) with the number density of electrons per unit energy $f(E, r, z)$ (in cm^{-3} GeV^{-1}) discussed above

$$j_{\rm syn}(\nu, r, z) = 2\int_{m_e}^{M_{\rm DM}(/2)} dE\;\mathcal{P}_{\rm syn}(\nu, E)\,f(E, r, z) \tag{4.50}$$

where the minimal and maximal energies of the emitting electrons are determined by the electron mass and the mass of the DM particle. The '/2' notation applies to the decay case. The overall factor 2 takes into account that, besides the electrons, an equal population of positrons radiates.

Finally, the observable in which we are interested is the intensity $\mathfrak{I}$ of the synchrotron emission (in erg cm^{-2} s^{-1} Hz^{-1} sr^{-1}) from a certain direction of observation. This is obtained by integrating the emissivity of eq. (4.50) along the line-of-sight. Schematically:

$$\mathfrak{I}(\nu, b, \ell) = \int_{\rm l.o.s.} ds \, \frac{j_{\rm syn}(\nu, r, z)}{4\pi} \tag{4.51}$$

where it is intended that a point in (r, z) is identified by the the parameter s along the line of observation individuated by the galactic latitude b and longitude ℓ: $r(s, b, \ell), z(s, b, \ell)$.

Recollecting eq. (4.51) and eq. (4.17), the synchrotron intensity $\mathfrak{I}$ at a given frequency ν and for given galactic coordinates (b, ℓ) can be cast as:

$$\mathfrak{I}(\nu, b, \ell) = \frac{r_\odot}{4\pi} \begin{cases} \dfrac{1}{2}\left(\dfrac{\rho_\odot}{M_{\rm DM}}\right)^2 \displaystyle\int_{m_e}^{M_{\rm DM}} dE_s \sum_f \langle\sigma v\rangle_f \frac{dN^f_{e^\pm}}{dE}(E_s)\; I_{\rm syn}(\nu, E_s, b, \ell) & \text{(annihilation)} \\ \left(\dfrac{\rho_\odot}{M_{\rm DM}}\right) \displaystyle\int_{m_e}^{M_{\rm DM}/2} dE_s \sum_f \Gamma_f \frac{dN^f_{e^\pm}}{dE}(E_s)\; I_{\rm syn}(\nu, E_s, b, \ell) & \text{(decay)} \end{cases} \tag{4.52}$$

with the *generalized synchrotron halo function* $I_{\rm syn}(\nu, E_s, b, \ell)$ defined as

$$I_{\rm syn}(\nu, E_s, b, \ell) = \int_{\rm l.o.s.} \frac{ds}{r_\odot} \left(\frac{\rho(r,z)}{\rho_\odot}\right)^\eta \, 2\int_{m_e}^{E_s} dE \frac{\mathcal{P}_{\rm syn}(\nu, E)}{b(E, r, z)} \; I(E, E_s, r, z), \tag{4.53}$$

where $\eta = 1, 2$ for the decay or annihilation cases respectively and again implicitly $r(s, b, \ell)$, $z(s, b, \ell)$.

4.6 Propagation of neutrinos from the center of the Sun

The propagation of neutrinos from DM annihilations from the center of the Sun deserves a dedicated section since it is quite involved and represents a subject by itself.

The final energy spectrum of the neutrino flux at the detector location is written as

$$\frac{d\Phi_\nu}{dE_\nu} = \frac{\Gamma_{\rm ann}}{4\pi d^2} \frac{dN_\nu}{dE_\nu} \tag{4.54}$$

where d is the Sun–Earth distance, $\Gamma_{\rm ann}$ is the total DM annihilation rate in the Sun, dN_ν/dE_ν is the energy spectrum of $\nu_{e,\mu,\tau}$ and $\bar\nu_{e,\mu,\tau}$ produced per DM annihilation after taking into account all effects. What we present here is the computation of $\frac{dN_\nu}{dE_\nu}$, starting from the spectra obtained in sec. 3.3 and discussing the propagation. The latter features the superposition of flavor oscillations and (at energies above tens of GeV) Neutral Current (NC) and Charged Current (CC) interactions with solar matter, which give rise to absorption and (when a τ lepton is produced) to regeneration of neutrinos with lower energies.

4.6.1 Formalism

Flavor oscillations are a quantum coherent process while interactions with matter are coherence-breaking, but both processes simultaneously affect neutrino propagation. The appropriate formalism that marries in a quantum-mechanically consistent way these two aspects, consists in studying the spatial evolution of the 3×3 matrix of densities of neutrinos, $\boldsymbol{\rho}(E_\nu)$, and of anti-neutrinos, $\bar{\boldsymbol{\rho}}(E_\nu)$. The diagonal entries of the density matrix represent the population of the corresponding flavors, whereas the off-diagonal entries quantify the quantum superposition of flavors.[12] The matrices $\boldsymbol{\rho}(E_\nu)$ and $\bar{\boldsymbol{\rho}}(E_\nu)$ satisfy a coupled system of integro-differential equations in the distance r from the center of the Sun:

$$\frac{d\boldsymbol{\rho}}{dr} = -i[\boldsymbol{H},\ \boldsymbol{\rho}] + \left.\frac{d\boldsymbol{\rho}}{dr}\right|_{\rm NC} + \left.\frac{d\boldsymbol{\rho}}{dr}\right|_{\rm CC} \tag{4.55}$$

with an analogous equation for $\bar{\boldsymbol{\rho}}$.

- The first term describes oscillations, computed including the vacuum mixing and the MSW matter effect [112]. The effective Hamiltonian reads

$$\boldsymbol{H} = \frac{\boldsymbol{m}^\dagger \boldsymbol{m}}{2E_\nu} \pm \sqrt{2} G_{\rm F} \left[N_e \text{ diag}\,(1,0,0) - \frac{N_n}{2} \text{ diag}\,(1,1,1) \right], \tag{4.56}$$

  where $\boldsymbol{m}$ is the 3×3 neutrino mass matrix, and the $+$ $(-)$ sign applies for neutrinos (anti-neutrinos). One has $\boldsymbol{m}^\dagger \boldsymbol{m} = \boldsymbol{V} \cdot \text{diag}(m_1^2, m_2^2, m_3^2) \cdot \boldsymbol{V}^\dagger$ where $m_{1,2,3} > 0$ are the neutrino masses and $\boldsymbol{V}$ is the neutrino mixing matrix given by

$$\boldsymbol{V} = R_{23}(\theta_{23}) \cdot R_{13}(\theta_{13}) \cdot \text{diag}\,(1, e^{i\phi}, 1) \cdot R_{12}(\theta_{12}) \tag{4.57}$$

  where $R_{ij}(\theta_{ij})$ represents a rotation by θ_{ij} in the ij plane and we assume the present best fit values for the mixing parameters [113][13]

$$\tan^2\theta_{\rm sun} = 0.45, \qquad \theta_{\rm atm} = 45^\circ, \qquad \theta_{13} = 8.8^\circ,$$
$$\Delta m^2_{\rm sun} = 7.5\ 10^{-5}\,\text{eV}^2, \qquad |\Delta m^2_{\rm atm}| = 2.45\ 10^{-3}\,\text{eV}^2.$$

- The second term in eq. (4.55) describes the absorption and re-emission due to NC scatterings $\overset{(-)}{\nu} N \leftrightarrow \overset{(-)}{\nu} N^*$ (where N is any nucleon in the Sun and with N^* we denote its possible excited state after the collision), which remove a neutrino from the flux and re-inject it with a lower energy. So they contribute to the evolution equation as:

$$\left.\frac{d\boldsymbol{\rho}}{dr}\right|_{\rm NC} = -\int_0^{E_\nu} dE'_\nu \frac{d\Gamma_{\rm NC}}{dE'_\nu}(E_\nu, E'_\nu)\boldsymbol{\rho}(E_\nu) + \int_{E_\nu}^\infty dE'_\nu \frac{d\Gamma_{\rm NC}}{dE_\nu}(E'_\nu, E_\nu)\boldsymbol{\rho}(E'_\nu) \tag{4.58}$$

  where

$$\Gamma_{\rm NC}(E_\nu, E'_\nu) = N_p(r)\ \sigma(\nu_\ell p \to \nu'_\ell X) + N_n(r)\ \sigma(\nu_\ell n \to \nu'_\ell X). \tag{4.59}$$

- The third term in eq. (4.55) describes Charged Current (CC) scatterings $\overset{(-)}{\nu}_\ell N \to \ell^\pm X$ of an initial neutrino ν_ℓ with energy E_ν, which remove the ν_ℓ from the flux and produce a charged lepton ℓ and scattered hadrons X. They decay back into neutrinos $\nu_{\ell'}$ and

[12] Alternatively, the fully numerical approach pursued in Wimpsim [114] consist in writing down an event-based MonteCarlo that follows the path of a single neutrino undergoing oscillations and interactions (with given probabilities). The two approaches yield results which are very well in agreement, for any practical purpose.

[13] We neglect the indications possibly in favor of a non-maximal $\theta_{\rm atm}$ and we do not consider the small dependence of the best fit values on the choice of the mass hierarchy.

anti-neutrinos $\bar{\nu}_{\ell'}$ with lower energy E'_ν: their energy distributions are described by the function $f_{\ell\to\ell'}(E_\nu, E'_\nu)$. When the initial neutrino is ν_τ ($\bar{\nu}_\tau$), the produced τ^- (τ^+) decays promptly before losing energy, giving rise to energetic $\nu_\tau, \bar{\nu}_e, \bar{\nu}_\mu$ ($\bar{\nu}_\tau, \nu_e, \nu_\mu$): this is the tau regeneration phenomenon [115]. When instead the initial neutrino is a ν_e or ν_μ we assume that the produced e, μ is totally absorbed and we neglect the corresponding low energy neutrinos. CC scatterings thereby affect the propagation of neutrinos with the term

$$\begin{aligned}\left.\frac{d\boldsymbol{\rho}}{dr}\right|_{\rm CC} &= -\frac{\{\boldsymbol{\Gamma}_{\rm CC}, \boldsymbol{\rho}\}}{2} + \int \frac{dE_\nu^{\rm in}}{E_\nu^{\rm in}} \Big[\boldsymbol{\Pi}_\tau \rho_{\tau\tau}(E_\nu^{\rm in}) \Gamma^\tau_{\rm CC}(E_\nu^{\rm in}) f_{\tau\to\tau}(E_\nu^{\rm in}, E_\nu) \\ &\qquad + \boldsymbol{\Pi}_{e,\mu} \bar{\rho}_{\tau\tau}(E_\nu^{\rm in}) \bar{\Gamma}^\tau_{\rm CC}(E_\nu^{\rm in}) f_{\bar{\tau}\to e,\mu}(E_\nu^{\rm in}, E_\nu) \Big],\end{aligned} \tag{4.60}$$

where $\boldsymbol{\Pi}_\ell$ is the projector on the flavor ν_ℓ: e.g. $\boldsymbol{\Pi}_e = \mathrm{diag}\,(1,0,0)$. The matrices $\boldsymbol{\Gamma}_{\rm CC}$, $\bar{\boldsymbol{\Gamma}}_{\rm CC}$ that describe the rates of CC interactions are given by $\boldsymbol{\Gamma}_{\rm CC}(E_\nu) = \mathrm{diag}\,(\Gamma^e_{\rm CC}, \Gamma^\mu_{\rm CC}, \Gamma^\tau_{\rm CC})$, where

$$\Gamma^\ell_{\rm CC} = N_p(r)\ \sigma(\nu_\ell p \to \ell X) + N_n(r)\ \sigma(\nu_\ell n \to \ell X). \tag{4.61}$$

In both NC and CC processes, we neglect low energy neutrinos that might emerge from the scattered hadrons and light leptons, i.e. the de-excitation of N^* in NC and the decay of X and e, μ in CC. E.g. in particular we neglect the very low energy neutrinos with $E_\nu \sim m_{\pi,K,\mu}$ coming from the decay at rest of light hadrons/leptons. In order to include them, one should implement neutrino/matter interactions in dedicated codes such as Geant, which currently do not include them. I.e. this would be analogous to the work we performed in sec. 3.3, now with neutrinos as primary particles. We estimate that such a neglected effect would only give a small enhancement in the final flux of neutrinos at very low energy.

Solving numerically the full evolution equation (eq. 4.55) starting from the initial condition dictated by the spatial distribution of DM annihilations inside the Sun, allows to compute the full transition probabilities $P_\pm(\nu_\ell(E') \to \nu_i(E))$ from the Sun to the Earth, with $\ell = \{e, \mu, \tau, \bar{e}, \bar{\mu}, \bar{\tau}\}$, $i = \{1, 2, 3, \bar{1}, \bar{2}, \bar{3}\}$ and $E \le E'$ in the two cases of normal (P_+) and of inverted (P_-) neutrino mass hierarchy. Some transition probabilities are plotted as examples in fig. 4.6. The transition probabilities incorporate thus all propagation effects and allow to obtain the spectra of neutrinos and anti-neutrinos at the Earth (in terms of mass eigenstates ν_i) via a simple convolution with the spectra at production (presented in sec. 3.3):

$$\frac{dN^\pm_{\nu_i}}{dE} = \sum_\ell \int_E^M dE'\ P_\pm(\nu_\ell(E') \to \nu_i(E)) \frac{dN^{\rm prod}_{\nu_\ell}}{dE'}. \tag{4.62}$$

The final step consists in taking into account the oscillations in the matter of the Earth. If neutrinos do not cross the Earth, the energy spectra for the neutrino flavour eigenstates are simply given by

$$\frac{dN^\pm_{\nu_\ell}}{dE_\nu} = \sum_i |V_{\ell i}|^2 \frac{dN^\pm_{\nu_i}}{dE_\nu}. \tag{4.63}$$

If instead neutrinos cross the Earth with zenith angle ϑ ($\cos\vartheta = -1$ corresponds to the maximal vertical crossing, and $\cos\vartheta = 0$ corresponds to the minimal horizontal crossing), the neutrino fluxes at detection are given by

$$\frac{dN^\pm_{\nu_\ell}}{dE_\nu} = \sum_i P^\pm_{\rm earth}(\nu_i \to \nu_\ell, E_\nu, \vartheta) \frac{dN^\pm_{\nu_i}}{dE_\nu}. \tag{4.64}$$

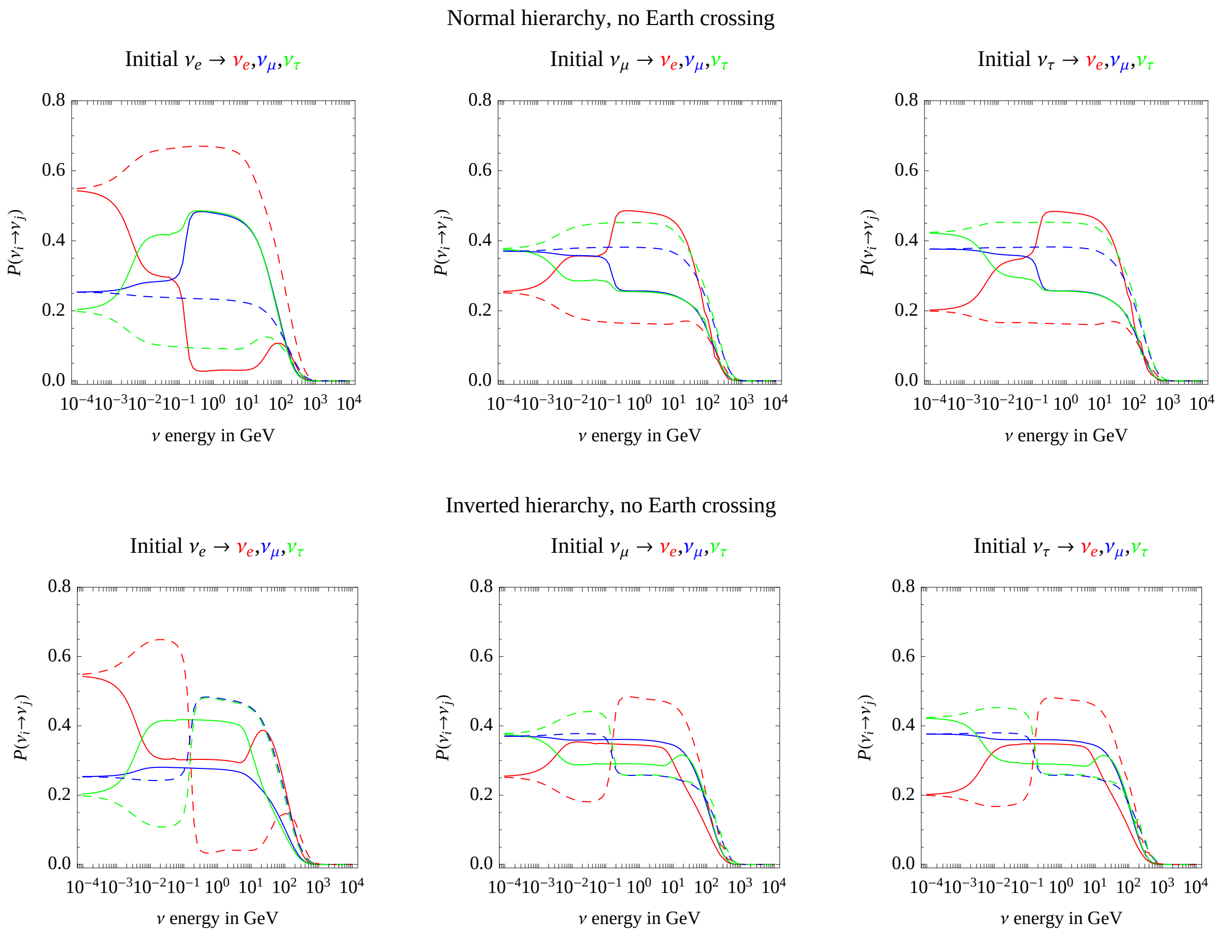

Figure 4.6: *Neutrino (continuous curves) and anti-neutrino (dashed)* ***transition probability from the Sun to the Earth****, assuming $\theta_{13} = 0$. At $E \gg 10\,\mathrm{GeV}$ the total probability $P(\nu_i \to \sum_f \nu_f)$ is smaller than 1 because of absorption. The probabilities plotted here do not include regenerated neutrinos, see text for details.*

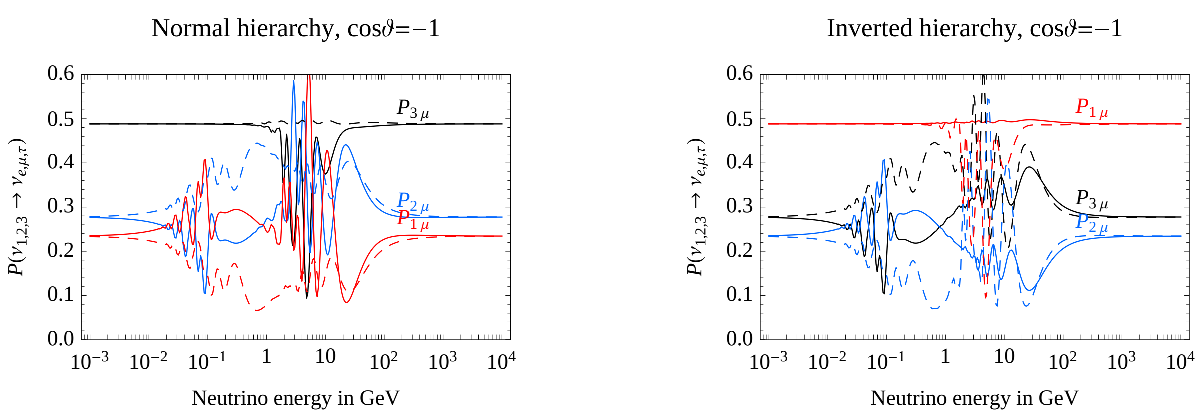

Figure 4.7: ***Earth crossing oscillation probabilities*** *into ν_μ (continuous curves) and into $\bar{\nu}_\mu$ (dashed), for neutrinos crossing vertically the Earth.*

where the oscillation probabilities $P_{\rm earth}$ are readily computed adopting the standard Earth density model. We neglect neutrino absorption within the Earth (they would be relevant only for energies above $\sim$ 10 TeV and neutrinos with those energy essentially do not emerge from the Sun, as discussed above). Some Earth oscillation probabilities are plotted in fig. 4.7 for illustration; for large and small neutrino energy they approach the limiting values $|V_{\ell i}|^2$.

4.6.2 Results

Fig. 4.8 presents, for reference, an example of our final results for the neutrino spectra at detection, analogously to fig. 3.3. The spectra are, as always, normalized per one annihilation of two DM particles.

In fig. 4.9 we present a more detailed comparison of the effect of propagation, for a few selected masses and channels. One sees, for instance:

- The effect of flavor vacuum oscillations: for an annihilation into $\tau^+\tau^-$ the flux of electron and muon neutrinos is greatly enhanced and the corresponding flux of tau neutrinos is depleted; for an annihilation into $\bar bb$, the opposite happens since $\nu_{e,\mu}$ mostly emerge from the b channel.

- The effect of solar matter absorption: moving towards higher masses, the spectra are significantly degraded in energy; the case of the Z spectrum (peaked at production) is the most apparent. For even larger $m_{\rm DM}$ all spectra approach a limit, 'bell-shaped' exponential spectrum dictated by the maximum energy to which the Sun is transparent [9].

- The effect of Earth crossing oscillations: the wiggles at around 1 to 10 GeV.

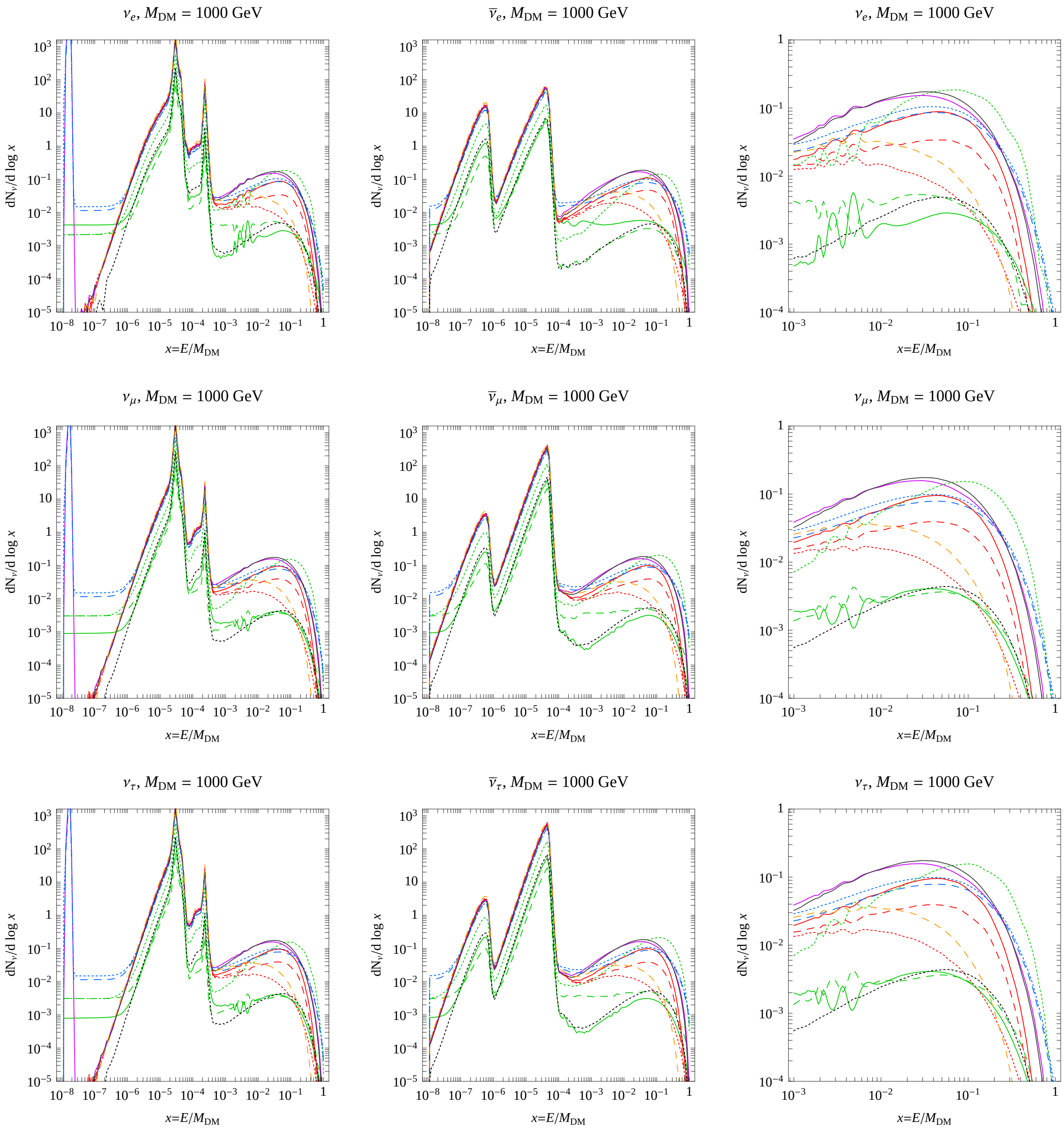

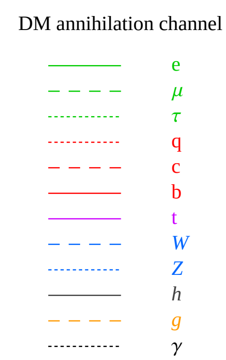

Figure 4.8: *Final results for the* ***neutrino spectra at detection****, including all propagation effects. For definiteness we choose the case of Normal Hierarchy and neutrinos crossing vertically the Earth. Left column: neutrino spectra. Central column: antineutrino spectra. Right column: zoom on the high energy portion of the neutrino spectra. Upper row: e flavor; middle row: μ flavor; bottom row: τ flavor. These plots can be directly compared with those in fig.* 3.3.

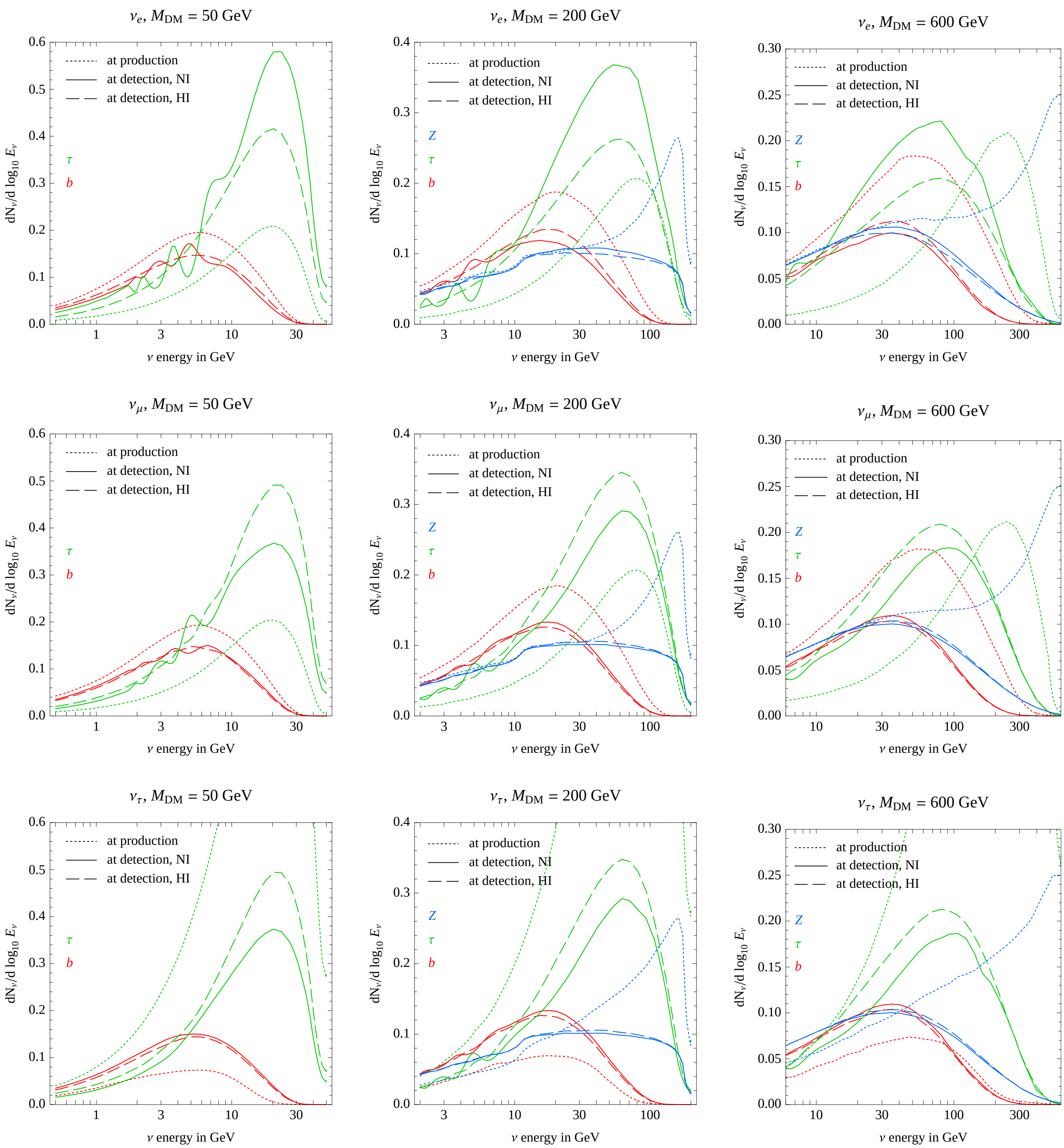

Figure 4.9: ***Comparison of the neutrino spectra*** *at production and detection, showing the effects of propagation. For definiteness we choose the case of neutrinos crossing vertically the Earth. Upper row: e flavor; middle row: μ flavor; bottom row: τ flavor. Different columns: different values of the DM mass.*

Chapter 5

Status of the searches

In this chapter I intend to briefly review the current status of the field, using the pretext of discussing four recent experimental 'anomalies' and the ensuing phenomenological activity. The four anomalies are: 1) the positron and electron excesses, first soundly detected by Pamela in 2008 in the positron fraction and then corroborated by many results from Fermi, Hess and recently Ams-02; 2) the '130 GeV line' from the Galactic Center (GC), first identified in 2012 by Christoph Weniger and collaborators in Fermi data; 3) the 'GeV Galactic Center γ-ray excess', promoted since 2010 most notably by Dan Hooper; 4) the 3.5 KeV X-ray line, supposedly detected in march 2014 in data from the Xmm-Newton satellite from several galaxy clusters and the Andromeda galaxy (M31).

5.1 The positron and electron excesses

There has been a flurry of positive results from a few indirect detection experiments looking at the fluxes of charged cosmic rays. In particular, the signals pointed to an excess of electrons and positrons at the TeV and sub-TeV scale:

- Notorius data from the Pamela satellite [116] showed, back in 2008, a steep increase in the energy spectrum of the positron fraction $e^+/(e^+ + e^-)$ above 10 GeV up to 100 GeV, compatibly with previous hints from Heat [117] and Ams-01 [118]. These findings have later been confirmed with independent measurements by the Fermi satellite [119] and, recently, by the Ams-02 experiment [120] and extended to about 430 GeV.

- Data from Pamela [121] also showed no excess in the $\bar{p}$ energy spectrum compared with the predicted background.

- In the $e^+ + e^-$ energy spectrum, the results of the Fermi satellite [122], combined with the results from the Hess telescope [123], hint to an excess (with respect to the expected background) reproduced by a simple power law up to about 1 TeV and eventually a steepening at energies of a few TeVs.

The data are displayed in fig. 5.1, together with the expected astrophysical 'backgrounds' and with the contribution from an annihilating DM particle which fits them reasonably well (see below). The properties of such a particle are pin-pointed quite precisely by the data. The DM has to be:

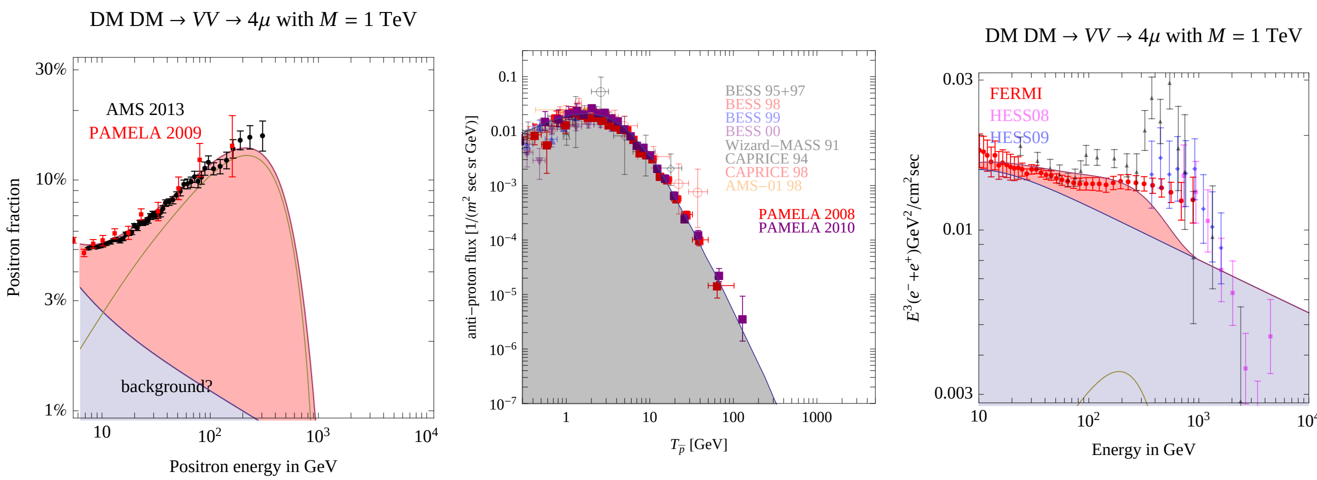

Figure 5.1: *A compilation of recent and less recent data in* ***charged cosmic rays****, superimposed on plausible but uncertain astrophysical backgrounds from secondary production and on the flux produced by Dark Matter annihilations for a specific model. Left: positron fraction. Center: antiproton flux. Right: sum of electrons and positrons. Figures from ref. [124].*

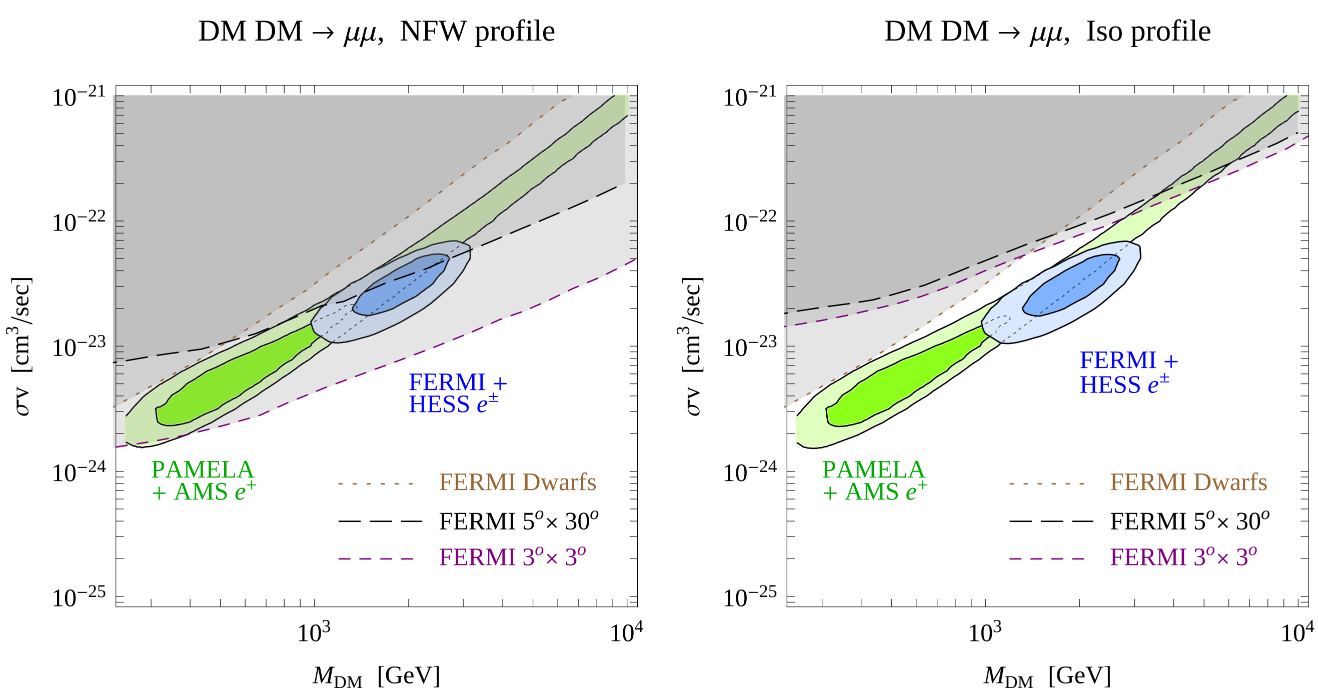

Figure 5.2: ***Best fit regions for the positron and electron excesses****, together with some representative* γ***-ray constraints****. Figure from ref. [124].*

- ▷ With a mass of *1 to few TeV*, in order to reproduce the feature in the $e^+ + e^-$ spectrum. Actually, the hint of a flattening in the positron fraction suggested by AMS-02 favours a DM mass below about 1 TeV with about 3σ statistical significance, depending on the DM annihilation channel, so that a little bit of a tension is present with the $e^+ + e^-$ spectrum, which requires a slightly larger value.

- ▷ *Leptophilic*, i.e. annihilating almost exclusively into leptonic channels, otherwise the antiproton measurements would be exceeded.

- ▷ With a *very large annihilation cross section*, of the order of $10^{-23}\,\mathrm{cm}^3/\mathrm{sec}$ or more (for the masses under consideration), much larger than the thermal one, in order to produce a large enough flux that can fit the positron rise and the $e^+ + e^-$ bump.

As tantalizing as these hints of DM can be, they have to be confronted with associated constraints. Many possible constraints can be considered, but here I will focus on two classes only. The first one is observations of γ-rays. In fig. 5.2 we show representative γ-ray bounds (the constraints are taken from [125, 126], more recent analyses find similar or slightly more stringent bounds). We see that the fit region shows some tension with γ-ray data (or it is rather clearly excluded) if (left) we have chosen a benchmark NFW galactic Dark Matter profile. Choosing the shallower isothermal profile (right), however, makes the constraints looser. It is therefore difficult to get a final answer from γ-rays. The second class of constraints comes from observations of the cosmic microwave background (CMB), which imposes bounds on DM annihilations (based on the fact that they would have re-ionized the primordial universe) that disfavor at various degrees and for most channels the DM interpretation of the positron excess [127].

5.2 The 130 GeV line

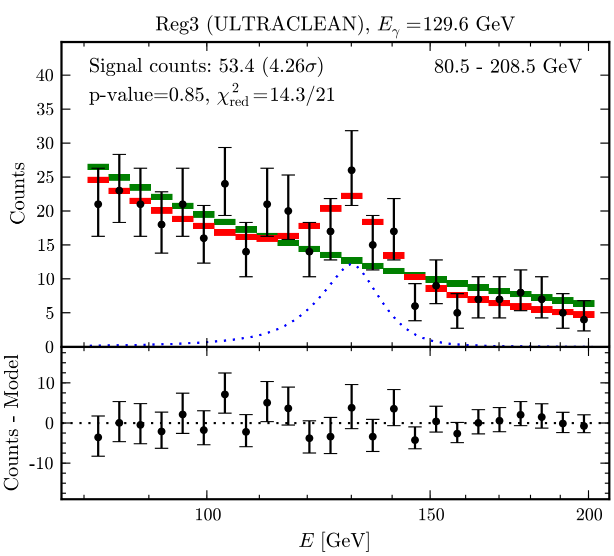

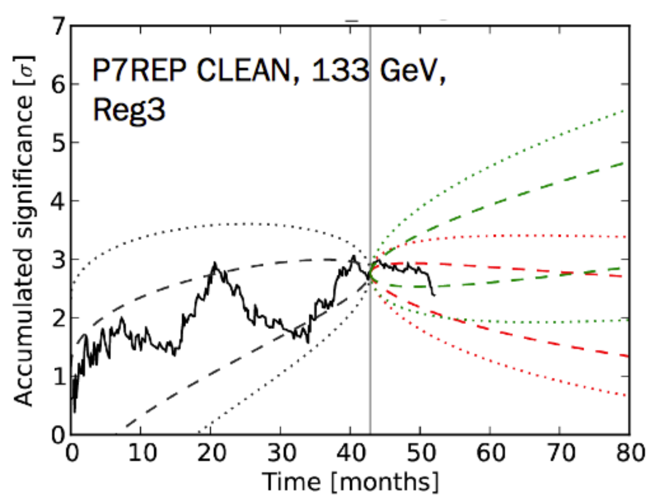

Figure 5.3: *Left:* FERMI *γ-ray data and fits pointing to a* ***line at about 130 GeV****. Right: behavior with time of the accumulated significance for this signal. Figures from ref. [130] and ref. [139].*

The '130 GeV line' claim has gathered a lot of attention in the past two years (for a more thorough review see [128]). Originally spotted by [129] and, above all, by [130] in the publicly available Fermi data from an extended region including the GC (fig. 5.3 left reports the most evocative of the original analysis' figures), it has later found support in other analyses [131, 132, 133, 134], with varying degrees of accuracy and claimed significance. [131, 134] have seen it in what could possibly be DM subhaloes of the MW, and there might be two lines, at 111 GeV and 129 GeV [135, 132]. [133] has seen it in galaxy clusters too. For a response, [136, 137, 138] challenged the analyses in a number of ways, suggesting that the line(s) could be due to unidentified instrumental, statistical or astrophysical origin. Although it is probably too early for a final conclusion on this claim, it is fair to say that the current consensus seems to be that the line has been a rather unfortunate combination of an instrumental effect and a statistical fluctuation. The right panel of fig. 5.3 illustrates that, as more data are accumulated, the significance of the signal lowers, hence pointing at something which is probably not an actual signal.

5.3 The GeV Galactic Center excess

Several authors have reported since 2009 the detection of a gamma-ray signal from the inner few degrees around the GC [140, 141], with the most notable early claims by Dan Hooper. Its spectrum and morphology are found to be compatible with those expected from annihilating DM particles: to fix the ideas, the results of one of the most recent analysis [142] confirm the presence of this excess at an incredibly high level of significance (if taken at face value) and find this signal to be best fit by 31-40 GeV DM particles distributed according to a (contracted) NFW profile and annihilating into $b\bar{b}$ with $\langle \sigma v \rangle = 1.4 \div 2 \times 10^{-26}$ cm^3/s. Fig. 5.4 displays the earliest fit to the data (from [140]) and one of the most recent ones (from [142]).

Of course, one should not forget that, in very general terms, the identification of an 'excess' strongly relies on the capability of carefully assessing the background over which the excess is supposed to emerge. The claim under scrutiny constitutes no exception, quite the contrary. The extraction of the residuals strongly relies on the modeling of the diffuse gamma-ray background (in particular the one publicly made available by the Fermi collaboration) as well as on additional modeling of astrophysical emissions, e.g. from Fermi bubbles, isotropic component, unresolved point sources, molecular gas... While this is probably the best that can be done, it is not guaranteed to be (and in general is not expected to be) the optimal strategy. Also, one should not forget that there might be alternative astrophysical explanations for the excess. A population of milli-second pulsars has been extensively discussed since the beginning [143], as well as the possibility of a spectral break in the emission of the central Black Hole [144]. More recently, the possibility has been suggested that isolated injections of charged particles (electrons [145] or protons [146]) sometime in the past, possibly connected with the activity of the central Black Hole, can produce secondary radiation able to account for the anomalous signal. While reproducing with these models all the details of the observed emission might be not easy, they represent plausible and useful counterexamples to the DM interpretation.

Still, it is interesting to insist on the tantalizing DM hypothesis and to explore ways to confirm or disprove the result within the DM framework. In particular, given the alleged hadronic origin of the signal, it is very useful to analyze the antiproton channel to put constraints on the DM interpretation of such excess. Ref. [147] delved precisely into this issue, and the condensed results are displayed in fig. 5.5. It considered several galactic propagation models for antiprotons (THN, CON, KOL, KRA, THK, roughly distinguished by the thickness of the diffusive halo, the diffusion

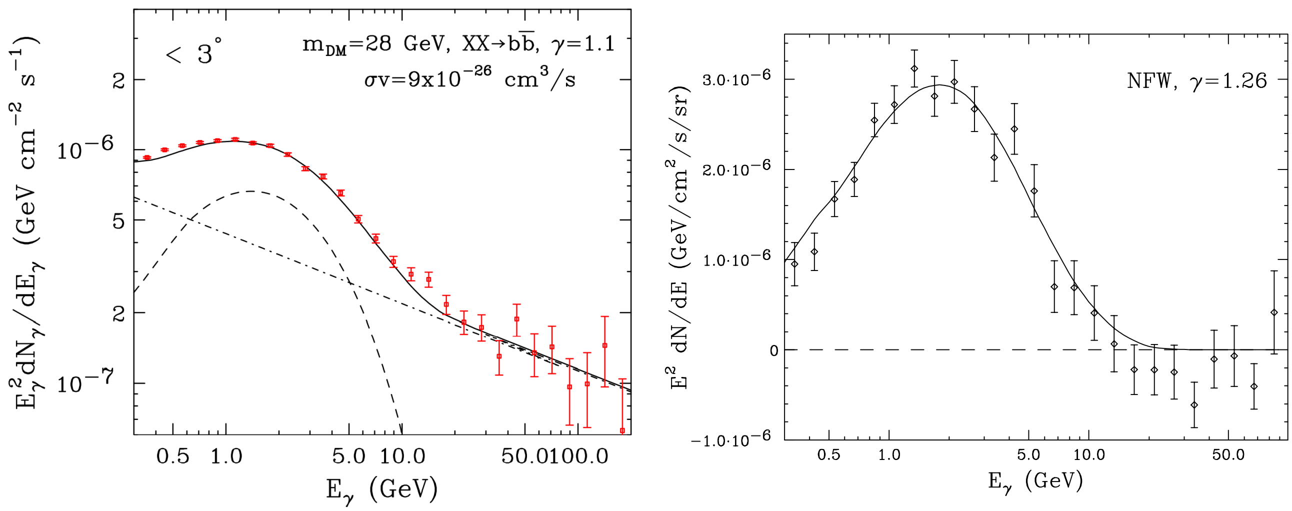

Figure 5.4: *Earliest and latest fits to the* ***GeV excess at the GC****. From ref. [140] and ref. [142].*

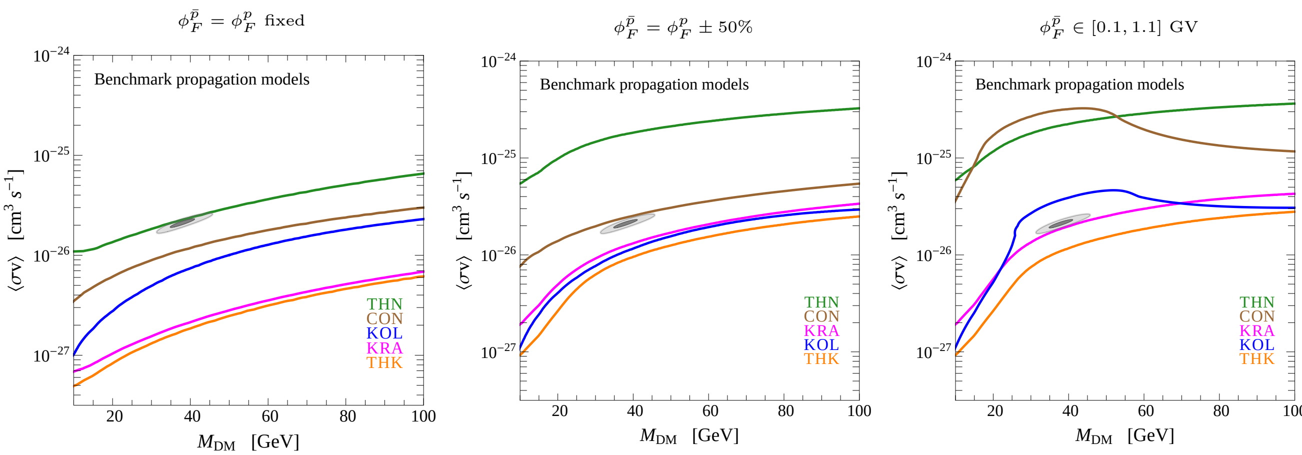

Figure 5.5: ***Antiproton constraints on the GC GeV excess****: 3-σ exclusion contours on $\langle\sigma v\rangle$ for 100% DM annihilation into $b\bar{b}$, for the three approaches to solar modulation briefly discussed in the text. The grey area is the best-fit region. Fig. from ref. [147].*

properties and the presence of side effects such as convection) and several assumptions for solar modulation. More precisely, it considered a solar force field for $\bar{p}$ fixed and equal to p one (left panel of fig. 5.5), variable within 50% (central panel) or free within a wide range (right panel).

The overall conclusions are the following: adopting the most realistic propagation models and well motivated choices for the solar modulation potential, the hadronic ($b\bar{b}$) DM interpretation for the GeV excess is definitely in strong tension with the antiproton data. Nevertheless, given that our knowledge of CR diffusion both in the Galaxy and in the heliosphere is far from being accurate and complete, there are still conservative choices of the parameters involved that do not result in ruling it out, namely thin halo models and large solar modulation potentials. [1]

[1]The authors of ref. [148] have also discussed the antiproton bounds. They find that the antiproton data can be marginally consistent with the GeV excess only if a very conservative propagation model with thin halo is used (a model roughly corresponding to our THN). The analysis in [147] differs from ref. [148] since: **1)** it considers a comprehensive set of propagation models, including several 'thin' models with different halo height, and models with high reacceleration or convection together with others where these effects are less important; **2)**

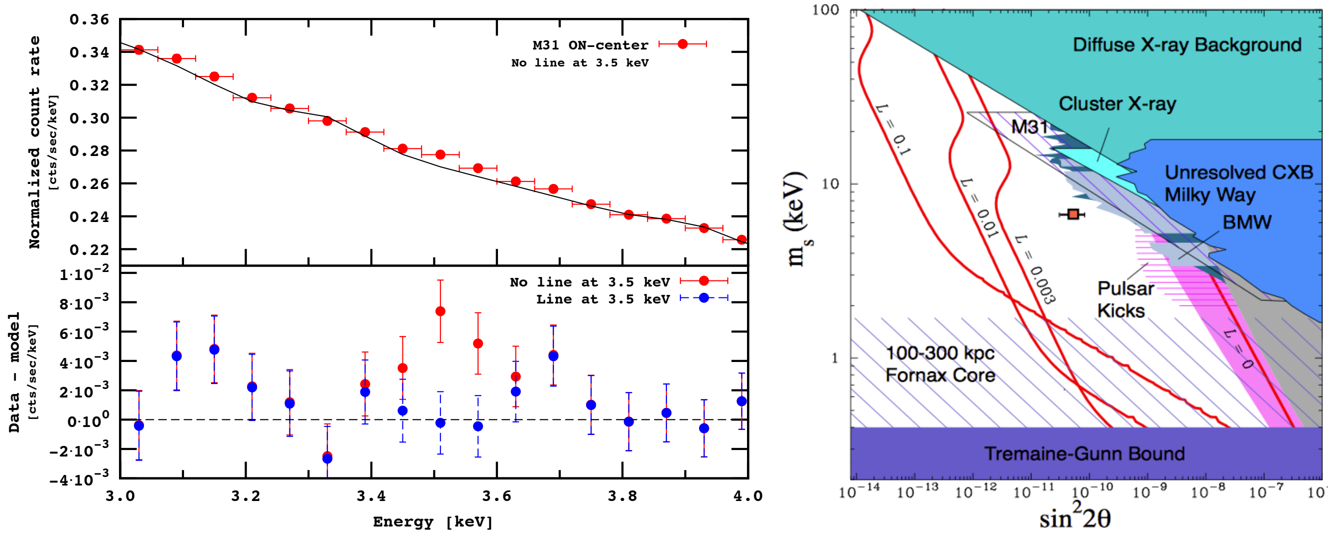

Figure 5.6: *Identification of the* ***3.5 KeV line*** *in* XMM-NEWTON *data (left) and the parameter space of its interpretation in terms of a* ***decaying sterile neutrino****. From ref. [150] and ref. [149].*

5.4 The 3.5 KeV X-ray line

One of the latest claims in the field of indirect detection comes from a different range of energies: X-rays. In datasets from the XMM-NEWTON satellite, two independent groups [149, 150] have found evidence for an unexplained line at 3.5 KeV. The former group found it in observations of a set of 73 galaxy clusters with redshift between 0.01 and 0.35. The latter one in observations both of the Perseus cluster and of Andromeda, with no detection in “blank sky” measurements. Fig. 5.6, left, displays an extraction of the spectrum showing the line, from [150].

The complication is that the X-ray spectrum in this range of energies is crowded with atomic de-excitation lines from elements such as Cr, Mn, K, Fe, Ni, Ca, Cu... Ref. [151] has indeed recently argued that previously-unaccounted-for potassium lines can well explain the signal. Ref. [152] reiterates, however, that data from Andromeda are instead solid and make the potassium interpretation problematic. On another side, ref. [153] has argued that no line is seen in Chandra data from the GC, although this conclusion depends on how one models the local background. The discussion is currently unfolding and probably more data from independent instruments will be needed.

If confirmed, however, the most straightforward explanation of the line in terms of new physics is of great interest for the field of DM indirect detection as it consists of a sterile neutrino of mass 7 KeV decaying into an ordinary neutrino and a photon (the detected X-ray). The decay rate turns out to be $\mathcal{O}(10^{-29})$ sec^{-1}. This, translated in terms of particle physics parameters by the effective mixing angle of the sterile and active neutrino, lies in a region of parameter space still allowed by other constraints, as illustrated by the right panel of fig. 5.6. The production mechanism of a population of sterile neutrinos in the early universe would involve active-sterile oscillations helped by the presence of a sizable leptonic asymmetry. Quite uncompelling, but possible.

it fully includes the subtleties associated to solar modulation: this turns out to be crucial since the more the Fisk potential for the antiprotons is allowed to vary the less stringent the bounds become.

5.5 Conclusions

There are arguably no firm conclusions in this field at this moment in time. There are tantalizing hints (the positron and electron excess, the gamma-ray line, the GeV GC excess and the X-ray line) and there are stringent constraints. Such constraints, however, are often relaxed by appropriate assumptions, which can be extreme or not (the illustration with the antiproton constraints on the GeV excess in section 5.3 is exemplar). The only firm albeit generic conclusions seem to be that:

- current experiments are clearly reaching (and in some cases have already reached) the sensitivities for which they were designed, and hence they probe very promising regions of the parameter space;
- astrophysics, in different manifestations, is the main killjoy, introducing alternative compelling explanation, irreducible uncertainties, unbeatable background noise...;
- hence, it is important to pursue a multi-messenger approach in all instances, investigating associated signals in other channels, cross-checking constraints and confirmations from independent targets etc;
- in any case, the profusion of data from the recent experiments have spurred a remarkable proliferation of DM models, so that 'traditional' DM models (such as SuSy DM) have, for better or for worse, been joined by many other possibilities.

Epilog

As stated at the beginning of this *mémoire*, my scientific career has developed so far at the borders between particle physics, cosmology and astrophysics, in what is commonly identified as the field of astroparticle physics. As perhaps all border areas, this is somewhat a dangerous zone. Particle physicists tend to think that you are escaping the formalities of their discipline (e.g. QFT, or group theory) by invoking mysterious '(g)astrostuff', while astrophysicists and cosmologists secretly (or not so) believe that you are just constructing the latest daydreaming particle theory which has little connection with what actually populates the night sky. On the individual side, it is easy to quickly lose memory of your roots and to develop a sense of arrogance stemming from the rapidity at which you seem to make some progress in a relatively less charted territory. One may soon find him/herself an 'expert' of several bits and pieces of all three disciplines, with unfortunately little connection among themselves. Yet, as perhaps all border areas, it is a field which is thriving with activity and it is where many efficient cultural exchanges are happening. It is undeniable that it tackles some of the most profound questions (What is the Universe made of? How did we come to exist? bla bla) and yet it is still in a state of *bricolage* in which some results can be obtained with relatively little effort. My efforts in this (sub)field so far have been the subject of this document, and I plan to continue in these directions for quite some time.

Dedicated to Alice and Fabio,
who did not give me the time
to do a better job.

Acknowledgements I wholeheartedly thank my collaborators on all the works that led to the material presented here: Nicolao Fornengo, Daniele Gaggero, Gaëlle Giesen, Andi Hektor, Mario Kadastik, Emmanuel Moulin, Paolo Panci, Martti Raidal, Filippo Sala, Pasquale Serpico, Alessandro Strumia, Marco Taoso, Alfredo Urbano, Aion Viana, Andrea Vittino and Gabrijela Zaharijas. I acknowledge the hospitality of the Institut d'Astrophysique de Paris, where part of this work was done. Funding and research infrastructure acknowledgements:

* European Research Council (ERC) under the EU Seventh Framework Programme (FP7/2007-2013)/ERC Starting Grant (agreement n. 278234 — 'NEWDARK' project),
* French national research agency ANR under contract ANR 2010 BLANC 041301.

Bibliography

My publications most relevant for this *mémoire*

[1] M. Cirelli, G. Corcella, A. Hektor, G. Hutsi, M. Kadastik, P. Panci, M. Raidal and F. Sala *et al.*, JCAP **1103** (2011) 051 [Erratum-ibid. **1210** (2012) E01] [arXiv:arXiv:1012.4515 [hep-ph]].

[2] M. Cirelli, M. Kadastik, M. Raidal and A. Strumia, Nucl. Phys. B 813 (2009) 1 [arXiv:arXiv:0809.2409].

[3] P. Baratella, M. Cirelli, A. Hektor, J. Pata, M. Piibeleht and A. Strumia, JCAP **1403** (2014) 053 [arXiv:arXiv:1312.6408 [hep-ph]].

[4] M. Cirelli and P. Panci, Nucl. Phys. B **821** (2009) 399 [arXiv:arXiv:0904.3830 [astro-ph.CO]].

[5] M. Cirelli, P. D. Serpico and G. Zaharijas, JCAP **1311** (2013) 035 [arXiv:arXiv:1307.7152 [astro-ph.HE]].

[6] M. Cirelli, D. Gaggero, G. Giesen, M. Taoso and A. Urbano, arXiv:arXiv:1407.2173 [hep-ph].

[7] C. B. Braeuninger and M. Cirelli, Phys. Lett. B **678** (2009) 20 [arXiv:arXiv:0904.1165 [hep-ph]].

[8] J. Buch, M. Cirelli, G. Giesen, M. Taoso, to appear.

[9] M. Cirelli, N. Fornengo, T. Montaruli, I. A. Sokalski, A. Strumia and F. Vissani, Nucl. Phys. B **727** (2005) 99 [Erratum-ibid. B **790** (2008) 338] [arXiv:hep-ph/0506298].

References for Chapter 2: Dark Matter distribution

[10] J. F. Navarro, C. S. Frenk and S. D. M. White, Astrophys. J. **462** (1996) 563 [arXiv:astro-ph/9508025].

[11] A. W. Graham, D. Merritt, B. Moore, J. Diemand and B. Terzic, Astron. J. **132** (2006) 2685 [arXiv:astro-ph/0509417].

[12] J. F. Navarro, A. Ludlow, V. Springel, J. Wang, M. Vogelsberger, S. D. M. White, A. Jenkins and C. S. Frenk *et al.*, arXiv:arXiv:0810.1522 [astro-ph].

[13] See e.g. O. Y. Gnedin, A. V. Kravtsov, A. A. Klypin *et al.*, Astrophys. J. 616 (2004) 16-26. [arXiv:astro-ph/0406247]; F. Prada, A. Klypin, J. Flix Molina *et al.*, Phys. Rev. Lett. 93 (2004) 241301. [arXiv:astro-ph/0401512].

[14] P. B. Tissera, S. D. M. White, S. Pedrosa and C. Scannapieco, arXiv:arXiv:0911.2316.

[15] K. G. Begeman, A. H. Broeils, R. H. Sanders, MNRAS 249, 523 (1991).

[16] J. N. Bahcall and R. M. Soneira, Astrophys. J. Suppl. 44, 73 (1980).

[17] A. Burkert, IAU Symp. 171 (1996) 175 [Astrophys. J. 447 (1995) L25] [arXiv:arXiv:astro-ph/9504041].

See also: P. Salucci and A. Burkert, arXiv:arXiv:astro-ph/0004397. G. Gentile, P. Salucci, U. Klein, D. Vergani and P. Kalberla, Mon. Not. Roy. Astron. Soc. 351 (2004) 903 [arXiv:arXiv:astro-ph/0403154] and P. Salucci, A. Lapi, C. Tonini, G. Gentile, I. Yegorova and U. Klein, Mon. Not. Roy. Astron. Soc. 378 (2007) 41 [arXiv:arXiv:astro-ph/0703115].

[18] J. Diemand, B. Moore and J. Stadel, Mon. Not. Roy. Astron. Soc. 353 (2004) 624 [arXiv:arXiv:astro-ph/0402267].

[19] M. Pato, O. Agertz, G. Bertone, B. Moore and R. Teyssier, Phys. Rev. D **82** (2010) 023531 [arXiv:arXiv:1006.1322 [astro-ph.HE]].

[20] C. M. Bidin, G. Carraro, R. A. Mendez and R. Smith, Astrophys. J. **751** (2012) 30 [arXiv:arXiv:1204.3924 [astro-ph.GA]]. C. M. Bidin, G. Carraro, R. A. Mendez and R. Smith, arXiv:arXiv:1204.3919 [astro-ph.GA].

[21] M. S. Turner, Phys. Rev. D **33** (1986) 889.

[22] M. S. Turner, Phys. Scripta T **36** (1991) 167.

[23] R. A. Flores, Phys. Lett. B **215** (1988) 73.

[24] K. Kuijken and G. Gilmore, Astrophysical Journal - Letters, vol. 367 (1991), p. L9-L13. Based on: K. Kuijken and G. Gilmore, MNRAS 239 (1989), p. 571-603. K. Kuijken and G. Gilmore, MNRAS 239 (1989), p. 605-649. K. Kuijken and G. Gilmore, MNRAS 239 (1989), p. 651-664.

[25] L. M. Widrow, B. Pym and J. Dubinski, Astrophys. J. **679** (2008) 1239 [arXiv:arXiv:0801.3414 [astro-ph]].

[26] R. Catena and P. Ullio, JCAP **1008** (2010) 004 [arXiv:arXiv:0907.0018 [astro-ph.CO]].

[27] M. Weber and W. de Boer, Astron. Astrophys. **509** (2010) A25 [arXiv:arXiv:0910.4272 [astro-ph.CO]].

[28] P. Salucci, F. Nesti, G. Gentile and C. F. Martins, Astron. Astrophys. **523** (2010) A83 [arXiv:arXiv:1003.3101 [astro-ph.GA]].

[29] P. J. McMillan, Mon. Not. Roy. Astron. Soc. **414** (2011) 2446 [arXiv:arXiv:1102.4340 [astro-ph.GA]].

[30] S. Garbari, J. I. Read and G. Lake, Mon. Not. Roy. Astron. Soc. **416** (2011) 2318 [arXiv:arXiv:1105.6339 [astro-ph.GA]].

[31] F. Iocco, M. Pato, G. Bertone and P. Jetzer, JCAP **1111** (2011) 029 [arXiv:arXiv:1107.5810 [astro-ph.GA]].

[32] J. Bovy and S. Tremaine, Astrophys. J. **756** (2012) 89 [arXiv:arXiv:1205.4033 [astro-ph.GA]].

[33] L. Zhang, H. W. Rix, G. van de Ven, J. Bovy, C. Liu and G. Zhao, Astrophys. J. **772** (2013) 108 [arXiv:arXiv:1209.0256 [astro-ph.GA]].

[34] T. Piffl, J. Binney, P. J. McMillan, O. Bienaymé, J. Bland-Hawthorn, K. Freeman, B. Gibson and G. Gilmore *et al.*, arXiv:arXiv:1406.4130 [astro-ph.GA]. See also: O. Bienaymé, B. Famaey, A. Siebert, K. C. Freeman, B. K. Gibson, E. K. Grebel, G. Kordopatis and U. Munari *et al.*, arXiv:arXiv:1406.6896 [astro-ph.GA].

[35] J. I. Read, J. Phys. G **41** (2014) 063101 [arXiv:arXiv:1404.1938 [astro-ph.GA]].

[36] M. A. C. Perryman, K. S. de Boer, G. Gilmore, E. Hog, M. G. Lattanzi, L. Lindegren, X. Luri and F. Mignard *et al.*, Astron. Astrophys. **369** (2001) 339 [arXiv:astro-ph/0101235].

[37] X. X. Xue *et al.* [SDSS Collaboration], Astrophys. J. 684 (2008) 1143 [arXiv:arXiv:0801.1232 [astro-ph]].

[38] T. Sakamoto, M. Chiba and T. C. Beers, Astron. Astrophys. 397 (2003) 899 [arXiv:arXiv:astro-ph/0210508].

[39] N. Przybilla, A. Tillich, U. Heber and R. D. Scholz, arXiv:arXiv:1005.5026.

[40] S. Gillessen, F. Eisenhauer, S. Trippe, T. Alexander, R. Genzel, F. Martins and T. Ott, Astrophys. J. 692 (2009) 1075 [arXiv:arXiv:0810.4674 [astro-ph]].

[41] J. Bovy, D. W. Hogg and H. W. Rix, Astrophys. J. 704 (2009) 1704 [arXiv:arXiv:0907.5423 [astro-ph.GA]]. A. M. Ghez *et al.*, Astrophys. J. 689 (2008) 1044 [arXiv:arXiv:0808.2870 [astro-ph]].

[42] F. J. Kerr and D. Lynden-Bell, Mon. Not. Roy. Astron. Soc. 221 (1986) 1023. See also M. Shen and Z. Zhu, Chin. Astron. Astrophys. 7, 120 (2007) for a recent compilation.

[43] M. C. Smith, G. R. Ruchti, A. Helmi, R. F. G. Wyse, J. P. Fulbright, K. C. Freeman, J. F. Navarro and G. M. Seabroke *et al.*, Mon. Not. Roy. Astron. Soc. **379** (2007) 755 [arXiv:astro-ph/0611671].

[44] M. Fairbairn and T. Schwetz, JCAP **0901** (2009) 037 [arXiv:arXiv:0808.0704 [hep-ph]].

[45] M. Kuhlen, N. Weiner, J. Diemand, P. Madau, B. Moore, D. Potter, J. Stadel and M. Zemp, JCAP **1002**, 030 (2010) [arXiv:arXiv:0912.2358 [astro-ph.GA]].

[46] M. Vogelsberger, A. Helmi, V. Springel, S. D. M. White, J. Wang, C. S. Frenk, A. Jenkins and A. D. Ludlow *et al.*, Mon. Not. Roy. Astron. Soc. **395** (2009) 797 [arXiv:arXiv:0812.0362 [astro-ph]].

[47] F. S. Ling, E. Nezri, E. Athanassoula and R. Teyssier, JCAP **1002** (2010) 012 [arXiv:arXiv:0909.2028 [astro-ph.GA]].

[48] M. Lisanti, L. E. Strigari, J. G. Wacker and R. H. Wechsler, Phys. Rev. D **83** (2011) 023519 [arXiv:arXiv:1010.4300 [astro-ph.CO]].

References for Chapter 3: Energy spectra of cosmic rays from DM, at production

[49] In M. Kachelriess and P. D. Serpico, Phys. Rev. D **76** (2007) 063516 [arXiv:arXiv:0707.0209 [hep-ph]] the authors first point out the potential relevance of the effect. See also: N. F. Bell, J. B. Dent, T. D. Jacques and T. J. Weiler, Phys. Rev. D **78** (2008) 083540 [arXiv:arXiv:0805.3423 [hep-ph]]. More recent analyses and a more complete appraisal of the phenomenological importance of the effect have been performed in: M. Kachelriess, P. D. Serpico and M. A. Solberg, Phys. Rev. D **80** (2009) 123533 [arXiv:arXiv:0911.0001 [hep-ph]]; P. Ciafaloni and A. Urbano, Phys. Rev. D **82** (2010) 043512 [arXiv:arXiv:1001.3950 [hep-ph]]; N. F. Bell, J. B. Dent, T. D. Jacques and T. J. Weiler, arXiv:arXiv:1009.2584 [hep-ph].

[50] P. Ciafaloni, D. Comelli, A. Riotto, F. Sala, A. Strumia and A. Urbano, JCAP **1103** (2011) 019 [arXiv:arXiv:1009.0224 [hep-ph]].

[51] G. Aad *et al.* [ATLAS Collaboration], Phys. Lett. B **716** (2012) 1 [arXiv:arXiv:1207.7214 [hep-ex]]. S. Chatrchyan *et al.* [CMS Collaboration], Phys. Lett. B **716** (2012) 30 [arXiv:arXiv:1207.7235 [hep-ex]].

[52] G. Corcella and D. Rebuzzi, in Proceedings of the Workshop on Monte Carlo's, Physics and Simulations at the LHC PART II', Frascati 2006, arXiv:arXiv:0902.0180.

[53] A. Djouadi, J. Kalinowski and M. Spira, Comput. Phys. Commun. **108** (1998) 56 [arXiv:hep-ph/9704448].

[54] F. E. Paige, S. D. Protopopescu, H. Baer and X. Tata, arXiv:hep-ph/0312045.

[55] S. Jadach, Z. Was, R. Decker and J. H. Kuhn, Comput. Phys. Commun. **76** (1993) 361.

[56] T. Bringmann, L. Bergstrom, J. Edsjo, JHEP 0801 (2008) 049. [arXiv:arXiv:0710.3169].

[57] X. -l. Chen, M. Kamionkowski, JHEP 9807 (1998) 001. [arXiv:hep-ph/9805383]. C. E. Yaguna, Phys. Rev. D81 (2010) 075024. [arXiv:arXiv:1003.2730]. L. L. Honorez, C. E. Yaguna, JHEP 1009, 046 (2010). [arXiv:arXiv:1003.3125].

[58] M. Kadastik, M. Raidal and A. Strumia, Phys. Lett. B 683 (2010) 248 [arXiv:arXiv:0908.1578].

[59] **Neutrinos from DM annihilations in the Sun and the Earth**. *In the Sun:* J. Silk, K. A. Olive and M. Srednicki, Phys. Rev. Lett. 55 (1985) 257. W. H. Press and D. N. Spergel, Astrophys. J. 296 (1985) 679. *In the Earth:* K. Freese, Phys. Lett. B 167 (1986) 295. L. M. Krauss, M. Srednicki and F. Wilczek, Phys. Rev. D 33 (1986) 2079.

[60] **Solar corona neutrinos**. G. Ingelman and M. Thunman, Phys. Rev. D 54 (1996) 4385 [arXiv:hep-ph/9604288]. G. L. Fogli, E. Lisi, A. Mirizzi, D. Montanino and P. D. Serpico, Phys. Rev. D 74 (2006) 093004 [arXiv:hep-ph/0608321].

[61] S. Agostinelli *et al.* [GEANT4 Collaboration], Nucl. Instrum. Meth. A 506 (2003) 250. J. Allison, K. Amako, J. Apostolakis, H. Araujo, P. A. Dubois, M. Asai, G. Barrand and R. Capra *et al.*, IEEE Trans. Nucl. Sci. 53 (2006) 270 (webpage).

[62] C. Rott, J. Siegal-Gaskins and J. F. Beacom, Phys. Rev. D 88 (2013) 055005 [arXiv:arXiv:1208.0827].

[63] N. Bernal, J. Martín-Albo and S. Palomares-Ruiz, JCAP 1308 (2013) 011 [arXiv:arXiv:1208.0834].

References for Chapter 4: Computation of the propagation and thus the observable fluxes at Earth

[64] For a lucid and pedagogical review of the CR propagation formalism relevant for DM, see: P. Salati, "Indirect and direct dark matter detection", Proceedings of the 2007 Cargèse Summer School: Cosmology and Particle Physics Beyond the Standard Models, PoS(cargese)009, pos.sissa.it/cgi-bin/reader/conf.cgi?confid=49.

[65] T. Delahaye, F. Donato, N. Fornengo, J. Lavalle, R. Lineros, P. Salati and R. Taillet, Astron. Astrophys. **501** (2009) 821 [arXiv:arXiv:0809.5268 [astro-ph]].

[66] The now standard "two-zone diffusion model" introduced in V.L. Ginzburg, Ya.M. Khazan and V.S. Ptuskin, Astrophysics and Space Science 68, 295-314 (1980). W.R. Webber, M.A. Lee and M. Gupta, Astrophysical Journal 390, 96-104 (1992).

[67] M. Perelstein and B. Shakya, Phys. Rev. D **82** (2010) 043505 [arXiv:arXiv:1002.4588 [astro-ph.HE]].

[68] K. Blum, arXiv:arXiv:1010.2836 [astro-ph.HE].

[69] M. Su, T. R. Slatyer and D. P. Finkbeiner, Astrophys. J. **724** (2010) 1044 [arXiv:arXiv:1005.5480 [astro-ph.HE]]. See also www.nasa.gov/mission_pages/GLAST/news/new-structure.html.

[70] M. Perelstein and B. Shakya, arXiv:arXiv:1012.3772 [astro-ph.HE].

[71] A. Putze, L. Derome and D. Maurin, Astron. Astrophys. 516 (2010) A66 [arXiv:arXiv:1001.0551 [astro-ph.HE]].

[72] G. Di Bernardo, C. Evoli, D. Gaggero, D. Grasso and L. Maccione, Astropart. Phys. 34 (2010) 274 [arXiv:arXiv:0909.4548 [astro-ph.HE]].

[73] R. Trotta, G. Johannesson, I. V. Moskalenko, T. A. Porter, R. R. de Austri and A. W. Strong, arXiv:arXiv:1011.0037 [astro-ph.HE].

[74] T. Delahaye, R. Lineros, F. Donato, N. Fornengo and P. Salati, Phys. Rev. D 77 (2008) 063527 [arXiv:arXiv:0712.2312].

[75] F. Donato, N. Fornengo, D. Maurin and P. Salati, Phys. Rev. D 69 (2004) 063501 [arXiv:arXiv:astro-ph/0306207].

[76] G. R. Blumenthal and R. J. Gould, Rev. Mod. Phys. **42** (1970) 237.

[77] Reinhard Schlickeiser, 'Cosmic ray astrophysics', Springer, 2002.

[78] I. Moskalenko, A. Strong, J. Ormes, M. Potgieter, Astrophys. J. **565** (2002) 280 [arXiv:astro-ph/0106567].

[79] R. Beck, AIP Conf. Proc. **1381**, 117 (2011) [arXiv:arXiv:1104.3749 [astro-ph.CO]].

[80] R. Jansson, G. R. Farrar, A. H. Waelkens and T. A. Ensslin, JCAP **0907** (2009) 021 [arXiv:arXiv:0905.2228 [astro-ph.GA]].

[81] M. S. Pshirkov, P. G. Tinyakov, P. P. Kronberg and K. J. Newton-McGee, Astrophys. J. **738** (2011) 192 [arXiv:arXiv:1103.0814 [astro-ph.GA]].

[82] X.Sun, W.Reich, A.Waelkens, T.Enßling, A&A **477**, 573 (2008) [arXiv:arXiv:0711.1572 [astro-ph]].

[83] R. Jansson and G. R. Farrar, Astrophys. J. **761** (2012) L11 arXiv:arXiv:1210.7820 [astro-ph.GA].

[84] R. Beck, AIP Conf. Proc. **1085**, 83 (2009) [arXiv:arXiv:0810.2923 [astro-ph]].

[85] A. W. Strong, I. V. Moskalenko and O. Reimer, Astrophys. J. **537**, 763 (2000) [Erratum-ibid. **541**, 1109 (2000)] [arXiv:astro-ph/9811296].

[86] J.L. Han, R.N. Manchester, A.G. Lyne, G.J. Qiao and W. van Straten, Astrophys. J. **642**, 868 (2006) [arXiv:astro-ph/0601357].

[87] A. W. Strong and I. V. Moskalenko, Astrophys. J. **509** (1998) 212 [arXiv:astro-ph/9807150].

[88] I. V. Moskalenko and A. W. Strong, Astrophys. J. **493** (1998) 694 [arXiv:astro-ph/9710124].

[89] A.W. Strong, E. Orlando and T.R. Jaffe, Astron. Astrophys. **534**, A54 (2011) [arXiv:arXiv:1108.4822 [astro-ph.HE]].

[90] I. Z. Rothstein, T. Schwetz and J. Zupan, JCAP 0907 (2009) 018 [arXiv:arXiv:0903.3116 [astro-ph.HE]], Appendix B.

[91] L. C. Tan and L. K. Ng, J. Phys. G 9 (1983) 227.

[92] J. Hisano, S. Matsumoto, O. Saito and M. Senami, Phys. Rev. D 73 (2006) 055004 [arXiv:arXiv:hep-ph/0511118].

[93] F. Donato, D. Maurin, P. Salati, A. Barrau, G. Boudoul and R. Taillet, Astrophys. J. 563 (2001) 172 [arXiv:arXiv:astro-ph/0103150].

[94] P. Chardonnet, G. Mignola, P. Salati and R. Taillet, Phys. Lett. B 384 (1996) 161 [arXiv:arXiv:astro-ph/9606174].

A. Bottino, F. Donato, N. Fornengo and P. Salati, Phys. Rev. D 58 (1998) 123503 [arXiv:arXiv:astro-ph/9804137].

See also: L. Bergstrom, J. Edsjo and P. Ullio, Astrophys. J. 526 (1999) 215 [arXiv:arXiv:astro-ph/9902012].

[95] D. Maurin, R. Taillet, F. Donato, P. Salati, A. Barrau and G. Boudoul, arXiv:arXiv:astro-ph/0212111.

[96] D. Maurin, F. Donato, R. Taillet and P. Salati, Astrophys. J. 555 (2001) 585 [arXiv:arXiv:astro-ph/0101231].

[97] L. Maccione, Phys. Rev. Lett. **110** (2013) 8, 081101 [arXiv:arXiv:1211.6905 [astro-ph.HE]].

[98] F. Donato, N. Fornengo and D. Maurin, Phys. Rev. D **78** (2008) 043506 [arXiv:arXiv:0803.2640 [hep-ph]].

[99] R. Duperray, "*Production and propagation de noyaux légers d'antimatière dans la Galaxie*", PhD thesis at the University of Grenoble, 2004.

[100] N. Fornengo, R. A. Lineros, M. Regis and M. Taoso, JCAP **1201** (2012) 005 [arXiv:arXiv:1110.4337 [astro-ph.GA]].

[101] E. Borriello, A. Cuoco and G. Miele, Phys. Rev. D **79** (2009) 023518 [arXiv:hhref0809.2990 [astro-ph]].

[102] E. Borriello, A. Cuoco and G. Miele, Nucl. Phys. Proc. Suppl. **190** (2009) 185 [arXiv:arXiv:0812.2932 [astro-ph]].

[103] T. Delahaye, C. Boehm and J. Silk, Mon. Not. Roy. Astron. Soc. Lett. **422** (2012) L16 [arXiv:arXiv:1105.4689 [astro-ph.GA]].

[104] Y. Mambrini, M. H. G. Tytgat, G. Zaharijas and B. Zaldivar, JCAP **1211** (2012) 038 [arXiv:arXiv:1206.2352 [hep-ph]].

[105] N. Fornengo, R. Lineros, M. Regis and M. Taoso, Phys. Rev. Lett. **107** (2011) 271302 [arXiv:arXiv:1108.0569 [hep-ph]].

[106] N. Fornengo, R. Lineros, M. Regis and M. Taoso, JCAP **1203** (2012) 033 [arXiv:arXiv:1112.4517 [astro-ph.CO]].

[107] D. Hooper, A. V. Belikov, T. E. Jeltema, T. Linden, S. Profumo and T. R. Slatyer, Phys. Rev. D **86** (2012) 103003 [arXiv:arXiv:1203.3547 [astro-ph.CO]].

[108] E. Carlson, D. Hooper, T. Linden and S. Profumo, JCAP **1307** (2013) 026 [arXiv:arXiv:1212.5747 [astro-ph.CO]].

[109] G. B. Rybicki and A. P. Lightman, 'Radiative Processes in Astrophysics', Wiley-Interscience, New York, 1979.

[110] P. Meade, M. Papucci, A. Strumia and T. Volansky, Nucl. Phys. B 831 (2010) 178 [arXiv:arXiv:0905.0480].

[111] G. Ghisellini, P. W. Guilbert and R. Svensson, ApJ 334, L5 (1988).

[112] **MSW effect**. L. Wolfenstein, Phys. Rev. D 17 (1978) 2369. S. P. Mikheev and A. Y. .Smirnov, Sov. J. Nucl. Phys. 42 (1985) 913 [Yad. Fiz. 42 (1985) 1441].

[113] **Neutrino oscillation parameters**. Particle Data Group Collaboration, Phys. Rev. D 86 (2012) 010001. F. Capozzi, G. L. Fogli, E. Lisi, A. Marrone, D. Montanino and A. Palazzo, arXiv:arXiv:1312.2878 [hep-ph]. A. Strumia and F. Vissani, arXiv:hep-ph/0606054, future version 4.

[114] M. Blennow, J. Edsjo and T. Ohlsson, JCAP 0801 (2008) 021 [arXiv:arXiv:0709.3898].

[115] **Tau regeneration**. F. Halzen and D. Saltzberg, Phys. Rev. Lett. 81 (1998) 4305 [arXiv:hep-ph/9804354]. J. F. Beacom, P. Crotty and E. W. Kolb, Phys. Rev. D 66 (2002) 021302 [arXiv:astro-ph/0111482]. E. Bugaev, T. Montaruli, Y. Shlepin and I. A. Sokalski, Astropart. Phys. 21 (2004) 491 [arXiv:hep-ph/0312295] and references therein. For background information, see also A. Stahl, *Physics with τ leptons*, Springer Verlag (Heidelberg, 2000), where spectra of τ decay products are reviewed. Some analytical approximations can also be found e.g. in S. I. Dutta, M. H. Reno and I. Sarcevic, Phys. Rev. D 62 (2000) 123001 [arXiv:hep-ph/0005310].

References for Chapter 5: Status of the searches

[116] O. Adriani *et al.* [PAMELA Collaboration], Nature 458, 607-609, 2009, arXiv:0810.4995.

[117] S. W. Barwick *et al.* [HEAT Coll.], Astrophys. J. **482** (1997) L191 [astro-ph/9703192].

[118] M. Aguilar *et al.* [AMS-01 Coll.], Phys. Lett. B **646** (2007) 145 [astro-ph/0703154].

[119] M. Ackermann *et al.* [The Fermi LAT Collaboration], arXiv:1109.0521 [astro-ph.HE].

[120] M. Aguilar *et al.* [AMS Collaboration], Phys. Rev. Lett. **110** (2013) 141102.
(An updated measurement has only been presented in a talk by S. Ting: `http://ams.nasa.gov/Documents/AMS_Publications/NASA%20JUNE-2014C.pdf` (and subsequent talks elsewhere).)

[121] O. Adriani *et al.* [PAMELA Coll.], Phys. Rev. Lett. **105** (2010) 121101 [arXiv:1007.0821].

[122] A. Abdo *et al.* [Fermi-LAT Coll.], Phys. Rev. Lett. **102** (2009) 181101, arXiv:0905.0025.
M. Ackermann *et al.* [Fermi LAT Coll.], Phys. Rev. D **82** (2010) 092004, arXiv:1008.3999.

[123] F. Aharonian *et al.* [H.E.S.S. Coll.], Phys. Rev. Lett. **101** (2008) 261104 [arXiv:0811.3894].
F. Aharonian *et al.* [H.E.S.S. Coll.], Astron. Astrophys. **508** (2009) 561 [arXiv:0905.0105].

[124] M. Cirelli, M. Kadastik, M. Raidal and A. Strumia, Nucl. Phys. B **813** (2009) 1 [Addendum-ibid. B **873** (2013) 530] [arXiv:0809.2409 [hep-ph]].

[125] M. Cirelli, P. Panci and P. D. Serpico, Nucl. Phys. B 840 (2010) 284 [arXiv:0912.0663]. M. Papucci and A. Strumia, JCAP 1003 (2010) 014 [arXiv:0912.0742].

[126] Fermi-LAT collaboration, Phys. Rev. Lett. 107 (2011) 241302 [arXiv:1108.3546]. Fermi-LAT collaboration, Astrophys. J. 761 (2012) 91 [arXiv:1205.6474]. For this figure we used the dwarfs data presented by A. Drlica-Wagner at the 2012 Fermi symposium.

[127] S. Galli, F. Iocco, G. Bertone and A. Melchiorri, Phys. Rev. D 80 (2009) 023505 [arXiv:0905.0003]. T.R. Slatyer, N. Padmanabhan, D.P. Finkbeiner, Phys. Rev. D 80 (2009) 043526, 0906.1197. G. Huetsi, A. Hektor, M. Raidal, Astron. Astrophys. 505 (2009) 999, arXiv:0906.4550. M. Cirelli, F. Iocco and P. Panci, JCAP 0910 (2009) 009, arXiv:0907.0719. See also: T. Kanzaki, M. Kawasaki and K. Nakayama, Prog. Theor. Phys. 123 (2010) 853, arXiv:0907.3985. Q.Yuan, B.Yue, X.-J.Bi, X.Chen, X.Zhang, JCAP 1010 (2010) 023, arXiv:0912.2504. G. Hutsi, J. Chluba, A. Hektor and M. Raidal, arXiv:1103.2766. S.Galli, F.Iocco, G.Bertone, A.Melchiorri, Phys. Rev. D 84 (2011) 027302, arXiv:1106.1528. A. Natarajan, arXiv:1201.3939. G. Giesen, J. Lesgourgues, B. Audren and Y. Ali-Haimoud, JCAP 1212 (2012) 008 [arXiv:1209.0247]. J. M. Cline and P. Scott, JCAP 1303 (2013) 044 [arXiv:1301.5908].

[128] T. Bringmann and C. Weniger, arXiv:1208.5481 [hep-ph].

[129] T. Bringmann, X. Huang, A. Ibarra, S. Vogl and C. Weniger, arXiv:1203.1312 [hep-ph].

[130] C. Weniger, JCAP **1208** (2012) 007 [arXiv:1204.2797 [hep-ph]].

[131] E. Tempel, A. Hektor and M. Raidal, arXiv:1205.1045 [hep-ph].

[132] M. Su and D. P. Finkbeiner, arXiv:1206.1616 [astro-ph.HE].

[133] A. Hektor, M. Raidal and E. Tempel, arXiv:1207.4466 [astro-ph.HE].

[134] M. Su and D. P. Finkbeiner, arXiv:1207.7060 [astro-ph.HE].

[135] A. Rajaraman, T. M. P. Tait and D. Whiteson, arXiv:1205.4723 [hep-ph].

[136] A. Boyarsky, D. Malyshev and O. Ruchayskiy, arXiv:1205.4700 [astro-ph.HE].

[137] N. Mirabal, arXiv:1208.1693 [astro-ph.HE].

[138] A. Hektor, M. Raidal and E. Tempel, arXiv:1208.1996 [astro-ph.HE].

[139] C. Weniger, presentation at the FERMI meeting http://fermi.gsfc.nasa.gov/ssc/proposals/alt_obs/white_papers_eval.html for alternative observations, 25 Jul 2013.

[140] L. Goodenough and D. Hooper, arXiv:0910.2998 [hep-ph].

[141] V. Vitale *et al.* [Fermi-LAT Collaboration], arXiv:0912.3828 [astro-ph.HE].
D. Hooper and L. Goodenough, Phys. Lett. B **697** (2011) 412 [arXiv:1010.2752 [hep-ph]].
D. Hooper and T. Linden, Phys. Rev. D **84** (2011) 123005 [arXiv:1110.0006 [astro-ph.HE]].
D. Hooper, Phys. Dark Univ. **1** (2012) 1 [arXiv:1201.1303 [astro-ph.CO]].
K. Abazajian, M. Kaplinghat, Phys. Rev. D **86** (2012) 083511 [arXiv:1207.6047.
D. Hooper, T. Slatyer, Phys. Dark Univ. **2** (2013) 118 [arXiv:1302.6589 [astro-ph.HE]].
C. Gordon and O. Macias, Phys. Rev. D **88** (2013) 083521 [arXiv:1306.5725 [astro-ph.HE]].
W.-C. Huang, A. Urbano and W. Xue, arXiv:1307.6862 [hep-ph].
K. N. Abazajian, N. Canac, S. Horiuchi and M. Kaplinghat, arXiv:1402.4090 [astro-ph.HE].

[142] T. Daylan, D. P. Finkbeiner, D. Hooper, T. Linden, S. K. N. Portillo, N. L. Rodd and T. R. Slatyer, arXiv:1402.6703 [astro-ph.HE].

[143] K. N. Abazajian, JCAP **1103** (2011) 010 [arXiv:1011.4275 [astro-ph.HE]].
D. Hooper, I. Cholis, T. Linden, J. Siegal-Gaskins and T. Slatyer, Phys. Rev. D **88** (2013) 083009 [arXiv:1305.0830 [astro-ph.HE]].
Q. Yuan and B. Zhang, arXiv:1404.2318 [astro-ph.HE].

[144] A. Boyarsky, D. Malyshev and O. Ruchayskiy, Phys. Lett. B **705** (2011) 165 [arXiv:1012.5839 [hep-ph]].

[145] J. Petrovic, P. D. Serpico and G. Zaharijas, arXiv:1405.7928 [astro-ph.HE].

[146] E. Carlson and S. Profumo, arXiv:1405.7685 [astro-ph.HE].

[147] M. Cirelli, D. Gaggero, G. Giesen, M. Taoso and A. Urbano, arXiv:1407.2173 [hep-ph].

[148] T. Bringmann, M. Vollmann and C. Weniger, arXiv:1406.6027 [astro-ph.HE].

[149] E. Bulbul, M. Markevitch, A. Foster, R. K. Smith, M. Loewenstein and S. W. Randall, Astrophys. J. **789** (2014) 13 [arXiv:1402.2301 [astro-ph.CO]].

[150] A. Boyarsky, O. Ruchayskiy, D. Iakubovskyi and J. Franse, arXiv:1402.4119 [astro-ph.CO].

[151] T. E. Jeltema and S. Profumo, arXiv:1408.1699 [astro-ph.HE].

[152] A. Boyarsky, J. Franse, D. Iakubovskyi and O. Ruchayskiy, arXiv:1408.4388 [astro-ph.CO].

[153] S. Riemer-Sorensen, arXiv:1405.7943 [astro-ph.CO].